Warwick Mobile Robotics

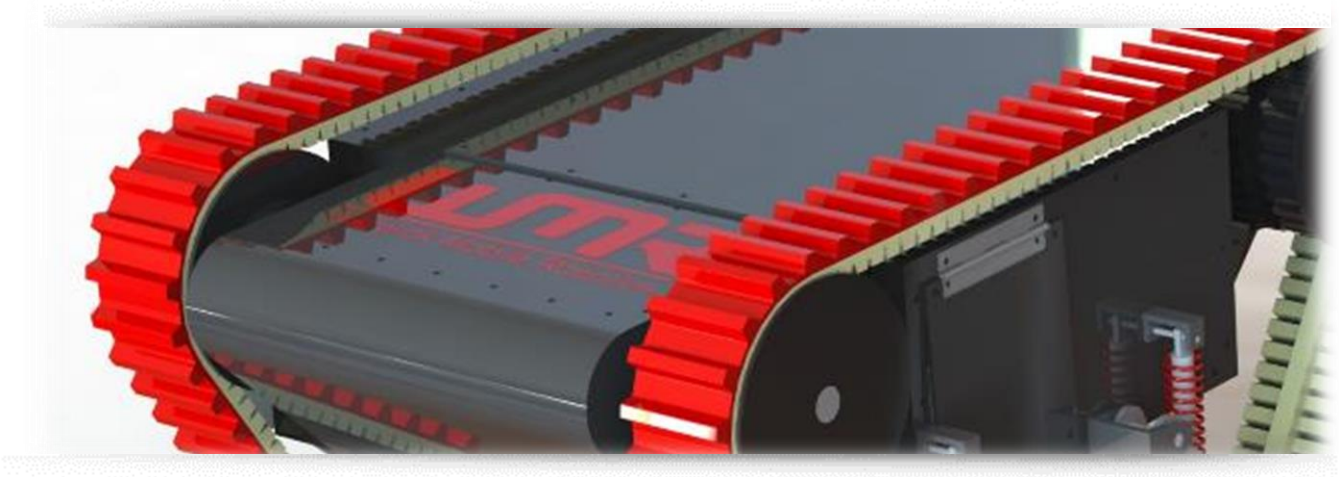

Urban Search & Rescue Robotics

Design & Development of a Miniature, Urban Search & Rescue Robot, 2014/15

Authors: 0910923 1015945 1102283 1124745
1114694 1117210 1117884 1124285

Sponsored By

WMG Innovative Solutions

School of Engineering

Transdev

MakerBeam

maxon motor driven by precision

I. DECLARATION

We hereby declare that this project work entitled "Urban Search & Rescue Robotics: The Design and Development of a Miniature, Urban Search & Rescue Robot" submitted to the University of Warwick, is the work done by Leigh Dawson, Craig Fox, Michele Galbusera, Paul Martin, Mara Nkere, Avnish Popat, Rebecca Saunders and John Strutton, under the guidance of Dr Emma Rushforth.

Authors:

Leigh Dawson

Craig Fox

Michele Galbusera

Paul Martin

Mara Nkere

Avnish Popat

Rebecca Saunders

John Strutton

II. ABSTRACT

Natural and man-made disasters cause dangerous environments in which response teams must risk their lives in rescue operations. This risk can be eliminated with the deployment of Urban Search and Rescue (USAR) robots. The Warwick Mobile Robotics (WMR) 2014/15 team has designed and developed the novel Mini-USAR robot, Orion, with project aims of:

- Delivering the mechatronic framework for an innovative Mini-USAR (M-USAR) robot by May 2015 as the first stage of a three-year plan
- Provisioning for design development by future WMR teams
- Exhibiting the robot as an educational platform to inspire younger generations

The design work was achieved through implementation of a full strategy and methodology. Analysing and benchmarking existing robots helped identify key challenges in USAR robot functionality. These exercises informed the development of a coherent mechatronic design comprising of a robust and accessible chassis with high clearance over obstacles, a resilient suspension and track system for optimal mobility, and a modular electronic architecture for precise control and provision for future developments. All features were validated through design calculations and simulations, and subsequently tested to confirm that the specification had been met. A critical review revealed the mass distribution of the robot could be improved for stability.

The 2014/15 WMR team was concluded to have successfully achieved its aims: delivering an innovative mechatronic framework for an M-USAR robot. This work represents a strong platform for further development and completion of a competitive M-USAR as part of the new WMR three-year plan. A dossier for further work has been generated, which includes the additions of a robotic arm and stabilisers.

The team has contributed to numerous Outreach events including, Imagineering 2014 and the 3D Printing in Schools Showcase at the Herbert Art Gallery. The project was delivered 15% under budget, with many benefits including the contribution to society in Search and Rescue applications and the inspiration of future Engineers.

This report documents the WMR 2014/15 project; including research and testing of WMR robots, design processes for a Chassis, Drivetrain and Electronic architecture, and manufacturing of the robot Orion.

Acknowledgements

With many thanks to our supervisor, Emma, for keeping us on track (pun intended); to our technician, Carl, for making endless brackets and monitoring our designs; to all the technicians and staff in WMG and the School of Engineering, who were always ready to lend a helping hand; to Margaret for giving us the opportunity to help inspire the next generation of engineers with Outreach projects; and to our sponsors: WMG, School of Engineering, Transdev, MakerBeam and Maxon Motor, for all their support.

TABLE OF CONTENTS

TABLE OF FIGURES

1 INTRODUCTION

"Whoever saves one life, saves the world entire."

– Itzhak Stern

Disaster zones are commonplace worldwide; from hurricanes and tsunamis, to earthquakes and nuclear meltdowns; humans are often in need of rescue. In such circumstances rescuers often jeopardise their lives to save others; however this risk can be hugely reduced through development and use of Urban Search and Rescue (USAR) robots (Kruijff, et al., 2012).

Warwick Mobile Robotics (WMR) is a research group at the University that runs several on-going projects in the field of robotics. In recent years, the Masters-level Group Project has been responsible for the development of USAR robots. The 2014/15 team inherited two robots: a large USAR robot developed over many projects requiring extensive refitting to regain functionality, and a small Mini-USAR (M-USAR) robot, designed by the 2013/14 team, which was not operational and was identified to have fundamental design flaws. WMR's robots are a platform for research, innovation and education.

This year, the team analysed and reviewed the existing robots from previous WMR projects, and developed a high-level three-year plan for an entirely new M-USAR robot. The development strategy for the new robot for the 2014/15 project year included detailed objectives, specifications and schedule. This report details the technical aspects of the project, while the corresponding Cost Benefit Analysis documents project information including budget, logistics and outcomes.

2 STRATEGY

The strategy set out by the 2014/15 WMR team included the following points:

- Review the current M-USAR robot through testing in a workshop environment to benchmark the design and inform decision making
- Plan achievable objectives for delivery this year and for future WMR teams
- Integrate mechatronic design philosophy across a multi-disciplined team
- Employ business practice throughout the project lifecycle including Design for Manufacture and Assembly (DFMA)
- Focus on durability and reliable performance
- Set testing objectives which replicate real world USAR challenges, and use these results to identify progress and achievement for the 2014/15 team
- Acquire sponsorship for the project to assist with capital and hardware requirements, and build relationships with suppliers to support the project and publicise their involvement in return
- Differ from previous WMR strategies in foregoing the 2015 RoboCup competition (see Section 3.3) in order to focus on a competitive design for future years

2.1 Aims

- Deliver a mechatronic framework for an innovative M-USAR robot by May 2015 as the first stage of a three-year plan
- Provision for design development by future WMR teams
- Exhibit the robot as an educational platform to inspire younger generations

2.2 Objectives

- Analyse the design of current USAR robots and other multi-terrain vehicles
- Benchmark both of WMR's existing USAR robots to inform the design process
- Define an achievable specification for robotic performance – complying with industry standards and RoboCup rules – by considering the results of benchmarking and strengths and weaknesses of previous WMR robots
- Design a mobile, multi-terrain robot incorporating novel technology and innovative features to push the boundaries of established design
- Adapt the design for ease of manufacture, maintenance and safety

- Test components and features to validate the design against the specification, analyse capability in real world applications and identify progress and achievement by the 2014/15 team
- Document designs, provision for further work and produce a handover programme for future projects and developments
- Showcase the robot through technology conferences and exhibitions such as the Imagineering Fair 2014, media publicity and open days to promote engineering, robotics and other STEM subjects

2.3 Team Structure

The 2014/15 team consisted of eight engineers: two Mechanical, two Systems, one Manufacturing, one Automotive, one Computing and one Electrical. This provided a strong mix of skill sets, although limited electrical expertise on a technical robotics project did present a challenge for the team.

All members took on both admin and engineering roles in order to encourage individuals to oversee the managerial aspects of the project as well as provide input on technical tasks. Administrative roles included Project Manager, Secretary, Procurement Officer, Sponsorship, Media and Health & Safety. To tackle the engineering challenges of designing and manufacturing a durable robot, the team was divided into mechanical and electronics sub-teams of five and three engineers respectively. This suited the disciplines of the engineers involved and aligned with the project objectives, as there were significant mechanical design and manufacture challenges in producing a completely new robot.

2.4 Project Lifetime

The project duration was 30 weeks, which was broken down into several milestone-monitoring points. It was recognised from the outset that it would be a challenge to produce a quality USAR vehicle within the allotted timeframe, and as such it was decided that a 3-year development plan would be implemented. For a Graphical representation of the 3-year WMR ‘roadmap’ see Figure 1. During the course of the project the group had to identify a project direction, benchmark the current robots, generate a design, conduct simulations, produce technical drawings, specify and order components, manufacture, assemble, program and finally test the robot. This would clearly prove demanding within the short project timeframe.

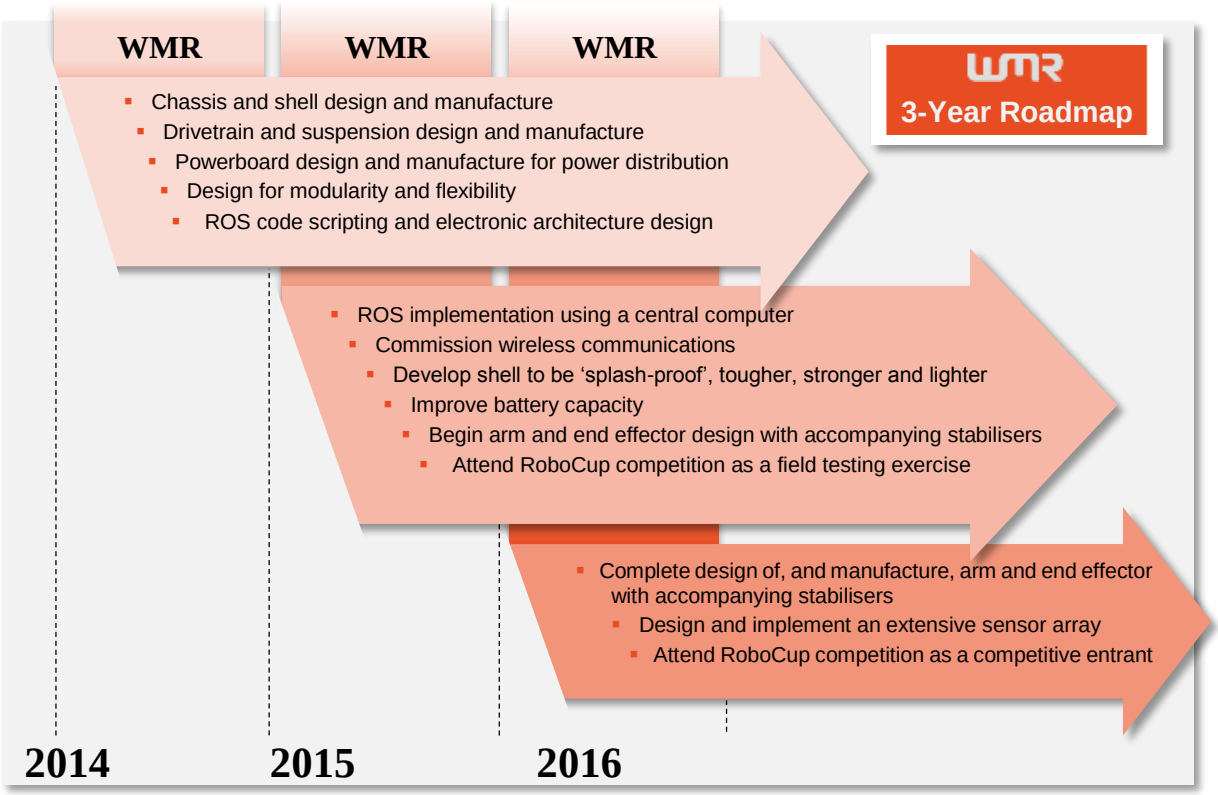

Figure 1 - WMR three-year road map

2.5 Management and Logistics

Individual timesheets, team budget, components and manufacturing logs were all coordinated on online platforms for the team to manage progress, technology and expenditure. These can be viewed in Appendix A, and are also detailed in the Cost Benefit Analysis, along with the Outreach and sponsorship activities. Through funding from the School of Engineering and Warwick Manufacturing Group (WMG), the WMR 2014/15 Team had a budget of £5,000 to cover all expenditure including materials, components, manufacturing, tools and other expenses. An additional £500 was secured through the School of Engineering Outreach programme, whereby the funding was promised in return for completing a quota of Outreach events and workshops.

3 MOTIVATION

3.1 Urban Search and Rescue Robotics

USAR robots are used to locate survivors in hazardous areas, reducing the requirement for response teams and minimising the risk to human life. As of June 2014, USAR robots had been used in more than 35 incidents, the first of which was at the World Trade Centre catastrophe in 2001. There they were used to navigate confined spaces to locate stairwells and entrances in the hope of finding survivors. Since then, USAR robots have been utilised on many occasions including the use of airborne rescue robots after hurricane Katrina (BBC, 2014).

USAR robots demonstrated their worth most notably after the nuclear accident in Fukushima, Japan. The robots used included the Japanese robot, Quince, a research project developed at Sendai University; The Talon developed by UK defence firm QinetiQ and the 710 Warrior, from Massachusetts-based company, iRobot (Forum on Energy, 2013).

Figure 2 - (From left to right) Quince, The Talon and 710 Warrior

Currently, the leader in the USAR robotics field is CHIMP, seen in Figure 3. The CHIMP (CMU Highly Intelligent Mobile Platform) is being developed at Carnegie Mellon University with funding from DARPA (The Defence Advanced Research Projects Agency) and has many capabilities. These included the ability to open doors, turn valves, connect a hose, use power tools, drive a vehicle, clear debris and climb a stair ladder (Carnegie Mellon University, 2015). CHIMP has been designed to take part in the DARPA Robotics Challenge in June 2015. One of its competitors is Momaro, developed at Bonn University in Germany, shown in Figure 3 (University of Bonn, 2015). Commercial funding for the development of USAR robots is low and hence research institutions are crucial in driving forward technology development.

Figure 3 – Momaro (left) and CHIMP (right)

3.2 Warwick Mobile Robotics

Warwick Mobile Robotics (WMR) is an on-going group research project carried out by a team of fourth year MEng students at The University of Warwick. This project is jointly run by the School of Engineering and Warwick Manufacturing Group (WMG) and has been designing and manufacturing USAR robots since 2008. Between 2008 and 2013 the team developed a large USAR robot, the evolution of which is shown in Figure 4.

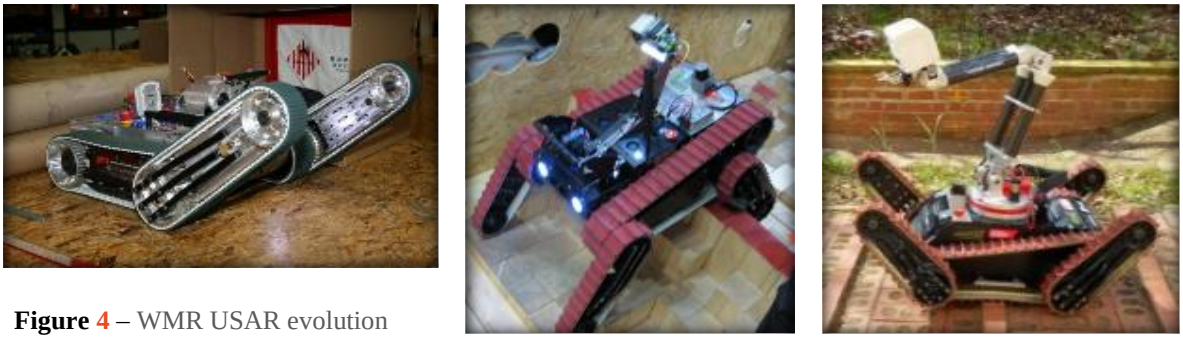

Figure 4 – WMR USAR evolution

The strengths and weaknesses of the large USAR are listed in Table 1.

Table 1 – Large USAR strengths and weaknesses

Strengths	Weaknesses
+ Strong manipulator	- Very Bespoke
+ Mobile	- Difficult to diagnose and repair faults
+ Wide range of sensors	- Unreliable drivetrain
	- Heavy
	- Large and Unwieldy

Noting the extensive disadvantages of the large USAR robot, the 2013/14 team chose to design an M-USAR robot, seen in Figure 5.

Figure 5 - 2013/14 M-USAR design and progress by project completion

The 2013/14 design successfully considered the reduction in size and weight of the robot and incorporated an innovative drivetrain system; however there were several fundamental design flaws which were highlighted in discussions with the NIST (National Institute of Standards and Technology) at the 2014 RoboCup competition (WMR, 2014). These faults were confirmed through the completion of benchmark testing, outlined in Section 3.4.

3.3 RoboCup Competition

The RoboCup Rescue competition is an event where USAR robots compete to compare their overall performance and '*evaluate best-in-class robotic solutions*' (Robocup, 2015). International teams operate in a simulated disaster area where they must search and locate survivors - points are awarded for each survivor found, as well for other disciplines including manipulation and mapping. The RoboCup competition is a good platform for the development of USAR robots and WMR have participated in previous years. Quince, the Japanese USAR mentioned in Section 3.1, has competed multiple times (RoboCup, 2013).

3.4 Benchmarking of Current WMR M-USAR

Part of the 2014/15 strategy was to assess and benchmark the 2013/14 M-USAR robot, analysing its capabilities and design, in order to improve upon results. The faults found were used to inform the specification for the new 2014/15 robot.

3.4.1 Tests

The 2013/14 M-USAR robot was unfortunately not in a position to be tested as thoroughly as intended, as it was largely dysfunctional. The following tests that could be conducted highlighted key areas for improvement, and a list of additional tests can be found Appendix B.

3.4.2 Battery Change and Critical Component Access

In the event of an issue with the lithium polymer (Li-Po) battery it may be safety-critical to be able to remove the battery from the robot swiftly. To permit this, and ensure ease of use, the chassis and shell need to allow a method of quickly accessing and removing the battery. The battery change time can be defined as the time taken to disassemble the robot, remove the current battery, replace it with a new battery and reassemble the robot for continued use.

The USAR robot had a battery change time of 20 seconds – using an access panel which easily opened on a hinge, giving access directly to the battery. The battery itself was housed in a rapid prototype case - removed via a small handle, as shown in Figure 6.

In comparison the 2013/14 M-USAR robot had a battery change time of 6 minutes and 54 seconds, with the main contributor to this time being the removal and replacement of 12 small bolts. A similar problem was found with accessing the computer. From these tests it was evident that access panels and a battery case should be used to allow quick battery changes (maximum of 30 seconds) and easy access to internal components.

Figure 6 – Battery change on large USAR

3.4.3 Chassis Clearance

As a benchmark test the robot was placed on a 90° corner kerb of height 100mm - a test which highlighted major issues with the chassis. Whilst climbing the kerb the two areas most likely to beach the robot were the front lower and underside areas of the chassis, as circled in Figure 7. This could lead to damage or catastrophic failure if attempted at high speeds. The clearance could be improved by chamfering the front and rear of the chassis and by raising the underside further above the ground. This method had been used successfully on the large USAR robot, and as such was considered in the 2014/15 design.

Figure 7 – Kerb climb test on 2013/14 robot

3.4.4 Benchmarking Conclusions

Table 2 summarises the strengths and weaknesses of the 2013/14 M-USAR robot which were used to define the new 2014/15 specification.

Table 2 – Strengths and weaknesses for WMR's 2013/14 M-USAR robot

Strengths	Weaknesses
+ Weight < 25kg (deployable by 1 person)	- Long battery change time
+ Strong Makerbeam® chassis	- Difficult to access internal components
+ Small size	- Poor chassis clearance, and external strength
+ Uses off-the-shelf components	- No method of cooling
	- Exposed Motors and wiring through moving components
	- Inadequate battery management
	- Brushed motors
	- Overly complicated and poor provision for electronics

4 SPECIFICATION

The specification was informed by testing and benchmarking of the previous robots developed by WMR, as mentioned in Section 3.4. Values have been extracted from the RoboCup rules, building regulations and real world obstacles; these are listed in Table 3.

Table 3 – 2014/15 Specification M-USAR Robot

ID	Parameter	Value / Description	Expected Achievement
1	Accessibility		
1.1	Accessible Hatch Design	30 Seconds for a Battery Change	May 2015
1.2	Deploy integrated USB access	Combine connections into a single USB Port hub	May 2015
2	Clearance		
2.1	High Track Radius	Climb stairs with a step height of 190mm at an angle of 38°	May 2015
2.2	Low possibility of beaching	Minimum clearance of 100mm	May 2015
3	Dimensions		
3.1	Capable of turning within a standard door width	Length < 580.0 mm, Width < 410.0 mm, Height < 350.0 mm	May 2015
3.2	Validate internal volume with calculations of cooling needs	Volume minimum of 3.9×10^{-3} m^3	May 2015
3.3	Fan cool with ventilation	Minimum Flow rate of 0.0052 m^3s^{-1}	May 2015

4	Weight		
4.1	Deployable by one person	Maximum weight of 25kg	May 2015
4.2	Low lying centre of gravity	Centre of Gravity acts within the base on a 38° incline slope	May 2015
5	Durability		
5.1	Vulnerable components inside chassis	Survive a 350mm drop impact	May 2016
5.2	No cable connections through moving parts	Stationary, fixed internal connections	May 2015
6	Drive		
6.1	Provide traction on both solid and permeable terrain	Mud, hard floor, sand, wood, surface water etc.	May 2016
6.2	Simple track design for high contact area and grip	Monolithic, rubber based tracks	May 2015
6.3	Emphasis on controlled positioning	Accelerate at 0.3 m/s^2 Standard operation at 1m/s	May 2015
6.4	Return to base when upside down	Chassis within tracks	May 2015
6.5	Sufficient Torque to Climb Stairs	Minimum Torque of 20N/m	May 2015
7	Electronics		
7.1	Provision for Development	Modular Architecture and additional ports	May 2015
7.2	Capable of full tele-operated control when out of sight	Range of Speeds, standard operation at 1m/s	May 2015
8	Sensory Array Design		
8.1	Map position	Utilise LiDAR Technology	May 2016
8.2	Sense heat from targets	Incorporate an IR Camera	May 2016
8.3	Sense CO_2 from targets	Incorporate a CO_2 Sensor	May 2016
8.4	Intuitive operation	Incorporate Stereoscopic Cameras	May 2016

4.1 Justification

In this section the parameters affecting the overall design of the robot (listed in Table 3) are justified.

4.1.1 Dimensions

The external robot dimensions are based on NHBC (National House Building Council) building regulations - whereby the robot must be able to pass through and rotate inside a standard hallway (NHBC, 2014). See Appendix C for further explanation.

4.1.2 Weight

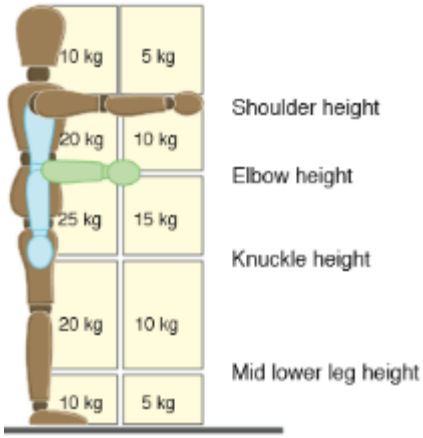

Figure 8 – Manual handling weight restrictions

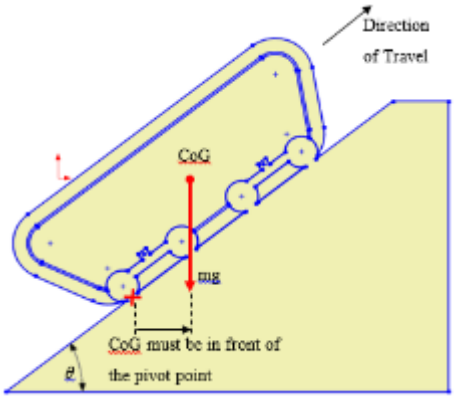

Figure 9 – Schematic used for analysis of robot design stability

The robot should be light enough such that it can be lifted and deployed by a single person. The Manual Handling Operations Regulation (1992) published by the Health and Safety Executive (HSE) recommends that the maximum weight, to be lifted to knuckle height by a male, should be no more than 25kg (NHBC, 2014) as outlined in Figure 8. Figure 9 shows how a tracked vehicle must be designed for the centre of gravity to act through the base of the robot on a 38˚ slope. A full analysis of the implications of this, with moment and force calculations, can be found in Appendix C.

5 DESIGN

5.1 Methodology

The project was split into two parallel streams: mechanical and electronics. Within each stream, individuals or sub-teams took responsibility for separate components or systems. Frequent communications of design intention were shared between all individuals and sub-teams during design to ensure integrated capability between all features and a ‘Total Design’ approach. This created multiple cross-discipline teams who worked together to generate concepts, develop and validate these designs and devise a final design in which all components were fully compatible with one another.

In all cases, design concepts were developed from benchmarking of other robots alongside broader limiting factors, such as space restrictions, power limitations, sponsorship

commitments etc. Subsequently, the concepts were developed to take account of further research, specification refinement and input from other members of the team and workshop technicians. Following this, designs were validated with other sub-teams to check compatibility and with technicians to ensure feasibility of manufacture. A final design was then created from this validation before being forwarded for manufacture and assembly. Figure 10 details the map of the design process. Finally it was decided that the new 2014/15 USAR robot should be named - with 'Orion' selected as a suitable title.

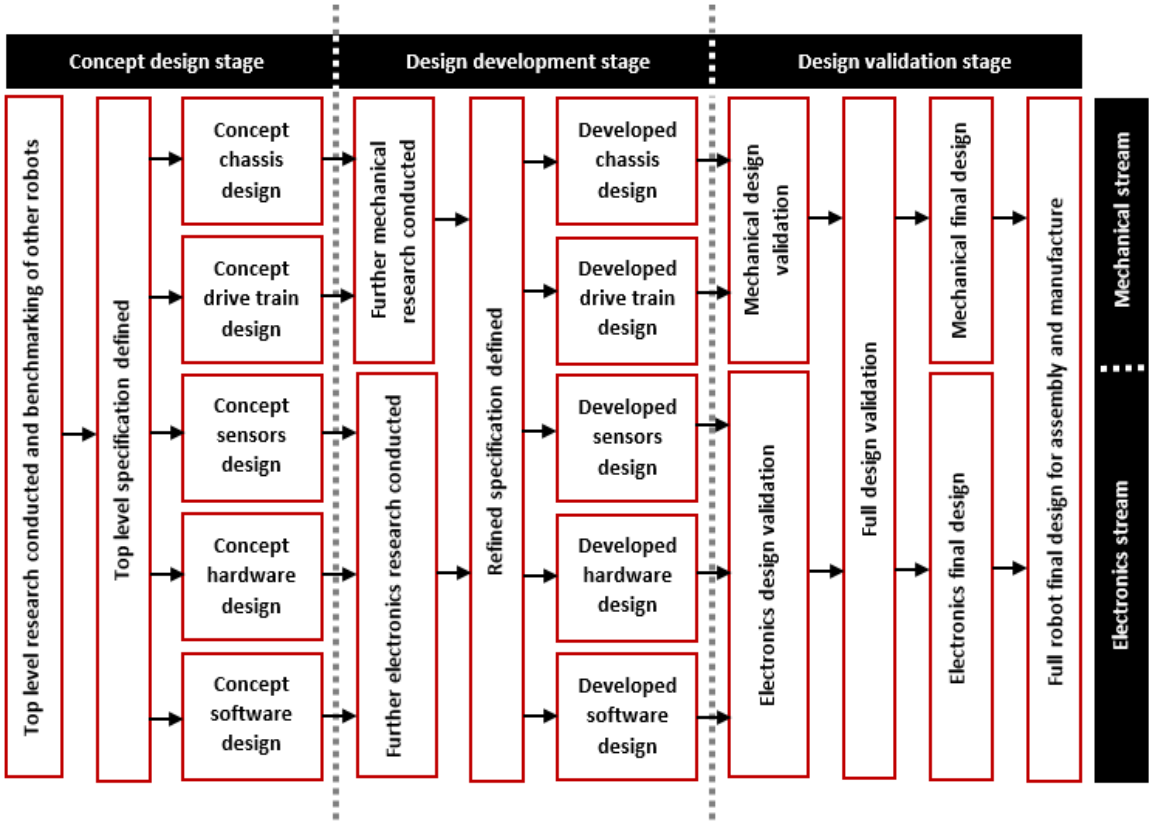

Figure 10 – Design methodology map

5.2 Chassis and Shell

5.2.1 Literature Review

USAR robots work in harsh and demanding environments and hence there is a high risk of damage (Hudock, 2003). Internal components are vulnerable to impact, cyclic loading, liquids and heat (Gunderson, 2009). For this reason, USAR chassis design often incorporates robust structures with a durable and resistant outer lining (shell) (Buckstone, et al., 2013). Chassis shape and design with respect to strength and heat distribution, internal volume, mobility and integration with drivetrain are important factors in design. Another critical consideration is material choice.

Steel and aluminium are often the material choices for chassis for their desirable properties, despite their relatively high cost (Milliken, 2002). Aluminium is favourable as it is both strong and lightweight, with a higher strength-to-weight ratio than stainless steel, it provides an excellent basis for robot chassis design. Stainless Steel, a relatively resilient metal, is more susceptible to cracking than Aluminium under working.

Once primary requirements of strength properties have been satisfied, research and lessons learned from previous WMR reports suggest ease of manufacture was a critical factor in success (Chavasse, et al., 2014). For this reason, Makerbeam® was highlighted as a strong contender, with its extruded aluminium products offering desirable mechanical properties, ease of manufacture and versatility in design.

Design and manufacture projects such as WMR, highlight the fact that integrating concept design and assembly presents a challenge – with joining and fastening methods between components a prime example. The key aim for fastenings is to provide a rigid connection between components and members while minimising stress concentrations (Chetwynd, 1992). Available options included mechanical fastenings and welding. Nuts and bolts are easy to assemble and non-toxic (unlike some adhesives), and readily available in standardised sizes. Stress concentrations are an issue, as well as corrosion between materials and access requirements in manufacture. Nuts and bolts have, however, proved to be sufficient in robot construction, whilst welding may add an extra dimension of durability (Ashby, 2005).

5.2.2 Specification Parameter Development

The following section details how the chassis specification was developed. For the full chassis specification, see Appendix D1.

4.2.2.1 Chassis Dimensions and Mass Parameters

The external dimensions of the robot were based on NHBC building regulations for doors and hallways. This equated to a maximum robot length, width and height of 580.0mm, 410.0mm and 350.0mm respectively. To ensure the robot remained within these limits, the chassis was to be no more than 90% of these values with a length, width and height of 522.0mm, 369.0mm and 315.0mm respectively.

The robot needed to house a range of electrical and mechanical components. Measurement of desired internal components determined an internal volume of at least 3.9×10^{-3} m^3, but excess space was desirable for cooling and space for development. For a full table of internal component volumes, see Appendix D2.

In the benchmarking tests in Section 3.4, it was highlighted that the front lower and underside areas of the chassis were likely to beach the robot. The clearance could be improved, as depicted in Figure 11, by chamfering the front and rear of the chassis, raising the underside away from the ground and increasing track radius. These changes did, however, come at the cost of some internal chassis volume loss and a higher Centre of Gravity (CoG).

Figure 11 – Chassis clearance improvement

An optimal robot CoG would be achieved by evenly distributing chassis and shell mass across the length of the robot. Mass should also be kept as low as possible and the chassis and shell CoG must be in front of the pivot point as detailed in Figure 10 in Section 4.1.2.

To ensure the robot meets a target weight of 25kg, the chassis should be lightweight, with an ideal weight no more than 20% of the overall robot mass (5kg).

4.2.2.2 Chassis Strength, Accessibility and Design Parameters

According to building regulations, if the robot were to fall off a staircase two steps up it would drop 350mm (NHBC, 2014). The chassis must withstand a fall from this height without damage.

If the robot drives at maximum speed head-on into a solid object it should still be fully operational with no visible damage to any of the shell or chassis. The chosen motor, a Maxon Motor EC-4 Pole 22 (323217) has a maximum speed of 16300 rpm, outputted at 133 rpm after the gearhead. This equates to a forward robot speed of 0.76 ms^{-1}. Adding a factor of safety, the considered forward speed is 1.0 ms^{-1}. Newton's 2nd Law and equations of motion were used to calculate the force in a fall or crash under the above conditions. For full derivations and application of these equations, see Appendix D3. As detailed in Table 4, the chassis must withstand a fall force of 650N and a crash force of 250N.

Table 4 – Fall resistance parameters

Parameter	Notation	Fall Resistance Values	Crash Resistance Values
Gravity	***g***	9.81 ms^{-2}	9.81 ms^{-2}
Acceleration During Impact	***a***	- 26.20 ms^{-2}	- 10.00 ms^{-2}
Robot Mass (Estimated)	***m***	25.0 kg	25.0 kg
Time of Impact	***t***	0.1 s	0.1 s
Distance of fall	***s***	0.35 m	N/A
Velocity at Impact	***v***	2.62 ms^{-1}	N/A
Force of Crash or Fall	***F***	655 N	250 N

In the event of a problem with the lithium polymer (Li-Po) battery, it may be safety critical to be able to remove the battery from the robot quickly. Access panels and a battery case should be included to allow quick battery changes (maximum of 30 seconds) and easy access to internal components, as shown in the benchmarking Section 3.4.2.

Standardised off-the-shelf parts should be used where possible in order that replacement parts are easy to source; hence facilitating damage repair. Where off-the-shelf components are not available, parts should be machined from easy to source material using basic machinery (lathe, mill, pillar drill, etc.). A flexible design should allow extra mounting points to be added as required.

5.2.3 Material Consideration

As discussed in the literature review, material choice is critical in determining the performance of USARs. Materials considered included 300 series stainless steel and 2000 and 6000 series aluminium alloys. For a comprehensive comparative review of these materials see Appendix D4. From research and reasoning demonstrated in the literature review, extruded 6000 series aluminium from MakerBeam®, available in pre-cut lengths, was deemed a versatile, desirable material choice. Testing and simulations in the following sections validate this selection.

5.2.4 Testing

The chassis needed to be lightweight and strong enough to withstand a drop impact of 655 N and a crash impact of 250 N. To determine the resistance to impact and crash forces, a specimen of each of the materials was subjected to a bending test. Each specimen (150 x 10 x 10 mm) was subjected to a central point load, which was increased until plastic deformation occurred.

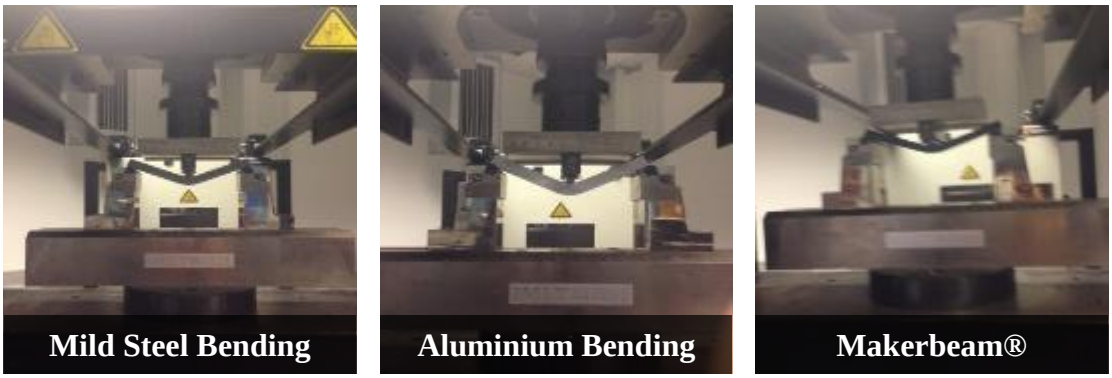

Figure 12 – Bending tests on mild steel, aluminium and MakerBeam®

The load vs. extension relationship for the 3 materials is displayed in Graph 1. Mild steel could withstand the highest load before undergoing plastic deformation. MakerBeam® however was able to withstand approximately 1000 N of load before beginning plastic deformation: a load 1.5 times what it would experience during a 350mm high drop.

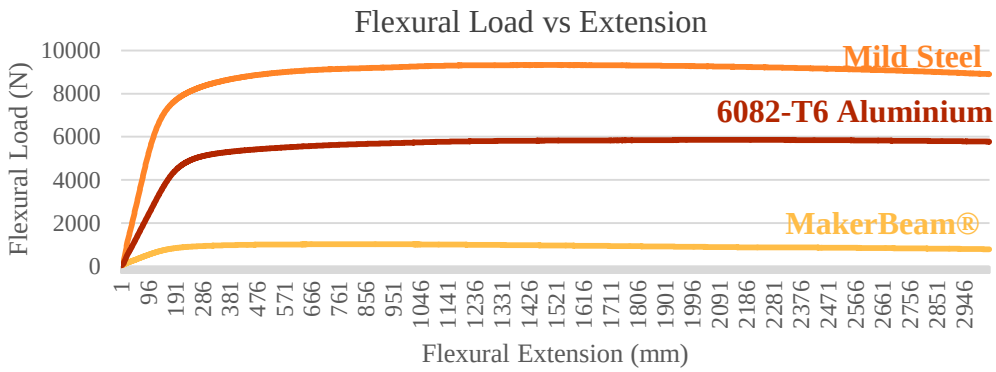

Graph 1 – Load vs. Extension for the 3 considered materials

These tests were confirmed through SolidWorks simulations. The results, pictured in Figure 13, show that MakerBeam® experienced a displacement of 0.32mm when subjected to a 500 N load. This is comparable to the extensions plotted from the physical bending test seen in Figure 12.

From these material tests it was found that mild steel offered the best strength, followed by 6082-T6 aluminium, and then MakerBeam®. However, MakerBeam® is proficient for WMR's specification with a 150% safety margin. For the brackets, 6082-T6 aluminium was used in order to keep the mass of the chassis low whilst maintaining desirable material properties. For future testing and simulations, it was a promising result that simulation and test results correlated closely.

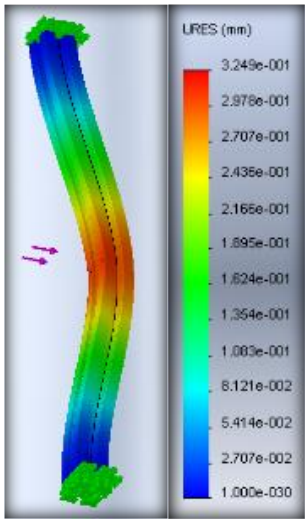

Figure 13 – Validation bending test in SolidWorks

5.2.5 Design Iterations

The chassis design underwent four major iterations following the concept design, identified as V1, V2, V3 and V4. Each of these chassis iterations was modelled in SolidWorks 2014.

The initial design, V1, looked to maximise the internal volume whilst creating a shape with good ground clearance. A large central rectangle was used to provide an area of usable internal volume which extended to within the track profile. Symmetrical front and rear nosecones were added from which to mount the drive pulleys, leaving a raised area of chassis for added clearance. Cutaways added to improve clearance are highlighted in red in Figure 14.

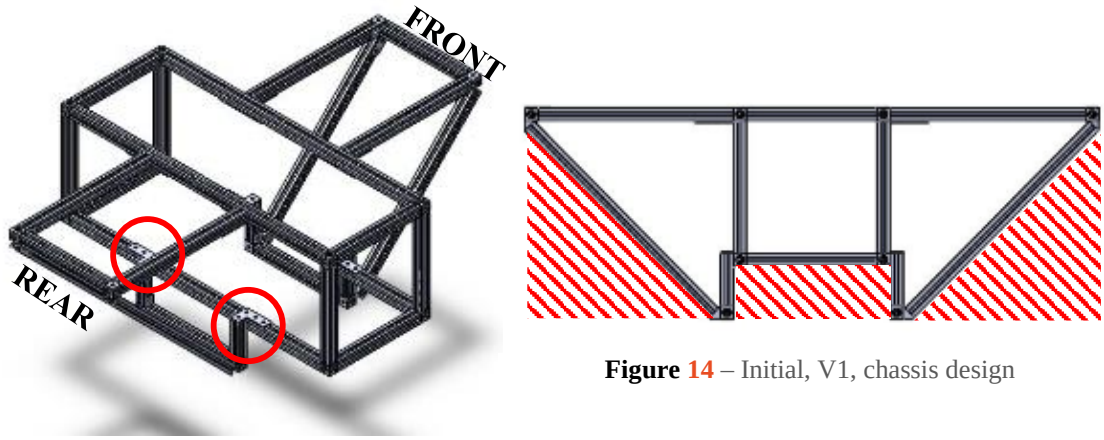

Figure 14 – Initial, V1, chassis design

The major disadvantage of chassis V1 was the low internal volume. To improve this, the central rectangle was extended to create chassis V2. The connections between the nosecones and the central rectangle were also weak (highlighted in Figure 14), and hence these were strengthened as part of the design changes.

The 2nd design iteration, V2, extended the space at the top of the central rectangle, increasing the internal volume. The side profile remained similar to that of chassis V1, offering large cutaway areas for improved clearance. The connection to the nosecones employed more fasteners and brackets, increasing the join strength.

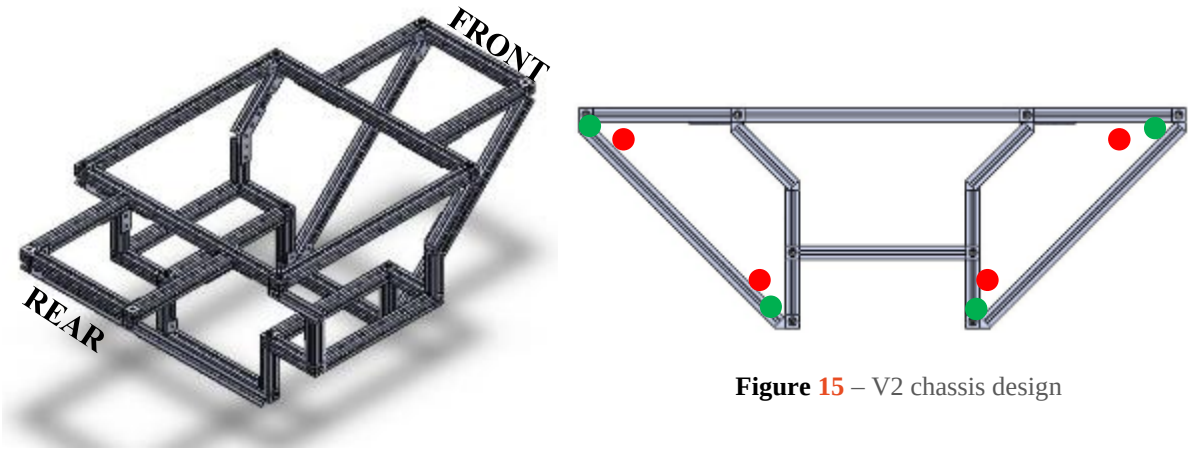

Figure 15 – V2 chassis design

The major disadvantage of chassis V2 was the space available for the track pulleys and axles in the corners of the nosecones. As the outer edges of the nosecones had acute internal angles, the axles couldn't be placed towards the edge of the chassis. This resulted in wasted space in the corners, as depicted in Figure 15 (green circles indicate ideal axle location, red circles indicate actual axle locations due to space constraints). The close horizontal proximity of the lower axles also put the robot in danger of flipping when on an incline due to CoG effects.

Chassis V3 addressed the issue of wasted space in the chassis by opening up the acute internal angles in the chassis. More space was also allowed for the track pulleys and the spacing between the lower axles was increased to help prevent the robot from flipping when on an incline.

The complexity of this design was its major drawback, however, it addressed all the key specification points relating to the chassis shape. It offered good clearance with the chamfered front and rear nosecones and raised central section alongside an adequate internal volume and minimised wasted space. As far as practically possible, standard lengths of MakerBeam® were used to reduce machining required during chassis assembly.

At this stage of the design development, the track system altered to use two large pulleys at the top corners and four small pulleys on a suspension system along the bottom (on each side) as opposed to a large pulley in each corner. The original (red) and revised (green) pulley locations and approximate sizes are depicted in Figure 16. With the new track and suspension system design, the complex shape of the chassis was no longer required and could be streamlined.

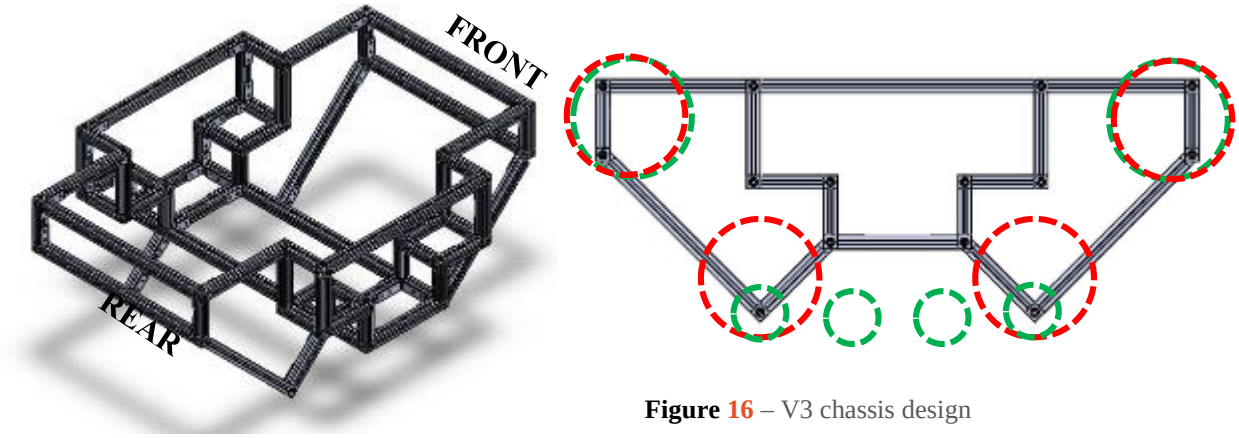

Figure 16 – V3 chassis design

The 4th design iteration, V4, effectively removed the bottom third of chassis V3. All angled components were removed except for the chamfered clearance edges at the front and rear. As the chassis was now supported on a raised suspension system, the clearance underneath the chassis was more than adequate. The simplicity of the design was improved for chassis V4 and as many beams as possible were modelled from standard parts available from MakerBeam® to reduce the use of custom machined parts; only 4 beams were non-standard. V4 is shown in Figure 17.

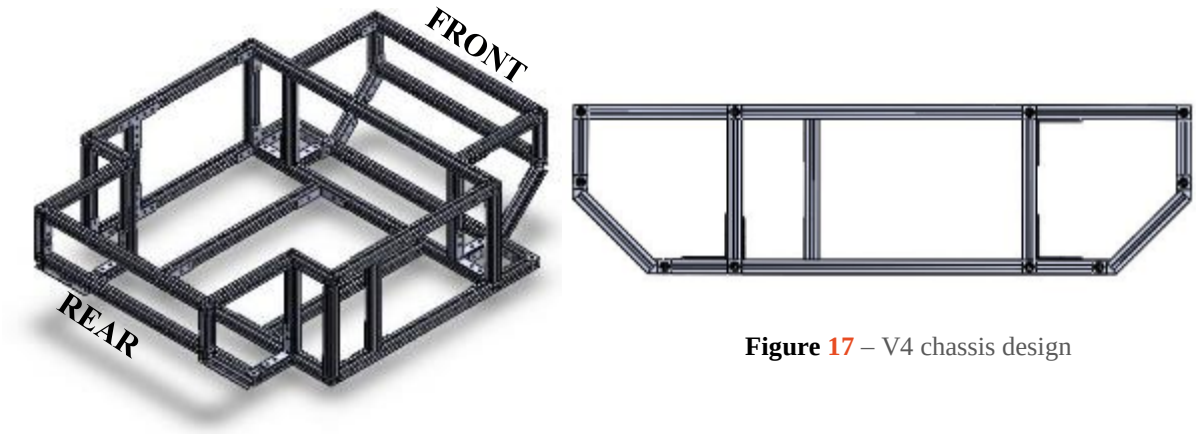

Figure 17 – V4 chassis design

The change in internal chassis volume and external chassis dimensions during development can be seen in Graph 3. At all times the external dimensions were within the 460mm length, 320mm width, 242.5mm height restrictions set by the specification. The ratio of internal volume to length x width x height (LWH) demonstrates how effectively the chassis shape makes use of the cuboid space envelope it occupies. A higher ratio is indicative of a more efficient design. As can be seen in Graph 2, when the chassis design was streamlined in V4, it vastly improved its use of the space available.

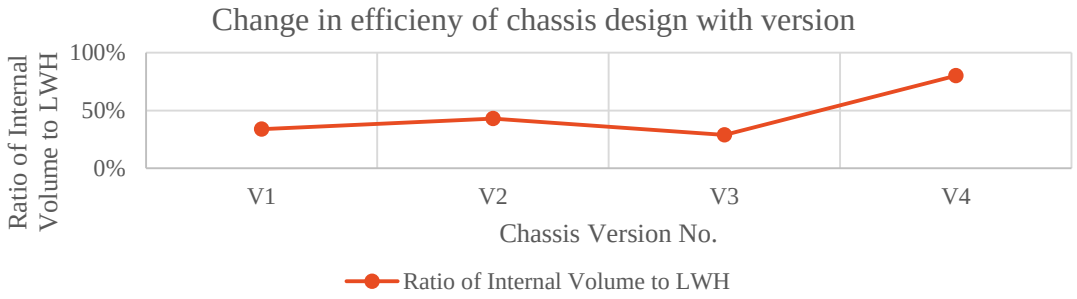

Graph 2 – Development of efficiency of chassis design

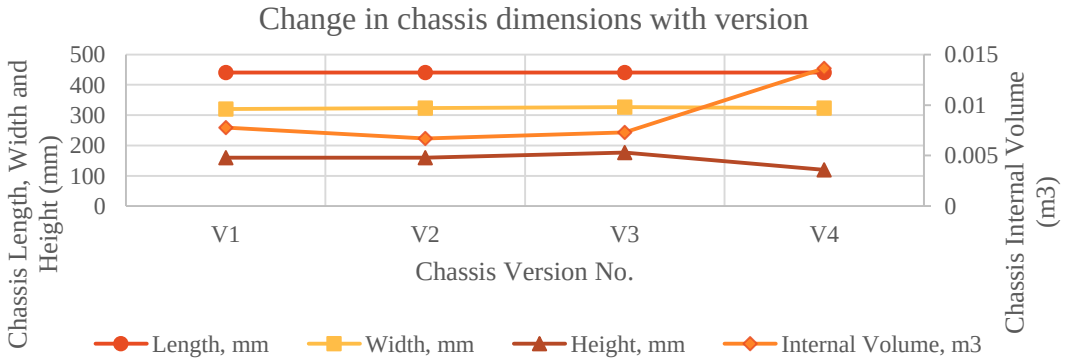

Graph 3 – Development of chassis external dimensions and internal volume

The shell was designed around the chassis V4 design and consisted of 17, 2mm thick aluminium plates and one 10mm thick base plate which bolted directly to the MakerBeam® chassis. Aluminium was chosen for being lightweight and offering excellent thermal conductivity properties, allowing the shell to act as a heat sink to the internal components.

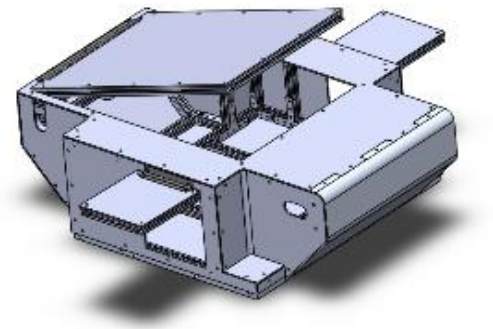

Figure 18 – Final design with open access panels

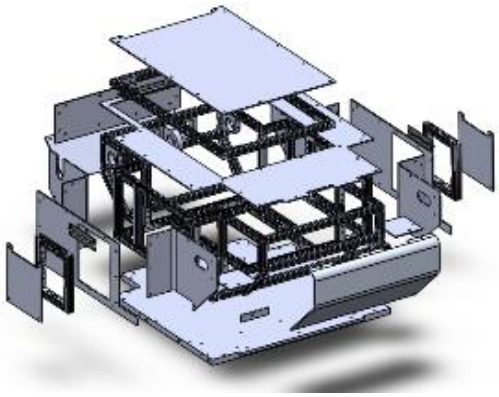

Figure 19 – Exploded view of chassis and shell

Shell design incorporated three access panels for quick access to internal components. Two small panels were located on the side of the robot (giving access to the battery and Pico ITX computer) and a large panel was located on top (giving access to the drivetrain system, power board, motor controllers, wireless router and Arduino) as shown in Figure 18 and Figure 19.

5.2.6 Simulations

4.2.6.1 Fall Resistance Simulation

The fall resistance of the chassis was simulated in SolidWorks using a buckling analysis. As per the chassis specification, the chassis model was subjected to a vertical impact force of 655N, applied at four locations to simulate suspension mounting points (orange arrows in Figure 20). The chassis was fixed at the centre to restrain the model (green arrows). The model was meshed to a high quality using approximately 128,500 7.2 mm elements.

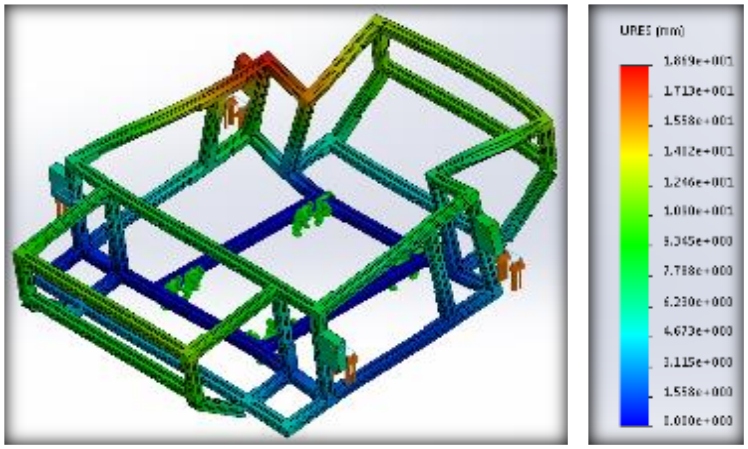

Figure 20 – Fall resistance SolidWorks simulation

Areas of highest deformation are signified by red colouring with blue being low deflection. The most deformation occurred by the rear suspension points, where cross bracing is at its lowest, reaching a maximum of 18.7 mm, still within the region of elastic deformation as determined in bending tests. Critically, the bending load factor (factor of safety) was -70.4, indicating the loads would not buckle the MakerBeam® in the chassis even if they were reversed. A buckling load factor of greater than 1 or less than -1 indicates that buckling was not predicted by the simulation. Once further brackets for the drivetrain system and internal components were mounted, coupled with the shell, the chassis stiffness was increased further, acting to improve the bending load factor. This also prevented the rear of the chassis from bending in as significantly during a drop impact.

4.2.6.2 Crash Resistance Simulation

The crash resistance of the chassis was also simulated in SolidWorks using a buckling analysis. Again from the specification, the chassis model was subjected to a forward impact force of 250N, applied uniformly across the front face of the nosecone (purple arrows in Figure 21). The chassis was fixed at the rear to restrain the model (green arrows). The model was meshed to a high quality using approximately 129,000, 7.2 mm elements. As could be expected, highest deformation occurs around the point of impact: reaching a maximum of 32.7 mm, still within MakerBeam®'s region of elastic deformation. Critically, the bending load factor (factor of safety) was 41.4, indicating load on the MakerBeam® in the chassis was well below the critical load so would not buckle. As with the fall resistance simulation, extra brackets and the shell stiffened the chassis acting to improve the bending load factor. This also reduced the chassis twist during a crash impact.

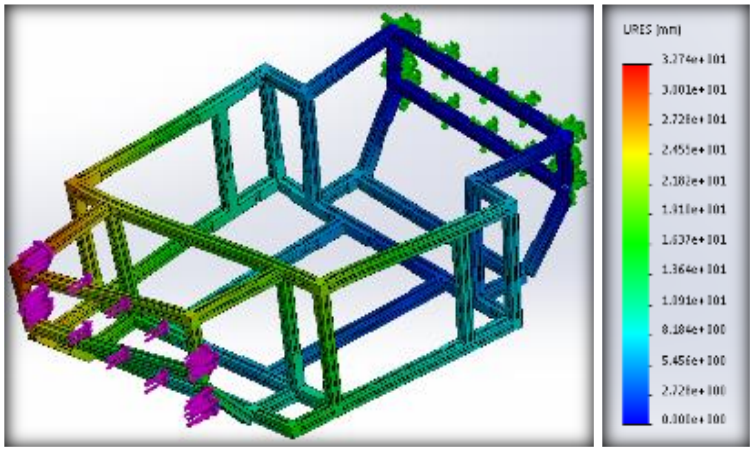

Figure 21 – Crash resistance SolidWorks simulation

4.2.6.3 Centre of Gravity Location Simulation

Using SolidWorks' mass properties function, the CoG of the chassis and shell assembly was found to be in front of the estimated location of the rear pivot point when on a slope of 38°. A pictorial representation of this is shown in Figure 22.

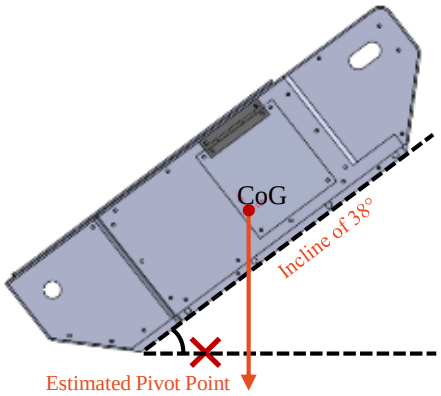

Figure 22 – Centre of gravity location of chassis and shell

5.2.7 Final Chassis and Shell Design

CAD models of the final designs for the chassis and shell are seen in Figure 23.

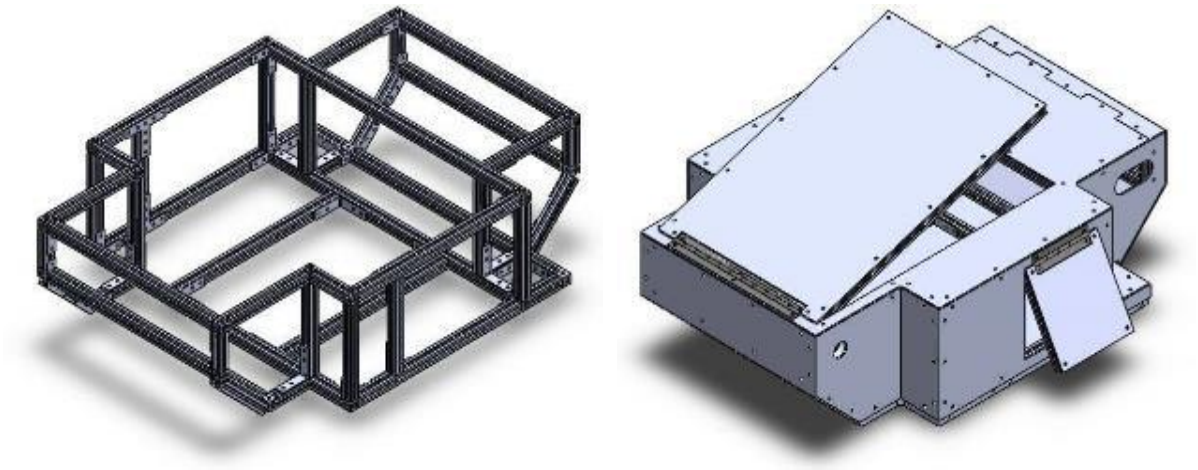

Figure 23 – Final shell and chassis design

5.2.8 Justification and Evaluation of Design

To validate the chassis and shell, the design was compared to the relevant specification points (fully defined in Appendix D1) – a comparison shown in Table 5. The only parameter to not meet the specification was the chassis and shell mass, being 0.57 kg heavier than desired. This was caused by a heavy base plate added in order to protect the underside of the robot and lower the centre of gravity. A mass 11% greater than intended was decided to be acceptable as the mass of the drivetrain system was able to be kept under the specified limit, counteracting the extra mass in the chassis and shell.

Table 5 – Evaluation of chassis and shell design against relevant specification

Criterion	Achieved Results	Status
Chassis length – maximum 522.0 mm	Chassis length - 454.0 mm	✓
Chassis width – maximum 369.0 mm	Chassis width - 331.0 mm	✓
Chassis height – maximum 315.0 mm	Chassis height - 135.0 mm	✓
Internal chassis volume – minimum 3.9 x 10^{-3} m^3	Internal volume - 13.61 x10^{-3} m^3	✓
Clearance over obstacles – chamfered front and rear and underside must be as high off the ground as practically possible	Front and rear of underside must be chamfered or curved and underside should be as high as practically possible above the ground	✓
CoG must lie in front of the pivot point and be equally spread front to back along the chassis	CoG in front of pivot point and central in the chassis	✓
Chassis and shell mass – maximum 5.0 kg	Chassis and shell mass - 5.57 kg	✗
A fall from 350.0 mm must not damage chassis	Chassis does not buckle when experiencing fall	✓
A crash into an immovable object at 1.0 ms^{-1} must not damage chassis	Chassis does not buckle when experiencing crash	✓
Battery must be able to be accessed quickly	A small side access panel in the shell allows quick battery access	✓
Access to internal components should be quick and easy	A small side access panel and top large access panel in the shell allows quick and easy access to internal components	✓
Chassis should be easy to assemble and fix in the case that some components get damaged	MakerBeam® allows relatively easy assembly and repair of the chassis	✓
Chassis design should be modular and flexible	MakerBeam® facilitates a flexible and modular design	✓

5.3 Drivetrain

5.3.1 Literature Review

Drivetrain is considered to be made up of three main areas: Steering, Suspension, & Tracks.

4.3.1.1 Steering

A clear and accessible evaluation of the major tracked vehicle steering systems may be found in (McGuigan & Moss, 1998). A more rigorous, mathematical analysis of steering methods for tracked vehicles is provided by (Wong, 1993) wherein the author investigates the kinetics and kinematics of skid steering amongst other areas, as well as mathematical modelling of various transmission mechanisms. This is useful knowledge for designing a new system.

4.3.1.2 Suspension

An interesting project from (DARPA, 2012) introduced a modified Remote Controlled (RC) tracked robot, '*equipped with an advanced suspension system*'. Inspection of the accompanying documentation and video footage showed considerable improvement in transit over rough terrain from a relatively simple suspension design – achievable within the project timeframe. Another vehicle investigated was the Ripsaw UGV from Howe & Howe Technologies– the world's fastest unmanned track-layer (Defense Update, 2009) – which is also renowned as one of the most rugged off-road vehicles in existence (see Figure 24). The Ripsaw, although much larger, incorporated suspension not dissimilar to that of the DARPA robot – indicating that this might be a possible root for the USAR's suspension system to follow.

Figure 24 – The Ripsaw UGV

4.3.1.3 Tracks

Investigations were carried out into various possibilities for track designs for the USAR, with one piece by (RCTanks, 2008) proving particularly informative – providing a large number of possibilities for constructing tracks, which can be seen in Appendix E1. For in-depth information into rubber composite tracks as used on previous WMR robots, the team consulted closely with Transdev (a UK-based timing belt company who supplied the tracks for the previous large USAR robot) – gaining valuable insight into materials, tread profile and tread spacing.

5.3.2 Specification Parameters & Development

Unless otherwise specified, the development of the design parameters listed in Table 6 has been explained in Section 4.1.

Table 6 – Drivetrain specification

Criterion	Specification
Maximum Mass – 25kg	▪ Drivetrain to take up a maximum of 60% of overall mass: i.e. 15kg
External Dimension Restrictions	▪ Maximum dimensions - Length < 460mm, Width < 320mm, Height < 242.5mm
High Clearance	▪ High track radius required to enable stairs of step height 190mm and incline of 38° to be climbed
High Traction	▪ This parameter stemmed from the goal of producing a multi-terrain robot – able to provide traction in various conditions: i.e. travelling on mud, hard floor, sand, surface water etc.
Drive Requirements	▪ Invertible: arising from the goal of being able to still operate if the robot is turned over ▪ Able to achieve a range of speeds, with standard operation at 1m/s – approximating average walking speed to avoid possible injury to survivors if an accidental collision were to occur ▪ Able to accelerate at 0.3 m/s² up a 38° slope – reduced from the previous year's design specification of 1m/s² up a 45° slope as this was decided to be unnecessarily rapid – requiring overpowered motors which would have to operate well below their rating for the majority of the time
Durability	▪ Able to survive a 350mm drop impact

5.3.3 Steering

The only widely-utilised method of tracked vehicle steering is that of 'skid-steering', whereby the tracks are allowed to move at disparate speeds – hence forming the basis for steering. The main methods considered for achieving this form of steering included: Dual drive, Clutch Break and Double Differential; for an explanation of the latter two see Appendix E2.

4.3.3.1 Dual Drive

Dual drive was one of the first solutions for tracked vehicle steering - employed on several WW1 tanks - and as the name suggests, two motors are used, each powering a separate track as shown in Figure 25. The advantages and disadvantages of the design are listed in Table 7.

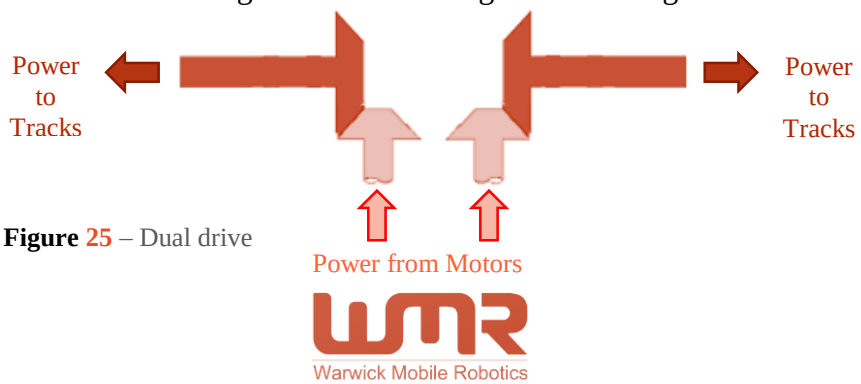

Figure 25 – Dual drive

Table 7 – Dual drive: advantages and disadvantages

Advantages	Disadvantages
+ Simplicity of design	- Can be difficult to supply same power to each track
+ Inexpensive	- Each track is unlikely to experience the same drag – hence potentially causing steering issues (negligible at low speed)
+ Allows true neutral turn	- If one motor does fail then robot practically immobilised
+ Commonly used on RC, tracked vehicles and successfully employed in previous WMR robots	
+ Reliability increased by low complexity & minimal components	

Dual Drive was ultimately selected, upon comparison with the other major mechanisms, as it was deemed the most suitable and most achievable design, given the temporal and monetary constraints inherent in the project.

5.3.4 Motors

At a glance the GR02 motors selected by the previous WMR team appeared to offer a great deal of mechanical power whilst also running at extremely high speed. Upon closer inspection, however, stall torque values rather than nominal values had been used when calculating the required torque and angular velocity outputs – meaning the calculations were out by a factor of 10. Therefore it was decided that new motors should be specified - once the steering system had been decided upon - based on the robot's stated requirements: namely being able to achieve an acceleration of $a = 0.3\text{ms}^2$ up a slope of $\theta = 38°$. The required output torque for each motor to achieve this – given that $g = 9.81\text{ms}^{-2}$, the mass $m = 25\text{kg}$, the wheel radius $R = 0.05\text{m}$, the efficiency $\varepsilon = 0.8$, & the number of motors $N = 2$ is given by:

$$\tau = \frac{(a + g\sin\theta)mR}{\varepsilon N} \approx 4.95\text{Nm} \qquad (5.3.1)$$

The required output angular velocity for a given speed, V is given by, $\omega = V/r$, hence with $V = 0.5\text{m/s}$, and $R = 0.05$,

$$\omega = \frac{0.5}{0.05} = \frac{10rad}{s} = \frac{600rad}{m} \approx 95.5rpm \qquad (5.3.2)$$

In order to avoid damage to the motors they must not be subjected to above ⅓ of the stall torque – hence motors with a minimum stall torque of 25Nm were required; alongside a motor and

gearhead combination producing an output torque of around 5Nm and an output angular velocity of around 95rpm.

Having taken all the aforementioned factors into account, the Maxon, EC-4pole 22 Ø22 mm, brushless, 90 Watt motor was selected in combination with the Maxon Planetary Gearhead GP 32 C Ø32 mm, Ceramic Version.

Table 8 - Table comparing the chosen motors and the previous design's motors

Motor	Gear ratio	Torque (Nm)	Angular Velocity (rpm)	Power (W)
EC-4pole 22 Ø22 mm, brushless, 90 Watt	123:1	6.4	119	91
GR02 DC Planetary Gearmotor	24:1	1.4	700	153

Table 8 shows the nominal values for both the EC-4pole motor and the GR02 motor – highlighting that the electrical power consumption of the GR02 is more than 1.5 times that of the EC motors. In addition, an extra gearing of 7:1 would be required if the GR02 motors were used, in addition to the inbuilt 24:1 gearing, to obtain the desired torque and angular velocity. The Maxon brushless EC-4pole motors were hence chosen – with further advantages including: no cogging torque, high efficiency, and excellent control dynamics.

5.3.5 Internal Layout

Once the motors had been selected, the next stage was to determine their positioning within the chassis, and how the driveshaft would be powered. Figure 26 shows the final drivetrain system with the sprocket-&-chain design, chosen because of the major advantages listed in Table 9.

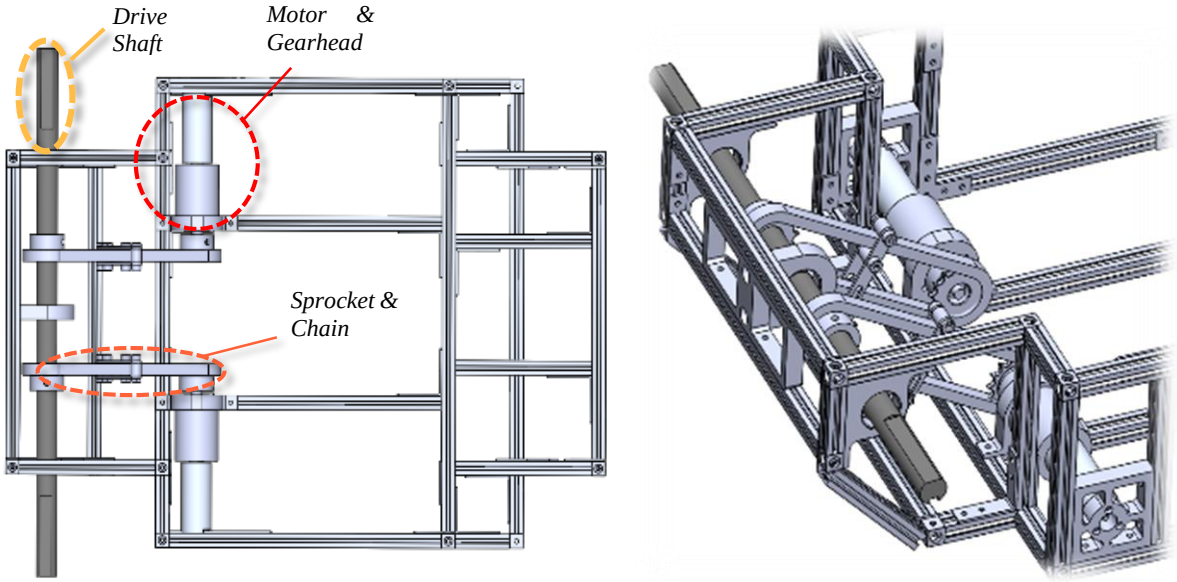

Figure 26 – Internal layout

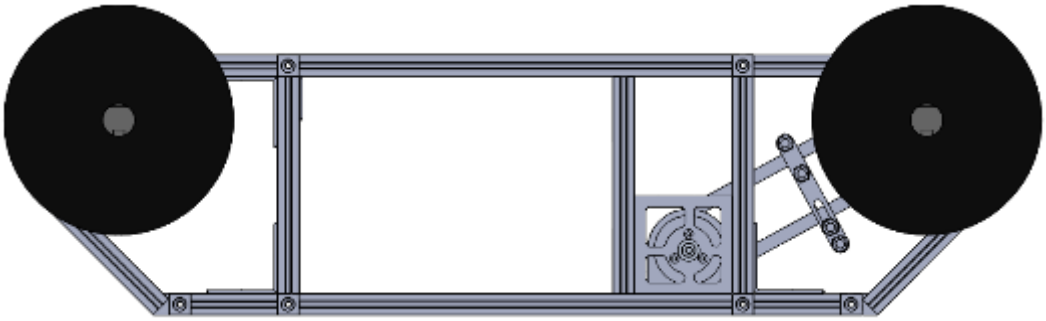

Figure 27 – Pulley positioning

Table 9 – Sprocket and chain drive: advantages and disadvantages

Advantages	Disadvantages
+ Simple design, easy to mount, uses hull space efficiently	- Requires a chain tensioning system
+ Avoids placing motors in close proximity and exacerbating overheating issues	
+ Avoids use of inefficient worm gears and of potentially-complex bevel gears	

Two separate drive shafts are hence driven – supported both centrally by a bracket housing two bearings, and at the hull sides by two further bearing brackets. The question of whether the drive shafts should be located in the front or the rear is less clear-cut for tracked vehicles than for their wheeled counterparts, as the torque is spread along the track as opposed to delivered at the driven cam. It was decided that the robot's drive should located at the rear as this would allow space for a frontal sensory array, as well as the fact that previous WMR robots had

achieved success employing this approach. For standardisation purposes two identical, large cams of 50mm radius were placed on the front and rear, shown in Figure 27, along with several smaller idlers which would form part of a suspension system, were used.

The necessary adjustable chain tensioner was also designed, as seen in Figure 28, as chains tend to lose tension after prolonged use. This comprised of two stationary and two rolling supports – with the position of one of the rolling supports adjustable along the length of its slotted housing – hence allowing tensioning to be achieved.

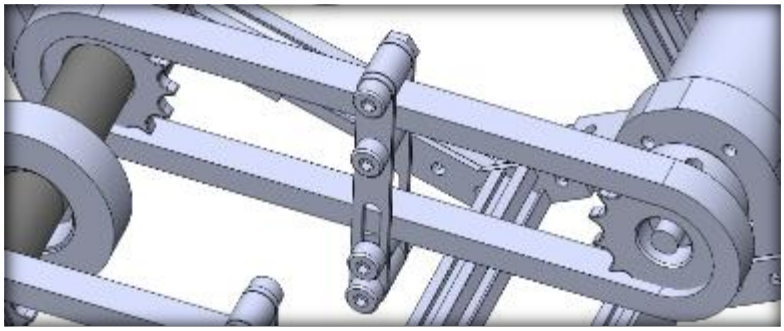

Figure 28 – Chain tensioner

5.3.6 Suspension

A number of designs were considered for the suspension system, which was to incorporate the lower idlers and allow the robot to easier traverse uneven and challenging terrain. The first major design considered was modelled off the VVSS (Vertical Volute Spring Suspension) system used by many US and Italian WW2 tanks. This concept was robust and well-proven, however the design would have been difficult to implement at small scale – requiring two extremely short shock absorbers with impractically-high spring rates. The final design took inspiration from several sources including both the DARPA robot and the Ripsaw (see Figure 24) mentioned in the literature review of Section 5.3.1. The concept (a simplified diagram of which may be seen in Figure 29) consisted of a crosspiece housing two pairs of idlers, which is pivoted (at point C) on the end of a suspension arm. This arm itself pivots about a point on the hull side (point A) and is attached (pivoted at point B) to a shock absorber which compresses upwards as the arm rotates and is attached to another pivot on the hull (at point D). From this design dual shock absorption can be achieved – with the pivoting T-piece handling smaller inconsistencies in terrain, with larger variations causing the main suspension arm and shock absorber to become active.

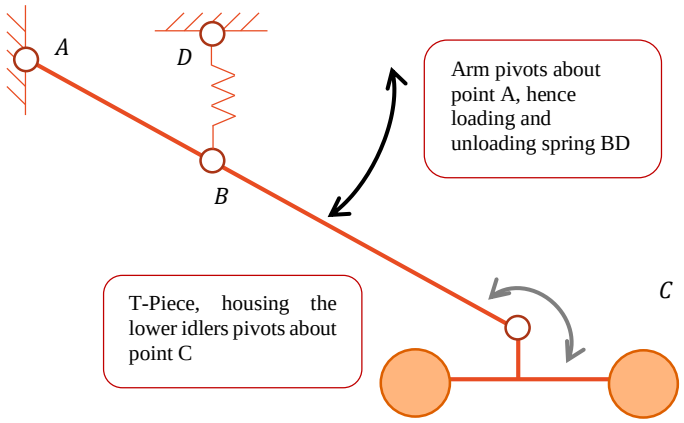

Figure 29 – Suspension schematic

4.3.6.1 Design iterations

Initial, basic designs used straight, single-piece suspension arms cut from flat plate, however it was soon realised that, as the arms were to be mounted upon the 'side pods' of the chassis, an offset would be required in order for the suspension idlers to align with the tracks and large pulleys. To achieve the required offset the next iteration, V2, (see Figure 30) consisted of an upper and a lower suspension arm joined parallel to one another, with each arm made up of two plates connected via pins to increase to the resistance to twisting. The crosspiece was redesigned into an arched shape to allow it to rotate further before the idlers came into contact with the suspension arm.

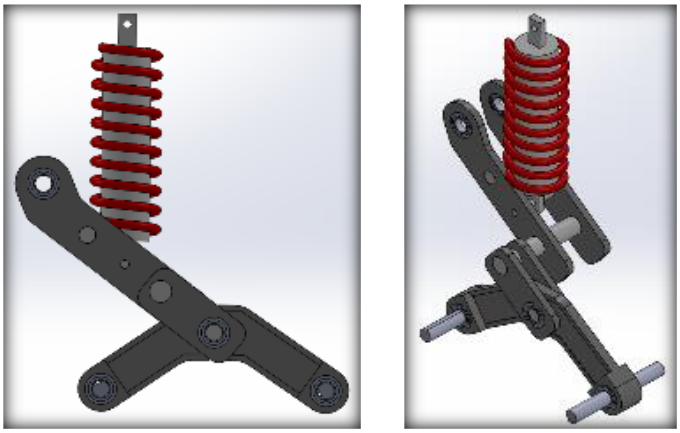

Figure 30 – Suspension V2

The third and final major design change, V3, was to replace the plates with channel sections in order to increase integrity and reduce machining work through buying standard lengths of channel (this may be seen in Figure 31). These were connected and secured via an M4 bolt and two 2.5mm dowels, with the chassis and crosspiece pivots consisting of shoulder bolts, and the spring pivot of a threaded M6 bolt. The crosspiece was also redesigned once more – with its

new T-piece design again allowing for more rotational travel, whilst also being simpler and sturdier than before.

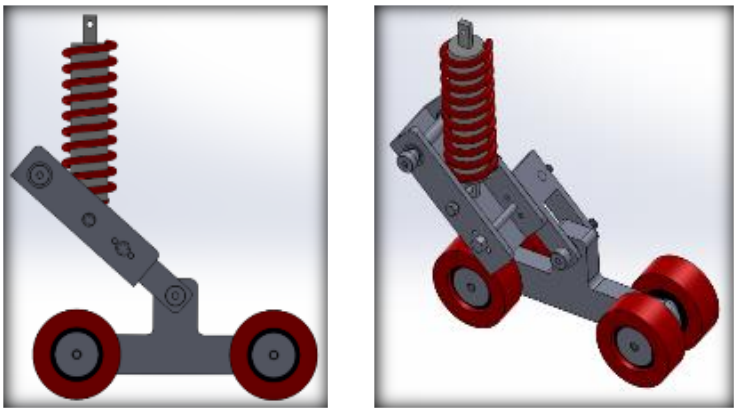

Figure 31 – Suspension V3 (final design)

4.3.6.2 Shock Absorbers & Springs

It was decided that shock absorbers would be bought in, as many suitable, good-quality options were available for RC cars and similar applications – although it was likely that the stock springs would have to be replaced by a set with a higher rate due to the relatively high robot weight. The shocks selected were BS903-004 95mm, oil-filled, aluminium RC shock absorbers from Blacksmith Products – providing a travel of 25mm, adjustable preload and an uncompressed length well below the maximum mounting length available. The stock spring rate was estimated experimentally, with the rate found to be approximately 1kN/m. The required rate was obtained from Equation 5.3.3, for deflection, $\delta = 12\text{mm}$, derived from the model of Figure 32.

$$k = \frac{L_1}{L_2}\frac{W}{4\delta} = \frac{0.03}{0.01} \times \frac{250}{4 \times 0.012} \approx \frac{15{,}000N}{m} \qquad (5.3.3)$$

Where W is robot weight and L_1 & L_2 are dimensions on the suspension arm. This calculation was validated using a simulation tool from US suspension supplier, Hyperco (Hyperco, 2014), which provided extremely similar results. Based upon these calculations three sets of springs of comparable dimensions to the stock springs were sourced from Lee Spring, with rates of 11.95, 14.35 and 17.28kN/m. For full derivation of suspension equations see Appendix E5.

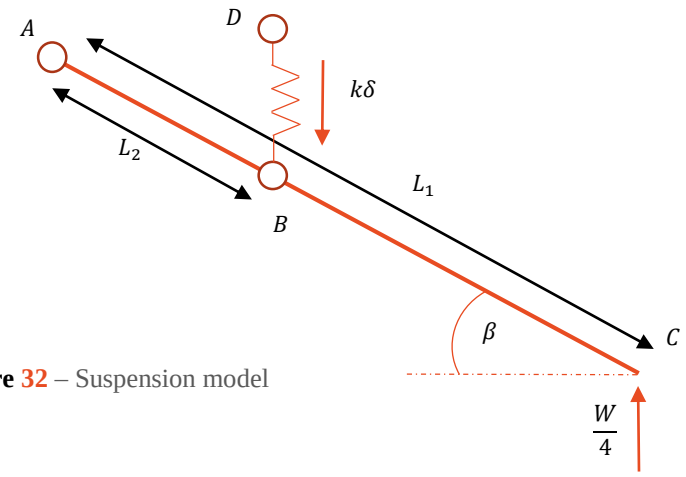

Figure 32 – Suspension model

5.3.7 Tracks

4.3.7.1 Positioning

The tracks should pass around the body of the robot, serving the dual purpose of maximising internal volume whilst also allowing the robot to be invertible. This led to the basic track layout shown in Figure 33.

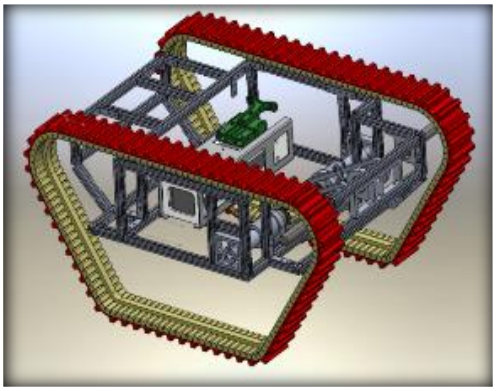

Figure 33 – Track positioning

4.3.7.2 Track Type

After comparison of several possible track concepts (see Appendix E1), it was decided that specialised, rubber tracks would be bought in – with previous WMR robots demonstrating the high durability, traction, and multi-terrain capability possible with similar designs.

4.3.7.3 Track profile design

Further major parameters to consider included material; rubber tread spacing & width; rubber tread alignment with polyurethane backing treads; and track guidance.

The choice of track material determines the friction coefficient on a given surface; as Orion was designed to traverse various terrains and this was taken into consideration. The material choice also impacts the durability of the tracks. The rubber tread spacing and width affects the proportion of the track in contact with the surface for a given terrain: e.g. more raised tread contact will provide better grip on hard surfaces as a greater surface area is in contact with the ground. During consultation with the track supplier, Transdev, it was established that aligning the main rubber treads with the backing treads leads to a significant increase the strength of the rubber tracks. This is because, when aligned, the rubber track is subjected to less force as it tightens when travelling over the pulleys. One major track issue on the previous USAR was the

occasional ‘slipping’ of tracks – i.e. lateral disengagement from the pulleys due to thrust forces perpendicular to the direction of travel. If this occurs and the track fully disengages, then the robot is effectively disabled, and hence it is a major concern to be addressed in the design.

5.3.8 Final Track Design

Several designs were considered including wider rubber treads, diagonal treads and even chevron-shaped treads, (the latter two had to be discounted due to lead time and price) however after consulting with Transdev (UK-based manufacturer of timing belts and pulleys) the design was finalised. The material chosen was Transdev’s AbbrX 55 – a silica-reinforced natural and synthetic rubber mix providing high strength and resilience alongside severeabrasion resistance. It has a low compression set and high elasticity, with a medium hardness from the available range. The kinetic friction coefficient between the AbbrX 55 and dry concrete was calculated to be high at 0.97 from lab testing (for calculation methods and full results see Appendix E3). The final profile design, (seen in Figure 34) employed a spacing of 20mm between the 10mm rubber treads, in order that it was a multiple of the backing tread width (10mm) – thus ensuring that the rubber treads were located above a backing tread, and therefore improving the integrity of the track. This spacing was also tighter than previous years with the aim being to provide a greater contact area on hard, urban surfaces where the robot will not sink in – meaning that more contact area and hence grip would be provided. On the PE backing track, a 10mm raised guide was included which would run in a groove on the large idlers, hence providing a thrust force to prevent lateral disengagement from the pulleys. In addition the large idlers were also designed with flanges to further assist track guidance.

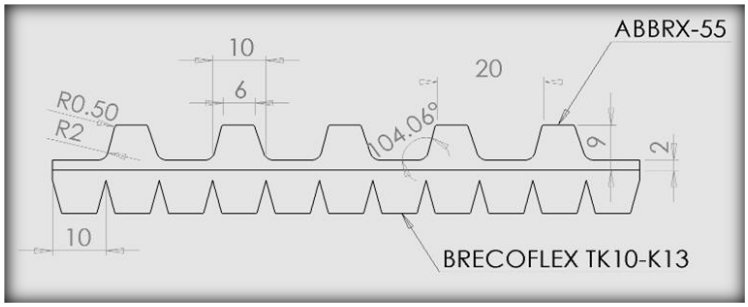

Figure 34 – Final track profile

5.3.9 Track Tensioner

The track tension impacts performance – with excess slack potentially causing misalignment between the backing treads and the pulley teeth, which in turn could lead to sub-optimal performance and transverse track slipping. Furthermore the effect of the suspension had to be accounted for – when it is compressed the track tension will drop, and as such some form of tensioning system was required. The initial concept utilised a linear pillow block bearing and a

sprung shaft which would be nominally fully compressed until the tracks began to slacken – the spring would then force the shaft outwards, thus dynamically re-tensioning the track.

This design, however, had to be rethought due to last-minute purchasing issues – with the pillow block repurposed to work both as the drive shaft bracket and the linear support, and the spring replaced by a piece of threaded bar, allowing for manual tension adjustment through tightening of a nut. The pillow block and wheel are supported by two 10mm steel dowels threaded into the pillow block itself and sliding through the support bracket, and by two 6.0 mm screws threaded into the support bracket and sliding through the pillow block. This final design may be seen in Figure 35.

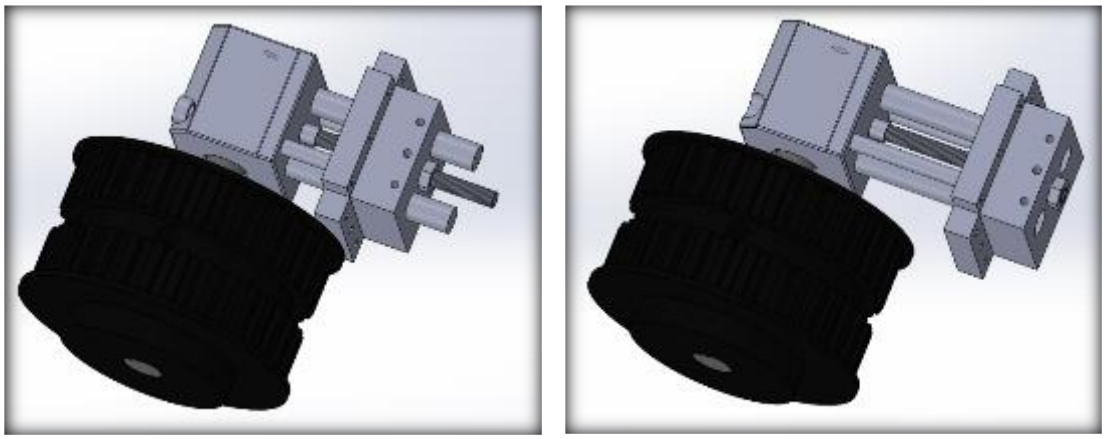

Figure 35 – Track tensioner

5.3.10 Stress Analysis

To ensure the suitability of components, both theoretical and simulated stress analyses were conducted. After some rough calculations it became clear that the most highly-stressed situation would be the reaction of the suspension system to its most severe loading case – the 0.35m drop test. Upon inspection, it was obvious that, once the shock absorber is fully compressed (and hence acting as a rigid element), the most heavily-loaded elements will be the two spring pivot rods at points B and D in Figure 36.

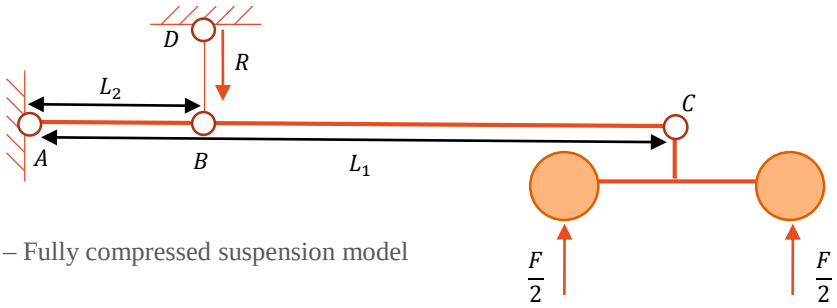

Figure 36 – Fully compressed suspension model

These were of particular concern given that they were single 6mm screws, and hence they were modelled theoretically to test the design's suitability. Summing moments about point A - which

is pin-jointed and hence cannot provide a resisting moment – with $L_1 = 3L_2$, gives the reaction force, $R = 3F$. The robot is to be dropped from a height of 0.35m - thus the velocity as it hits the floor is approximately $2.62m/s$. Then, assuming linear deceleration from this speed to zero over a time interval of 0.1s, this yields, $a \approx -26.2\ m/s^2$. The force at point C, may then be estimated as $R = (3m/4) \cdot a \approx 500N$. The pin then acts as a beam of circular cross-section, with both ends fixed, as seen in Figure 37.

Figure 37 – Spring pin model

Then, given $E = 210 \times 10^9$, $L = 0.025$, $r = 0.003$, and using the Simple Theory of Bending the maximum deflection, $y_{max} = 0.003$mm, the average stress, $\sigma_{avg} = 17.68$MPa, and the peak stress, $\sigma_{max} = 73.68$ MPa. These results were then compared with values obtained from simulations using Abaqus FEA software, shown in Figure 38 for the same loading. The maximum stress case obtained from the theory predicted a peak stress of around 75MPa – whilst the simulated stresses were an order of magnitude lower: with a maximum value of about 8MPa. Given that the yield stress for the stainless steel bolts used is 210MPa, then it is clear that the bolts are suitable for the task providing a minimum Factor of Safety (FoS) of 2.8, assuming the worst-case loading scenario from the theory.

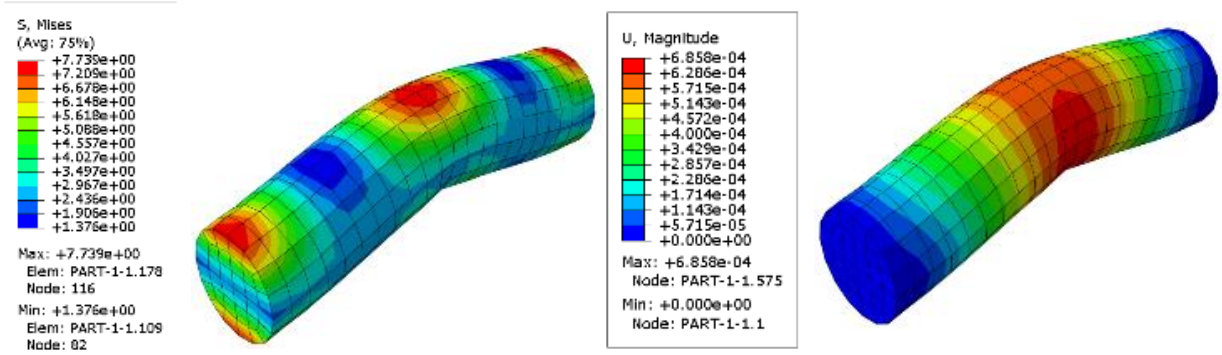

Figure 38 – Pin Abaqus analyses

5.3.11 Justification and Evaluation of Design

To validate the drivetrain, its design has been compared to the relevant specification points laid out in Table 3 of Section 4. The comparison may be seen in Table 10. The majority of criteria were met or surpassed, with only the motors not classed as having fully met requirements due to the lack of physical testing to validate theoretical capabilities.

Table 10 – Design evaluation and justification

Criterion	Achieved Results	Status
Maximum Drivetrain Mass – 15kg	Drivetrain mass calculated to be 10.5kg	✓
Maximum Allowable External Dimensions – 580 x 410 x 350	Length 502.0 mm, Width 405.0 mm, Height 270.0 mm	✓
High Clearance	Suspension system provides a high ground clearance of approximately 100mm	✓
High Traction	Track material selected with a high dynamic friction coefficient (0.97 with dry concrete). Tread design optimised to provide high traction levels on all terrains	✓
Invertibility	The design is invertible	✓
Range of Speeds including Standard 0.5m/s Operation Speed	Based upon specifications, the motors are theoretically capable of the speed requirements, although this has not been tested	-
0.3 m/s² Acceleration up 38° slope	Based upon specifications, the motors are theoretically capable of the acceleration requirements, although this has not been tested	-
Able to survive a 350mm drop impact	The most vulnerable components are capable of surviving the drop test with a FoS of 2.8	✓

5.4 Electronics

A Glossary of terms is available in Appendix F0.

5.4.1 Literature Review

Search and rescue robots have an inherent need for precise control and versatility. Many research groups use a wealth of sensor peripherals, teamed with high-end brushless motors and sophisticated control mechanisms (fuRo, 2014). What many of these USAR robots have in dynamism, however, they lack in failsafe operation and durability.

Although Orion is fundamentally a new design, previous WMR designs provide indications of areas for development. The multiple iterations of the large USAR robot have led it to become unwieldy (WMR, 2013), and although equipped with many complex controllers and sensors, lacking in a practical usability and capability for improvement. The chassis is also filled with poorly organised wiring and a large stack of dated computation boards.

Previous robots utilised bulky Powerboards with switchable outputs for power reduction and multiple output voltages to support various devices through design iterations. In an attempt to improve this, the M-USAR of 2013/14 used two Powerboards with TRACO DC-DC voltage

converters specifically targeted to provide 5V and 15V (Chavasse, et al., 2014). These provided 2A and 8A respectively, leaving little room for additional devices, in terms of output connections, PCB trace sizing, and current sourcing capability. The board used a large 50.8mm x 50.8mm 5V converter and switchable outputs, contributing to a main Powerboard area of 180x100 mm. Additionally, the proposed Arm Powerboard had an area of 140x100 mm.

Despite the dangers of using volatile Lithium-Polymer (LiPo) batteries highlighted in Appendix F1, no previous designs utilise battery management systems other than a simple 'danger' buzzer. In difficult terrains motors draw high currents at high loads, rapidly discharging the battery. This combined with the difficulty in changing batteries, could result in battery deep discharge during operation (Tjinguytech, 2013).

Programming a robot for first time programmers in such a short space of time was a very challenging task and so assistance was sought from third parties. The team chose to use the Robot Operating System (ROS), a collection of software frameworks, to provide the groundwork for the software to be created this year (ROS, 2013). Using ROS, therefore, ensured a reliable and modular system with the ability for the user to pick and choose "packages" of software components in future years.

The components that draw the most current are the motors (Maxon, 2015). In order to provide sufficient torque for the size and weight of the larger robot up to 2012-13, two large Maxon DC brushed RE50 drive motors were used, which were rated at 200W each. However, as these motors were brushed they had a low performance per-unit-volume weight and were unnecessarily powerful for more compact robots. Smaller Gimson GR02 brushed motors were employed on the M-USAR by the 2013/14 team: six motors were used drawing a massive 51A at maximum efficiency and occupying the majority of the robots 'real-estate'. With only a single 5Ah 6s LiPo battery this robot would have had a battery life of under 6 minutes.

5.4.2 Specification Parameters and development

4.4.2.1 Low Level Specification

Table 11 – Electronics parameters and specification

Criterion	Specification
Network	▪ Creating a secure Virtual Private Network for the client to connect to the robot via a point to point connection ▪ Having full control of the robot over this connection
SLAM	▪ Use of LiDAR for real time representation of the environment and Orion's position ▪ Identification of objects in the vicinity of the robot
Reliability	▪ Software should be able to detect any errors in connectivity

	▪ Software should have security/safety if stuck in an endless loop
Speed	▪ The software should be written in an efficient manner such that all functions can be used at full speed during competition
Motors and Controllers	▪ Use efficient brushless motors capable of providing sufficient power for motion of a 25kg Robot ▪ Controllers must prevent large stall currents and provide the option for reuse with potentially larger motors later
Sensors	▪ Incorporate capability for Stereoscopic Vision, Rearview Camera, Infra-Red (IR), CO2 and Audio Sensing
Sufficient heat exchange	▪ Ensure that circuitry can use the shell for sufficient heat sinking ▪ Distribute the heat evenly using a fan ▪ Fit all of the components safely within the 460x320x242.5mm chassis
Powerboard	▪ Design Powerboard with capability for further expansion of devices ▪ Design Powerboard without switchable outputs for space saving ▪ Design Powerboard with sufficient track sizes
Master Switching	▪ Utilise a MS circuit including battery monitoring and software E-stop ▪ Utilise a Physical E-Stop button to cut power to the system under conditions not resulting from battery or software problems
Modularity	▪ Have a structured and modular design to allow for swift and simple diagnostic at different levels of hardware ▪ Display Agility in design to allow future component upgrades ▪ Have a modular condition for Robot recovery should software or hardware bugs leave any part of the robot inactive ▪ Be designed with the intention of meeting RoboCup competition rules with respect to the electronic capabilities
Wiring & Fixings	▪ Secure wiring to prevent damage whilst minimising weight (length) within safe thermal limits. ▪ Make the wiring conform to a standard size connector and wire gauge

In order to meet the desired 25kg weight and the 580mm x 410mm x 350mm (l x w x h) dimensioning specifications for Orion, a middle ground between sophistication and mobility had to be found, as outlined in Table 11. Incorporating the capability for stereoscopic vision and rear view cameras enables the user to identify the robot's surroundings. Sensors such as IR, and CO_2 sensors as well as audio sensors and transceivers were deemed crucial for victim detection, following the RoboCup guidelines in future years. Brushless motors offer an extremely high power to volume ratio and as such it was decided that they would be used for Orion.

Alongside a low-effort battery removal system, it is best safety practice to prevent the dangerous deep discharge situation by monitoring the battery's individual cell voltage. Previous designs have attempted to measure total battery voltage, however this assumes a balanced discharge and may overlook one cell malfunctioning or reaching a dangerously low voltage. Such designs were never implemented and previous robots have used a small GARTT 1-8s battery buzzer, powered by the battery balance connector. The buzzer displays cell voltage

and sounds an alarm if an individual cell reaches a voltage below a user-specified minimum. This does not however incorporate an automatic master-switching stop should this event occur. Moreover, due to the use of potentially volatile LiPo batteries in hazardous environments, safety systems must ensure that the robot is safely shut down upon potential software bugs causing uncontrollable operation.

The Power Distribution Board should be designed to be compact in comparison to previous years due to the internal volume constraints of the robot. As a low level specification, the Powerboard, should not require switchable outputs. The 2013/14 M-USAR used very low power CMOS (Complementary metal-oxide semiconductor) switches on only three of the six 5V outputs, requiring complex software integration with an on-board MCU, a sizeable USB to FTDI interface, and a PROTO-PIC logic level converter module. It was apparent that the 2013/14 M-USAR saved negligible amounts of power, and if switched outputs were used they would only have been used for 5V devices such as the LiDAR and CO_2 sensor peripherals, rated as approximately 800mA and 500mA, which, compared to a continuous nominal current of 17A from two motors and far higher starting and stalling currents, is very small.

5.4.3 Modularity

The architecture of the robot was designed with the aim of achieving a modular structure suitable for future developments such as the addition of a robotic arm. The overall system was controlled by a central motherboard and operating system, which constituted the central input and output node of the robot. If the architecture were to be widened to a further level, sensors and the microcontroller would be added to the schematic, providing a more decentralized architecture. The architecture was then expanded to completion, adding a third level which actively controls the actuators and the battery, which constituted the final output.

Particular attention was paid to ensuring the reliability of the robot. This was achieved both by designing diagnostics tools and points, and by creating a software interrupt in the microcontroller. The software interrupt allows the user to control Orion's motors through a Bluetooth dongle connected to the Arduino if the signal from the Pico-ITX to the Arduino is lost.

The sensor package was designed to resemble a "sensor box" such that the layout and the parts can be readily taken out of the main body and into the robot arm. A schematic was also realised to aid future development and eventual relocation of the "sensor box" into an arm, which will be crucial to being successful at the RoboCup competition (see Appendix F2). This corresponds to the three year plan.

Finally, modularity matched the ambitions of the mechanical specification and the overall scope of the project. It allows a flexible choice of components which can then change to support the needs of different mechanical systems, such as the motors, or can be easily updated by future WMR teams should parts need replacement or development.

5.4.4 Component Choice

Orion's architectural design features various components in different logic levels. This section first analyses the control hardware of the architecture and then the remaining components features in the architecture diagram.

4.4.4.1 Motor controllers

The motor controllers chosen were the ESCON 50/50 P/N 409510. They receive inputs from the power supply and from the Arduino, which sends a Pulse-Width-Modulated (PWM) signal. The control signal from the Arduino is used to set the velocity target of the motor. The controllers' setup requires the tuning of their response to a known signal to tune the parameters of the PID controller built inside. Important in the setup and interface with the Arduino is to set a PWM signal well under the PWM controller duty cycle, following Nyquist criteria on signal aliasing. The chosen motor controller was selected for the following reasons:

- **Compatibility** - with motors and the Arduino.
- **Efficiency** - in limiting and managing the voltage and current input of the motors
- **Precision** – it uses incorporated Hall sensors ensuring precision; critical in the use of EC motors.

Finally, the motor controllers also feature a USB interface to allow for the monitoring, calibration and the diagnostic of the system from a PC. The motors were calibrated to have a maximum soft start and stall current of 15A maximum each using this interface. Figure 39 provides a schematic of the motor controller connection, setup parameters and monitoring interface, highlighting also why the device is extremely useful for diagnostic purposes.

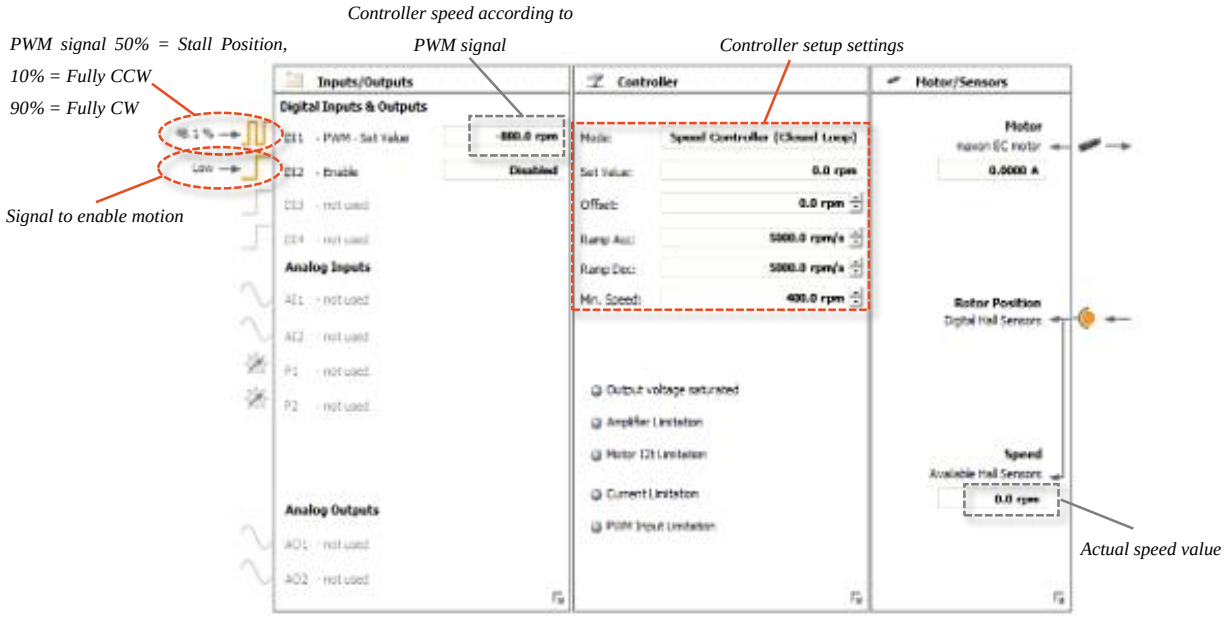

Figure 39 – ESCON software module

4.4.4.2 Arduino Mega 2560

The Arduino microcontroller (seen in Figure 40) is used to take inputs from a variety of sensors and devices such as the CO_2 sensor and the cameras, as well as controlling physical outputs such as the motors. The Arduino platform provides an Integrated Development Environment (IDE) to write software to the board. There were other motherboards that could have been used, such as the Raspberry Pi, but the Arduino was chosen for the following reasons:

- **Price** - At under £30, the Arduino Mega 2560 cost less than its competitors
- **Cross-Platform** - The chosen microcontroller needed to be compatible with both the Ubuntu and Windows Operating Systems.
- **Simplicity** - The IDE is easy to use and the programming can be done in C/C++.
- **Extensible** - Multiple shields (PCBs that plug into the Arduino pin headers) can be stacked

Figure 40 – Arduino Mega 2560

A more in-depth analysis of the Arduino is included in Appendix F3, stating its properties that make it useful for a project of this nature.

4.4.4.3 Pico – ITX 830

With a 1.86GHz dual core processor and requiring only a 5V power supply, the Pico 830 (see Figure 41) was seen as the ideal on-board computer for Orion. This computer runs the ROS master - facilitating the communication between the Arduino and the client laptop. Simultaneously, it stores the LiDAR data stream during the competition and in future years can be programmed using ROS to send the LiDAR data in real time over the wireless network to the client laptop. The Pico-ITX was chosen in preference to the previous robot's Mini-ITX for several reasons:

- **Size -** It is more than 4 times smaller (in terms of the board area L x W)
- **Computational power** – With a 1.86GHz dual core processor, the Pico is slightly more powerful than the Mini.
- **Efficiency** – It is more efficient than its predecessor and so does not require a fan

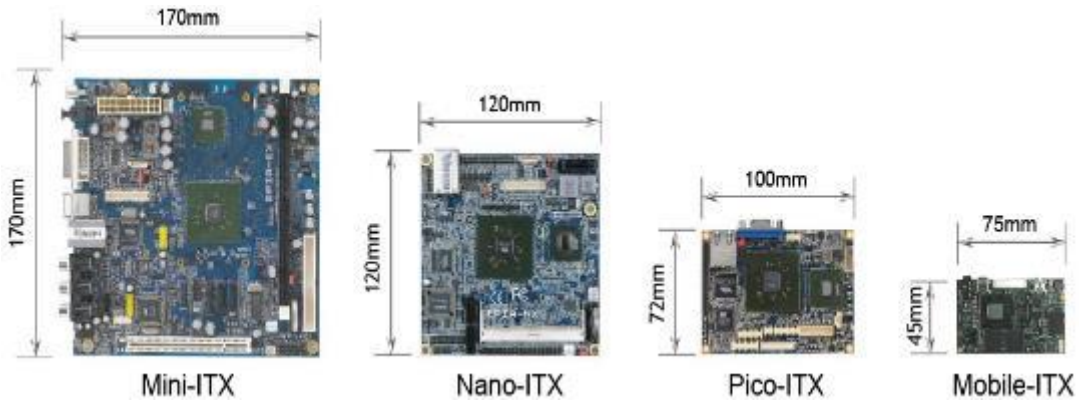

Figure 41 – Comparison of different motherboards

4.4.4.4 Wireless Router

The wireless router is used for the client laptop to communicate with and control the robot via the Pico-ITX. As the Pico is connected to the Arduino, the client will have full control over the robot through the Virtual Private Network (VPN) set up between the laptop and the Pico. Due to issues with incorrect advertising of an originally specified 5V router (see Appendix F4) the 12V Buffalo WZR-HP-G300NH used with the 2013/14 M-USAR was employed. It should be noted that this somewhat dated router only operates in the 2.4GHz range, which is technically a better fit for the RoboCup competition in terms of lower power consumption and greater usable range. Yearly rule updates for the competition's network use, however, should be considered in future iterations.

4.4.4.5 PlayStation Controller

A Sony PlayStation 3 bluetooth controller was used to control Orion's motors. Its control mechanism can be found in Appendix F5, which explains diagnostics of the controller that can be run through TurtleSim. For more information on TurtleSim see Appendix F6.

4.4.4.6 Sensor array

The determination of the sensors array followed a specific path. Firstly, previous project reports were examined, together with RoboCup rules, and further research was conducted into existing rescue robots to understand the sensors usually incorporated. Sensor choice was then based on criteria from the specification. While the revision of previous WMR reports provided a valuable starting point, the new system architecture and operating system demanded certain changes. Specifically, the M-USAR design lacked important sensors such as an IR camera and LEDs. The use of a Raspberry PI camera for rear vision was no longer compatible with the Arduino and a ROS-driven system. To gain maximum points at future RoboCups, a LiDAR system was included in the sensor array. The existing LiDAR was both proficient and compatible with the new architecture design, so was utilised rather than purchasing a new component. Position encoders were no longer needed for Orion, made redundant by precise four pole motors. Table 12 summarises the initial review and highlights problems and sources of innovation in Orion's design. The LiDAR and Gimbal can be seen in Figure 42.

Figure 42 – LiDAR & Gimbal

Table 12 – Sensor array review summary

Sensor	Previous design and analysis	Current analysis & design	Action	Chosen Sensor	Motivation
IR Camera	Missing	Included	To be added	Photon™ 160	High capability. The prompt availability from the 2012-2013 design
LiDAR	Included	Included	Use same sensor	-	High capability, already in house
CO_2	Included	Included	Use same sensor	-	High compatibility, Low cost
LED	Missing	Included	To be added	Cree xlamp xbd series led white	Ability to create a cone of light of 115°. Easy control of the flowing current
IMU	Included	Included	Use same sensor	-	Already in house, high precision, 10 DOf
Encoders	Included	Not to include	Consider in future arm	-	Not needed
Cameras	Included	Included	Add for rear view	Microsoft LifeCam HD-3000	Easy to interface, cost-effective , adequate frame rate

The Orion design couples the use of the LiDAR with a brushless Gimbal, which constituted a significant element of innovation compared to all previous designs. In all previous WMR designs of the SLAM system the final map was considerably confused due to the angular motion of the robot - thus making the final result blurry. The use of a gimbal obviates the problem, allowing thus to produce stable *geotiff* images.

4.4.4.7 Power Distribution Board

Although the use of precision isolated converters is recommended, the 2013/14 M-USAR converter TRACO TEN 40-2411 was only capable of supplying 8A at 5V (TracoPower, 2015). The number of 5V devices used draws a total of 9.585A before inclusion of a safety margin. A GE Hammerhead Series EHHD024A0A41 (GE Industrial, 2015) with the capability to supply 24A in a smaller ‘eighth-brick, low-height’ form factor (59 x 23 x 13 mm) was chosen for addition of further peripherals, with the additional benefit of being designed for extreme temperature variations (-40 to 85 °C) with 91% efficiency facilitating rugged operation.

Possibly most problematic, was the choice to power the bulky 19V ASUS AC1750 Gigabit Router (ASUSTek Computer Inc, 2015) used previously from a TRACO TEL30-2413 supplying 15V at 2A max. Without knowledge of router inner workings, supplying a voltage at under the required value will cause certain sporadic 'failure-like' behaviour, or at best a markedly sub-optimal performance. This is particularly important considering the 'serious connectivity issues' at the RoboCup competition due to high user volumes creating low bandwidth connections. A TRACO TEL 30-2412 DC/DC Converter was used instead of much more common 12V routers – allowing flexibility in future designs. See Appendix F10 for full analysis.

2-pin and 4-pin Harwin datamate Mix-Tek connectors were used for peripheral connection (Harwin PLC, 2014), and LittelFuse Nano-2 fuses alongside OmniBlok surface mount fuseholders were employed to provide physical circuit protection (LittelFuse Inc, 2014), as with previous USAR Powerboard designs.

The power requirements and parameters of the chosen components are listed in Table 13.

Table 13 – Electronics parameters and specification

Name	Voltage (V)	Current (A)	Power (W)	Fuse (A)	Inc. 135% Safety Margin(A)	Minimum Trace Width SS (mm)
Arduino Mega	5	<500m	2.5	(N/A)	0.675	N/A
IMU - Xsens motion tracker	5	70m	0.35	(N/A)	0.095	N/A
3 Lifecam 3000HD	5	<500m	<2.5	(N/A)	0.675	N/A
Pico ITX	5	3.5	17.5	5	4.725	2.56
LiDAR	5	1.5	7.5	2	2.025	0.795
Bright LED	5	350m	1.75	1	0.4725	0.107
CO2 Sensor	5	500m	2.5	1	0.675	0.175
IR Camera	5	<500m	<2.5	1	0.675	0.175
Fan	5	235m	1.6	1	0.317	0.0616
Router	12	<2A	24	3A	2.7	1.18

4.4.4.8 Wire Sizing Considerations

It was calculated that for flexibility, American Wire Gauge (AWG) 14 was to be used, with a 2.5mm cross section. Using this wire gives a current carrying capacity of between 15 and 25A,

allowing for all components including the motor controllers, which were calibrated and limited to drawing 15A at stall, to use the same wire (Farnell, 2015).

4.4.4.9 Battery Management and Master Switching

A master switching circuit, switching at a 'user specified' low cell voltage was required. The switching device must be rated to a current above this level; it was hence decided that a Vishay FB180SA10P Power MOSFET (rated to 180A) would be used as the primary switching device (Vishay Intertechnology Inc, 2014). The cell voltages from the balance connector, supplying 2.5A maximum, can be used to drive the gate of this MOSFET and switch it off upon low voltage. By using the balance connector, any circuitry powered by it does not turn off when the MOSFET switches off the rest of the circuit, powered by the main power wires. The full design methodology in Section 5.1 and Appendix F7 are used to best describe the master switching operation.

4.4.4.10 Internal Cooling

For designing and combining power electronic systems in a chassis, it is imperative to understand rudimentary thermal issues such as the heat emanating from motors and heat dissipation in integrated circuits. Due to this, there needs to be productive thermal management of electronic components to prevent draining the battery, premature failure, overexerting these devices and to improve power availability. In simple terms, these electronic components require cooling. Such techniques for heat dissipation include heat sinks and fan(s) for air cooling.

The total heat dissipated through the Aluminium shell was calculated to be 535.9KW which is more than sufficient to dissipate the 88W of heat from the internal components. The heat still required a more even distribution, however, as over half the heat in the robot will emanate from the motors. Therefore a fan with a flow rate of 11.0 CFM (cubic feet per minute) was chosen for this purpose. The calculations for these figures can be found in Appendix F8.

5.4.5 Software

4.4.5.1 Robot Operating System (ROS)

As previously mentioned, ROS is an excellent tool in robot software design. It offers some operating system like features and so helps resolve several specific issues in the development of software for robots such as mentioned in (O'Kane, 2013).

4.4.5.2 Distributed Computation

The system will have multiple computers which will need to bilaterally communicate with one another. For example, the user will need to send a command through the laptop to the motors in order to move the robot. For this to occur with the architecture of the chosen system, the client laptop would need to communicate with the Pico-ITX, via the wireless router, which in turn communicates with the Arduino to send a pulse directly to the motors. By having ROS on both the client laptop and on the Pico-ITX's Small Outline-Dual In-line Memory Module (SO-DIMM) (Axiomtek, 2015), communicating between the Pico and the laptop is made significantly easier. The rosserial_arduino package (ROS, 2011) provides the protocol for ROS to communicate with the Arduino over the latter's Universal Asynchronous Receiver/Transmitter (UART).

4.4.5.3 Software Reuse

As ROS is open-source, the algorithms for each of the packages are written by experts in the particular field, for example an individual with experience in Android would have created the ROS-Android packages such as the Android camera driver. These algorithms are only useful however if they can be refined to be applicable to different applications. As ROS is becoming a de facto standard for robot software interoperability, the packages available for ROS are generally compatible with the latest, most popular hardware used in robotics.

4.4.5.4 Rapid Testing

ROS provides a quick and simple way to record and playback data from sensors as well as other types of messages. Within ROS, these recordings (known as "bags") are recorded with a tool called "rosbag" and also replayed many times via the same tool to test alternative methods for processing the same data. ROS also allows the separation of the low-level hardware control programs and the high-level processing programs. Alternatively, the low-level programs can be replaced with a simulator which will replicate the corresponding hardware, allowing the user to test the high-level part of the system.

A running instance of a ROS program is called a node. Most nodes will need to interact with each other and this is done by sending messages. All messages are organised in ROS into topics. The methodology of a topic connection is outlined in Appendix F9. Therefore it is easy for nodes to communicate with each other; they either subscribe to a topic to receive information or they can publish messages on a particular topic to share information. The nodes can all be run simultaneously using the ROS master which facilitates the communication between the

different nodes. Nodes can be written in any programming language, making ROS the ideal framework for future WMR teams to use (O'Kane, 2013).

4.4.5.5 Communication Protocol

ROS allows multiple methods of transport for communicating over an IP network. Transmission Control Protocol/Internet Protocol (TCP/IP) is most popular because it is reliable and packets arrive in the same order they were sent. If a packet is lost, it is resent until the client has received it (ROS, 2014). In a room with multiple networks running, and hence much interference, such as in RoboCup competition, this protocol is ideal and ensures reliability. The alternative ROS permitted communication is User Datagram Protocol (UDP). UDP is another transport layer protocol for computers within the same network. It is more unreliable than TCP/IP because there is no guarantee of a message being delivered and messages can be duplicated. This unreliable protocol was therefore avoided to ensure Orion receives all messages it is sent at future RoboCup competitions (Fairhurst, 2008).

4.4.5.6 Heartbeat Generator

The heartbeat generator is a periodic signal sent from one device to another, for further information see Appendix F11. The Pico receives the messages from the client laptop via the wireless router, and relays the signal to the relevant Arduino pins via the serial connection to the Arduino. Simultaneously, the heartbeat signal created can be sent from the Pico to the Arduino periodically at 10Hz whilst other ROS topics are running on the Pico. The heartbeat signal may not be received for a multitude of reasons; such as the code being stuck in an endless loop, or loss of connection between the Pico and Arduino. Therefore the heartbeat generator can verify that the robot is fully functional and can prevent software and hardware glitch mishaps. If no heartbeat is recognised by the Arduino MCU, it can be used to send an output high, as an E-Stop signal and used to switch off the system as a precautionary measure.

5.4.6 Design Iterations and Analysis

4.4.6.1 Power Board

With internal space at a premium, the Powerboard was allocated a 180 x 80 x 40mm (l x w x h) area, considerably smaller than the inefficient 100 x 140 x 40mm of the previous year, which also used an additional 150 x 90 x 40mm of chassis volume for a separate Arm power board. Prior to incorporating trace width considerations, removing switchable outputs and miniaturising converters shrunk the board to 140x80x40mm, as shown in Figure 43.

Multisim and Ultiboard (Figure 44) were used for the design and layout of the board, with custom models and footprints produced for every component to populate the board.

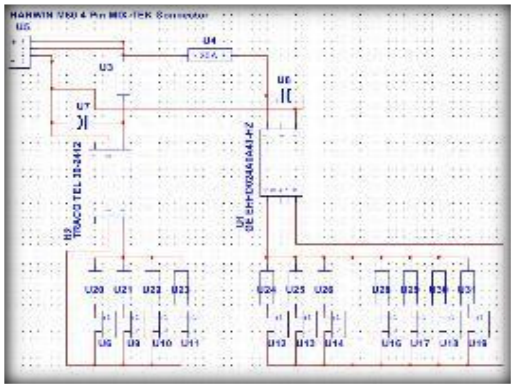

Figure 43 – Powerboard multisim schematic

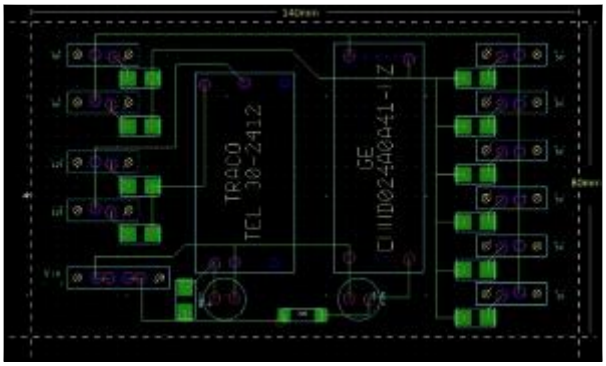

Figure 44 – Ultiboard layout schematic

Trace widths as per the IPC-2221 standard, using a 1 oz. ft^{-2} process for only a 15°C temperature rise on a current rating safety margin of 135% were calculated in Table 14 (4pcb, 2013), this indicated that the board should be printed using double sided traces at the power rails to the DC/DC converters (PEAK Electronics, 2012), and forced the removal of one 5V connection to remain within the specified geometric limits. The 12V rail was designed to be 3mm double sided to support current far beyond the 2.5A of the TRACO TEL 30 2412 to allow for future flexibility in exchanging with a more powerful converter. These double sided traces are shown in yellow on Figure 45.

Table 14 – Trace parameters

	Max Current (A)	With 135% Safety Margin (A)	Fuse (A)	Min Trace Width SS	Trace Size DS (Double Sided)
TRACO TEL 30 2412	2.5A	3.375A	5A	5.62	2.81
GE EHHD024A0A41	24A	32.4A	30A	35.8 (28.5 with 15°C temp rise)	17.9 (14.25 with 15°C temp rise)

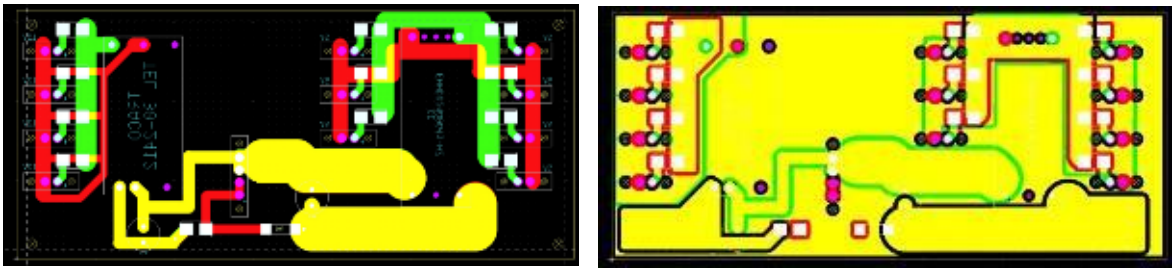

Figure 45 – Double sided traces

In terms of PCB design for manufacture, previous power boards had not included crucial ground returns and power supply polygon pours which reduce current density and prevent excessive board heating (Altium Ltd, 2004). This introduces risk of a floating ground issue due to the build-up of resistance in ground traces. Additionally with the power board using switching DC/DC converters, although they are self-contained modules, it is good practice to include large ground return pours for EMC shielding. External 47µF decoupling capacitors as specified on the converter data sheets were used to remove undesirable noise on the supply voltage (Intersil Americas Inc., 2011). The final board was produced within the sizing constraints and can be seen in Figure 46 with the polygon pours incorporated. The bottom view of the complete Powerboard can be seen in Appendix F12.

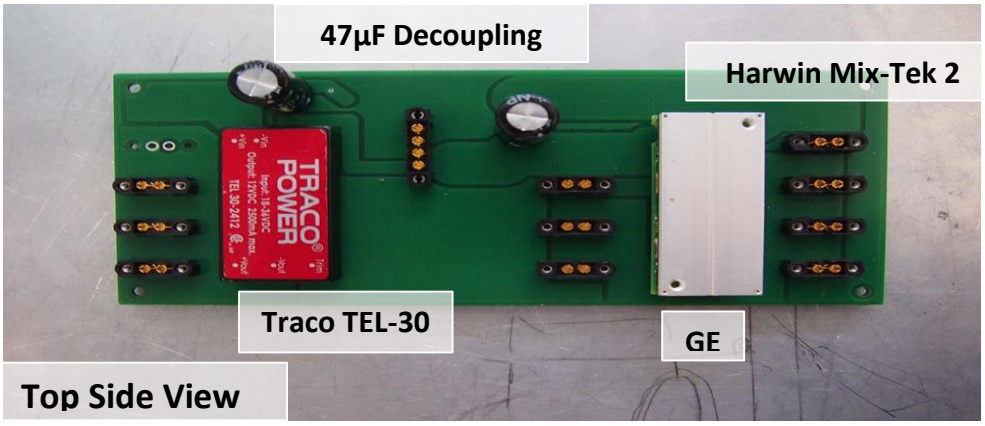

Figure 46 - Final Power Board Design (Top)

4.4.6.2 Sensor mounting

The sensors are controlled through both the Arduino and the PICO ITX and their disposition is designed to maximise their range. Due to the choice of the sensors, selected to have the best software and control interface, no mid-step components are needed. The overall arrangements of the sensors and their range is illustrated in Figure 47.

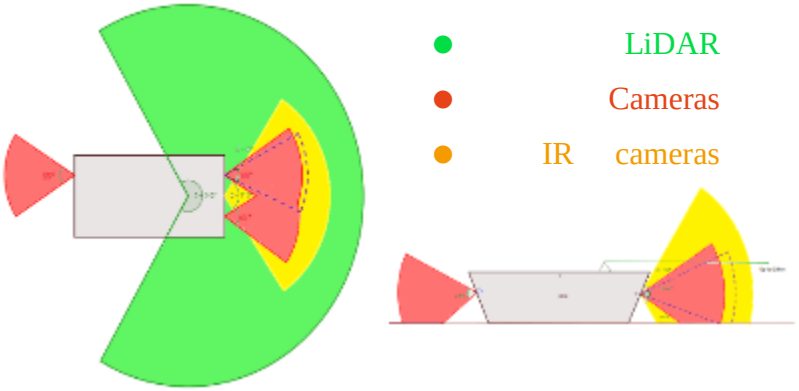

Figure 47 – Sensor range of sight

4.4.6.3 Battery Monitor and E-Stop Master Switching Circuit

An innovative new system was designed to repurpose this monitor with some additional latching circuitry to provide a signal to a power MOSFET to switch off the power to the Orion M-USAR, but also facilitate two different control methods for events after a software bug. The buzzer, which originally 'flashed' on and off during the alarm, was used as the 'SET' input to an NOR SR latching circuit. This meant that upon 'flashing' the output remained at a constant latched logical 'High' level. Figures 48-50 shows design iterations with bullet-pointed features.

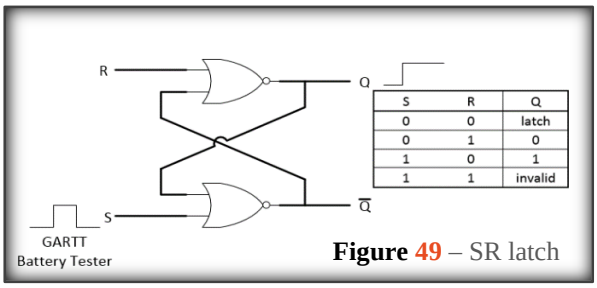

Figure 49 – SR latch

- Fundamental SR Latch.
- Q Latches high with S input high.
- Only R going high resets Q.

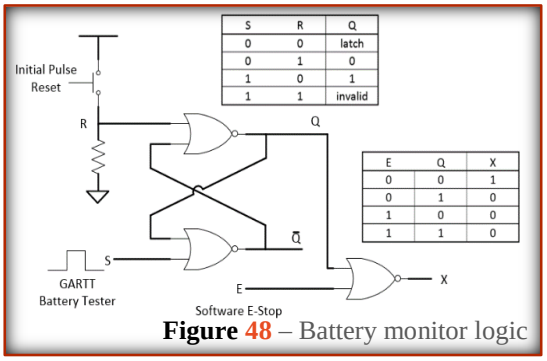

Figure 48 – Battery monitor logic

- GARTT buzzer 'flashes' upon plug in.
- Must include a 'pull up' reset switch.
- Final NOR uses E-Stop input E and Q.
- E-stop and Battery Monitor Combined.
- Output is now 'active high'.
- High input S and S' leads to low output.
- Useful now for switching off MOSFET.

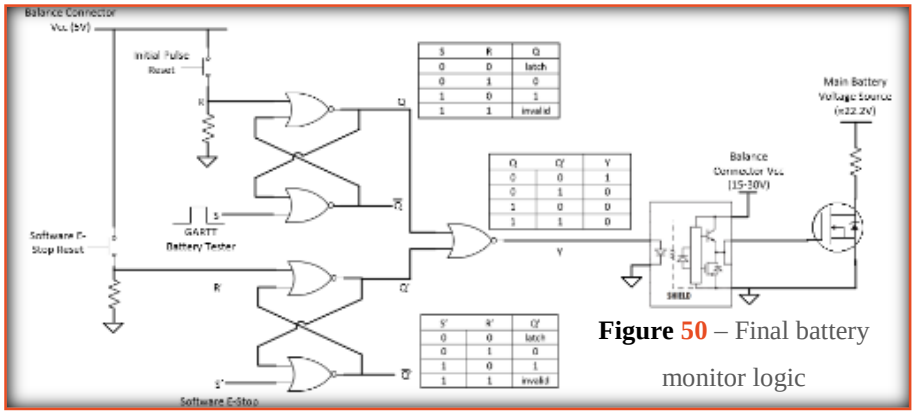

Figure 50 – Final battery monitor logic

- SR Latch for software E-stop after a loss of heartbeat signal to the Arduino MCU
- Latches even after E-stop MCU is powered off to maintain off state.
- Modular control mediums: When a Bluetooth dongle is plugged in after a power off due to software bug, Reset R' can restart the system whereby the Arduino MCU uses a switch statement to detect the dongle and use Bluetooth. This allows alternative control for retrieval.

A TI SN74AS805BN Hex 2-input NOR gate was used to prototype the NOR gate circuit (Texas Instruments, 1995). A Vishay FB180SA10P Power MOSFET, which is rated to 180A was chosen as the main power switch. An Avago HCPL-3120-300E Optocoupler was used as a gate driver between these two components, outputting sufficient voltage for the Power MOSFET to conduct and hence function correctly corresponding to the low voltage NOR output signal (Avago Technologies, 2013). Care was taken to ensure that the Vishay MOSFET was positioned far from the Opto-coupler Gate Driver to prevent undesirable tuning and coupling. Further explanation of circuit and component characteristics can be found in Appendix F7.

4.4.6.4 Integration with Mechanical Design

Frequent design consultations with the mechanical team ensured a coherent design, with components arranged on CAD and mounted using Makerbeam® brackets directly onto the chassis. Wiring was carefully considered to minimise total distance and thus chassis volume occupancy.

5.4.7 Justification and Evaluation of Design

4.4.7.1 Final Architecture

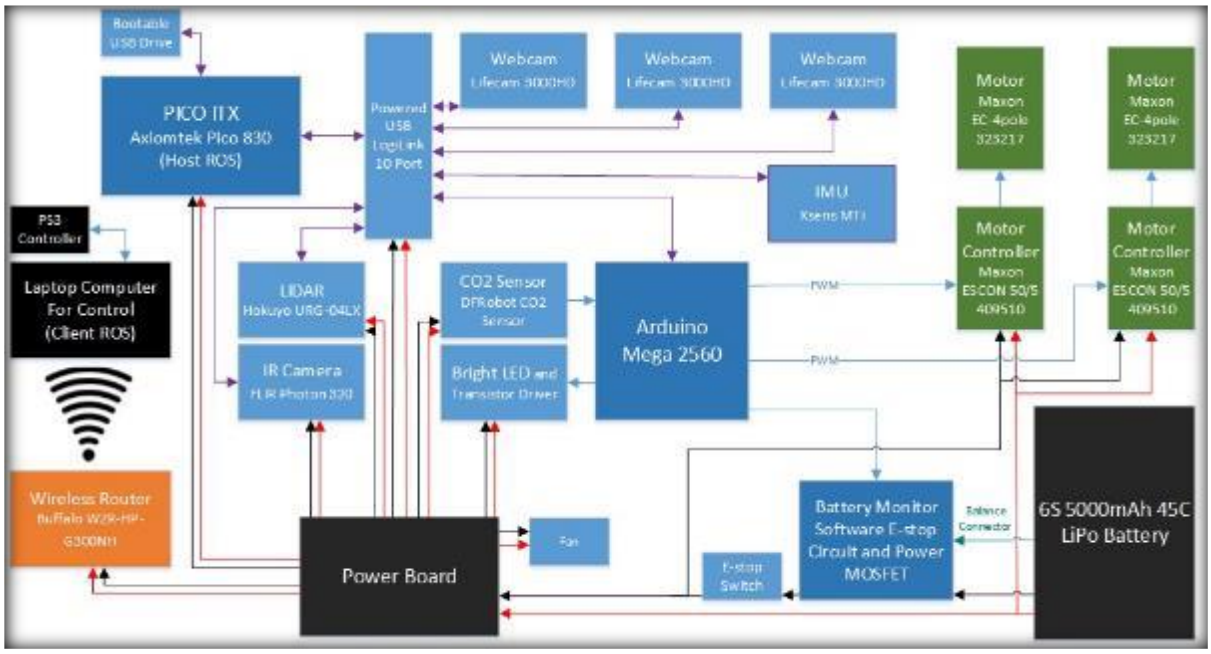

Figure 51 – Electronic architecture diagram

The final architecture of the system, shown in Figure 51, which also gives a summary of the different components included. Particularly useful is the overlaying of the schematic with the modularity concept expressed in the previous sections (see Figure 52 on subsequent page).

A careful analysis of the two schematics reveals how the design meets the required specifications. The design features several diagnostic and expansion points (USB symbol) and different control levels corresponding to the different logic level (Level 1 in red, Level 2 in green, Level 3 in orange). The integration with the other systems in the robot is mainly done through the motor controller making it an element of top priority in the design of mechanical systems. In fact, a dedicated logic level is designed for these components, and several higher logic systems are designed to prevent and diagnose any problem.

Specifications are also met in terms of the sensors and their integration with the remaining body of the robot and with the future developments of the project. Their location and mounting is designed not to constitute a hindrance to other systems and to be easily located in an external robot arm. The mounting of the other components follows the same principle. Specifically, for light parts such as the Arduino, a suspended mounting has been designed. Instead of fixing the board with screws, which would have limited its location and the future use, the board is held in place by tensioned ties which pass through holes already present on the board. This system, other than providing a flexible location, provides suspension-like mountings for the controller, which help in avoiding disconnections of wires.

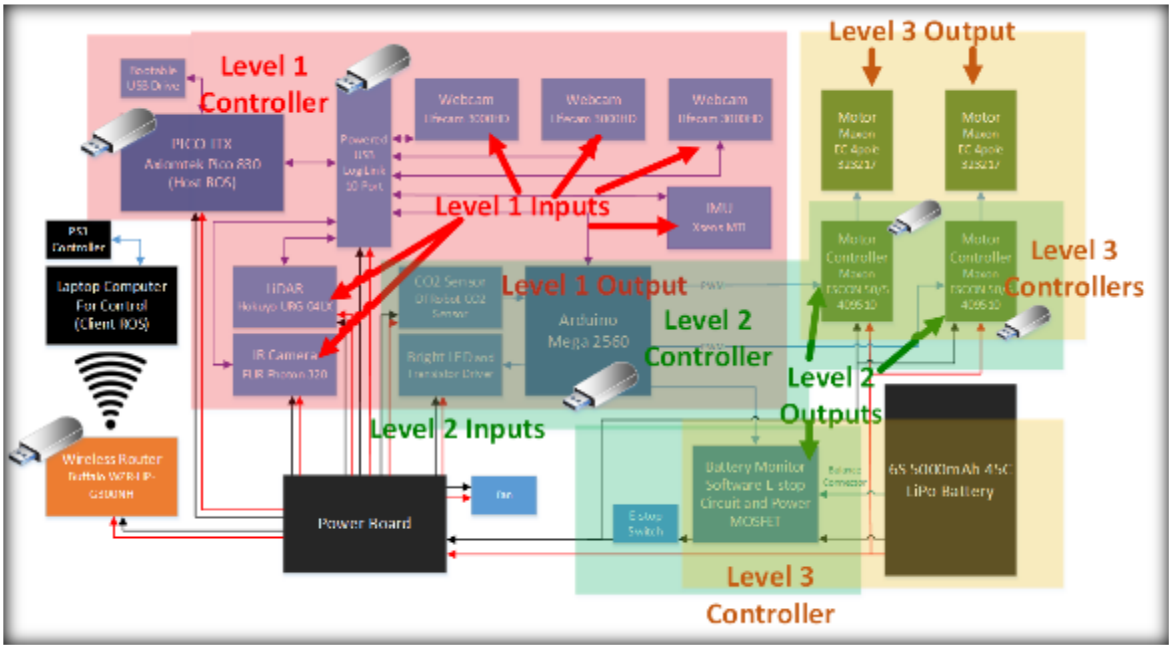

Figure 52 – Final level logic diagram

4.4.7.2 Final Power Board

The final Powerboard design and 3D representation can be found in Figure 53 (on the next page), with an image of the final populated board.

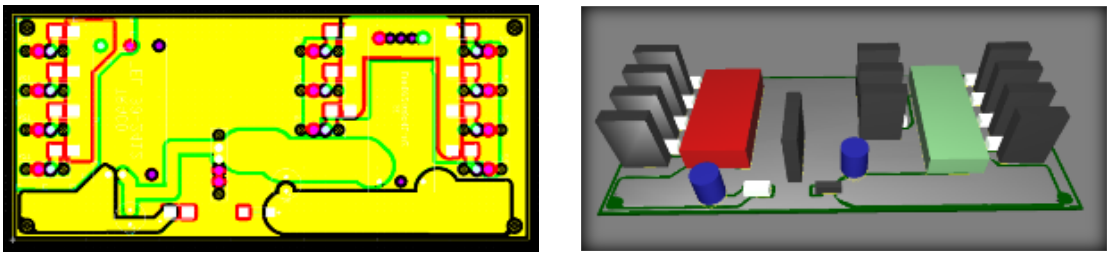

Figure 53 – Populated Powerboard design

As well as meeting the low-level electronics specifications, the Powerboard reinforced the concept of modularity, as it was capable of supplying additional 5V and 12V devices through use of 'spare' connections and large DC/DC converters with all output traces being 2.56mm for loads of 3.5A as per the Pico ITX computer. Complex internal 'bucking' circuitry regulates the load to provide a stable 5V and 12V voltages regardless of minimum load. This was particularly important for the 5V GE EHHD024A0A41, which was underutilised at 9.585A draw.

4.4.7.3 Final Battery Monitor and E-Stop Switching Circuit

The battery monitor circuitry is powered from the JST-XH balance connector, with a negligible current draw. Since the 'dangerous' cell voltage level is user-specified as a low voltage cut-off (LVC), it can be set to above the dangerous 3V per cell level to accommodate for the additional battery load of the monitor circuit. The cell LVC was set to 3.5V.

Since the modular design allows the sensor 'front-end' to be relocated upon later design iterations (e.g. within the 'head' of a Robotic Arm), space for an additional battery could become available. The Master Switching circuit has been designed on a proto-board with multiple input possibilities. The SR logic circuit and gate driver designed on the circuit board can be reused, leaving only the input to the system required to change. It is thus easily capable of using a miniaturised battery management IC in the future, to allow for more complex monitoring – possibly capable of monitoring 6 cells i.e. more than one battery in future designs.

As an additional recommendation it may be better to use the E-stop SR latch in a configuration that triggers a software E-Stop when the MCU output goes low rather than high. This would provide better protection from loose connections and double protection upon low cell voltage switch off. This can be achieved simply by using a transistor before the S input which turns on when the heartbeat is operational. Efforts to incorporate an Automatic E-Stop Reset upon Bluetooth dongle plug in could also be beneficial for instant recovery, however when considering that the MCU is off after E-Stop the situation is problematic and may interfere with power segregation.

Finally, the achieved results were compared with the design specification – with the results listed in Table 15.

Table 15 – Electronics and software specification achievements

Criterion	Achieved Results	Status
Network	A VPN was set up between two computers and tested using TurtleSim	✓
SLAM	The LiDAR was tested both with Windows and with ROS	✓
Reliability	The heartbeat generator code created and ready to be implemented	✓
Speed	The code was made as short and clean as possible	✓
Motors and Controllers	Motors are powerful enough theoretically but are yet to be tested in the robot	-
Sensors	Capability for Stereoscopic Vision, Rearview Camera, IR, CO2 and Audio Sensing	✓
Sufficient heat exchange	A fan has been installed to ensure even heat distribution	✓
Powerboard	Smaller Powerboard built with sufficient room for expansion	✓
Master Switching	Prototyped board capable of switching power off upon low voltage and software bugs. Fully resettable to allow Bluetooth or Wifi control	✓
Modularity	Modular design created in view of allowing expansion from both electronics and software point of views	✓
Wiring & Fixings	Harwin connectors are used to connect power distribution wiring. A minimum of AWG 14 was used for connections with sufficient fuse	✓

6 FINAL DESIGN

This final design was a result of several design iterations and input from, academics specialists and technical staff. It was influenced by lessons learned from previous teams and a detailed analysis of competitors in the field. Not only has Orion been designed to be durable and fit for purpose in its intended environment, but commercial viability has also been considered. Figure 54 shows the WMR 2014/15's final design.

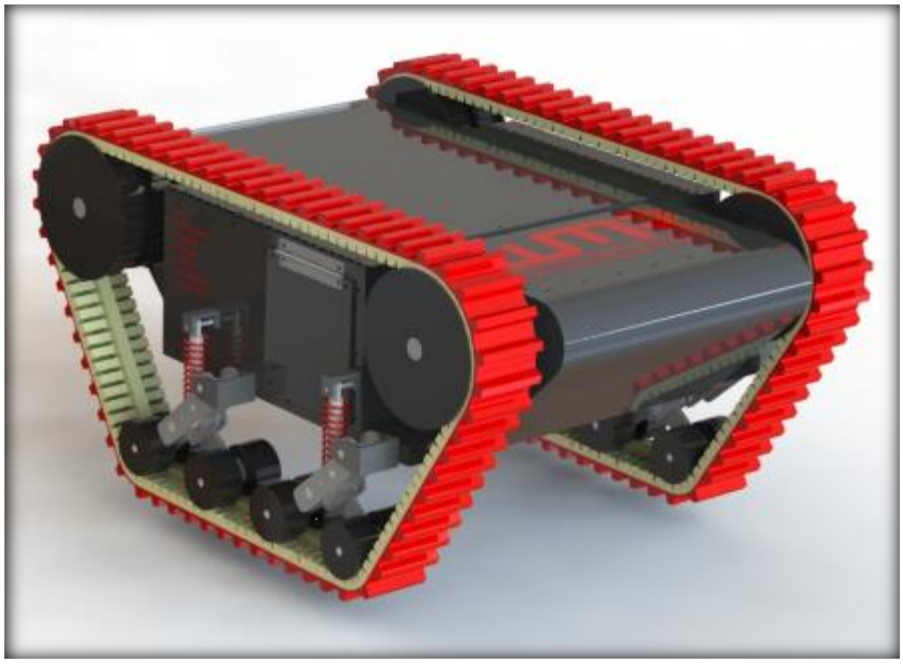

Figure 54 – WMR 2014/15's M-USAR, Orion

Areas of particular achievement and innovation were:

- Suspension system and high clearance that allows speed and mobility
- Tensioned tracks provided robustly with torque from high quality and well integrated motors - enabling inverted motion when needed
- Heightened accessibility for maintenance and safety, with all components designed with ease of manufacture and assembly
- A resettable and modular master switching, with LiPo battery monitoring allows an improved robot safety system and capability to switch between two different control strategies (Wifi and Bluetooth)
- Power board miniaturisation using standard size high power DC-DC converter blocks meant that Orion is capable of providing additional outputs to power further peripherals in the future, facilitating sustainable development whilst fitting effectively within a small chassis.

7 MANUFACTURE AND ASSEMBLY

This section documents one of the most challenging aspects of the project – the building of Orion. The WMR team conceptually designed the robot proficiently to meet objectives, however adapting the robot for feasible manufacture was more difficult. With relatively little practical engineering experience, this process took time, and multiple design iterations ensured all forms of designs (both mechanical and electronic) were integrated for manufacture, assembly and safety.

7.1 Design for Manufacture and Assembly

The purpose and importance of DFMA (Design for Manufacture and Design for Assembly) is widely reported in literature - with (Mascle, 2003) demonstrating that the key purpose is to decrease 'the product development' costs while simultaneously improving the overall quality of the component. Primarily DFMA has been become a philosophy for product optimisation from the viewpoint of assembly and part design. The generic guidelines include minimising part count, separate fasteners, orientation, improving ease of handling, utilising standardisation, using modular design and minimising operations that are non-value-adding. An important factor when manufacturing is safety and hence health and safety courses were taken throughout the year as outlined in Appendix G1.

7.2 Strategy and Method

Detailed concept designs on SolidWorks were based on many iterations and simulations which were of high quality from a theoretical viewpoint. Subsequently, the team approached WMG for consultation on engineering practice to adapt the designs for manufacture. This resulted in several changes of design details, including the addition of flats on shafts for grub screws, keyways, and bracket alterations. These changes were all to fix degrees of freedom and add restraints to motion, and also to meet the strategy objectives of durability and performance. Important factors in decision-making were reducing labour intensive processes, availability of material, and ease and speed of manufacture and assembly.

7.2.1 Technical Drawings

Every feature and component was modelled in SolidWorks to ensure designs were correct and precise. Moreover, the team generated approximately fifty technical drawings with all dimensions and detail documented, for WMG technicians to work from. An example of drawings and SolidWorks CAD are shown in Figure 55 with an accompanying image of the manufactured parts in situ.

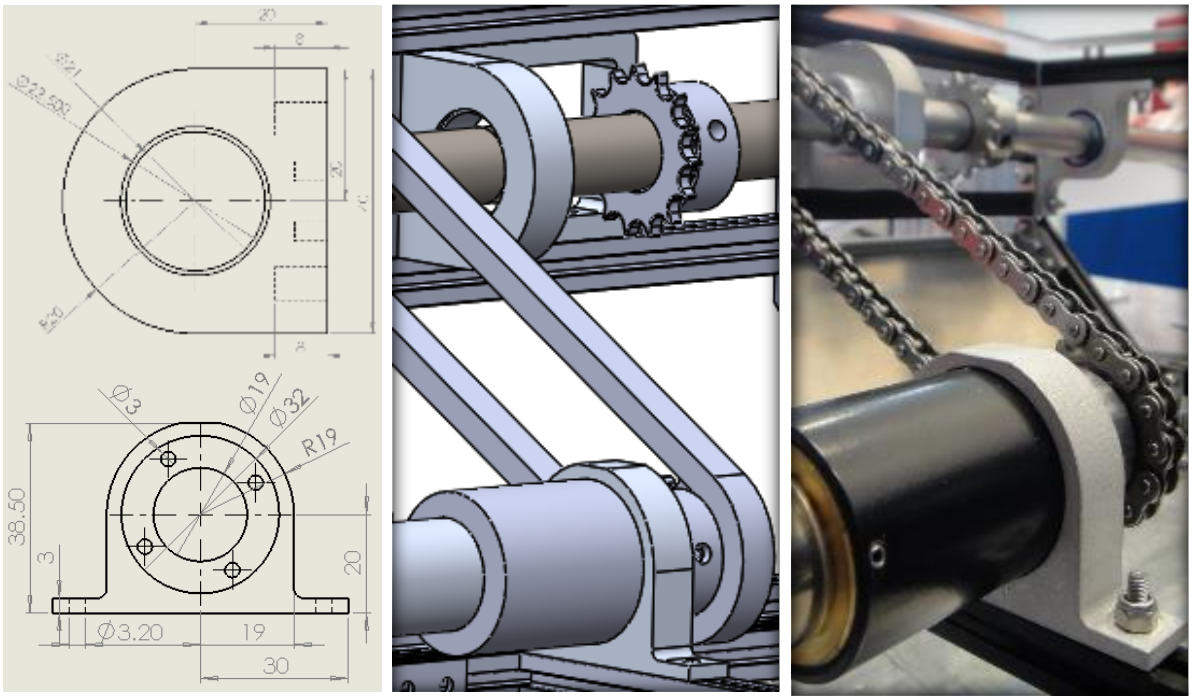

Figure 55 – Technical drawings, accompanying CAD and finished parts of Orion

7.2.2 Manufacturing Priority

Team members were responsible for various robot features as this was the most effective and efficient way to use the time and labour available. A manufacturing priority list of jobs was used to coordinate the effort, (see Appendix 7.1.) The high level summary of manufacturing priorities is shown in Figure 56. The assembly process began first with the chassis construction - then the transmission system was assembled so the electronics team could begin testing of motors in practice.

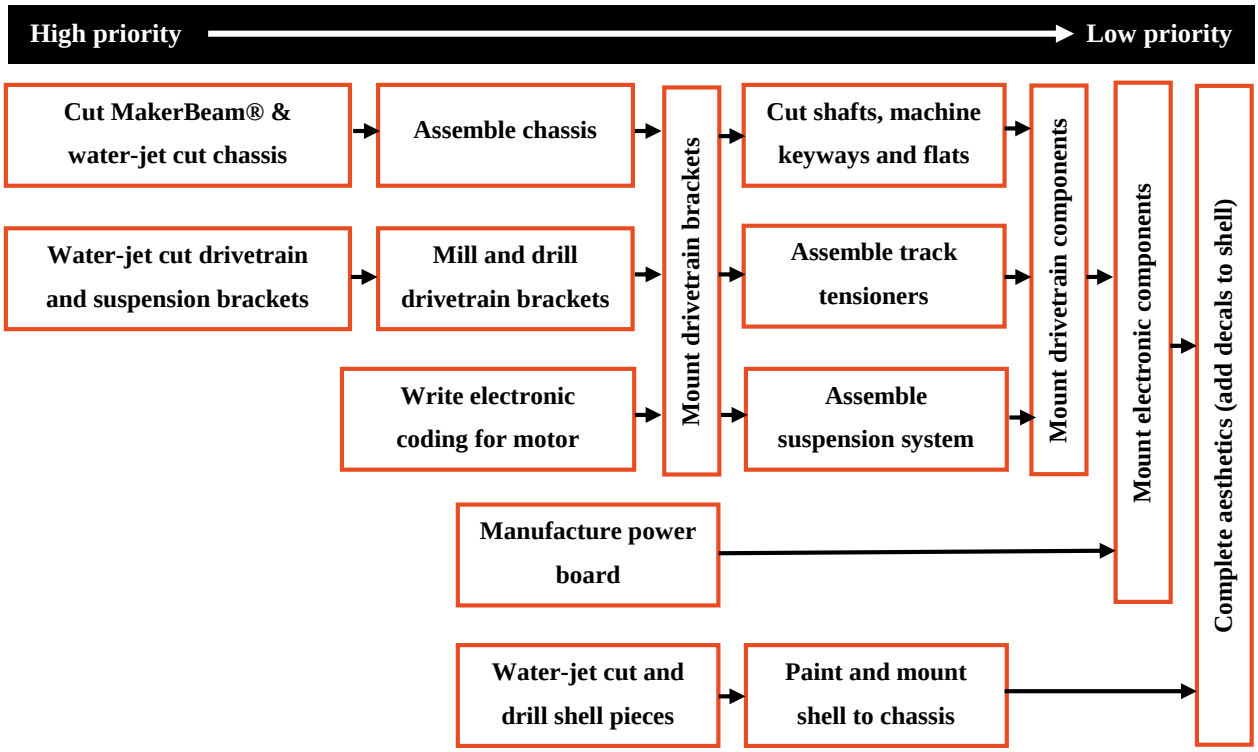

Figure 56 – Manufacturing priority diagram

7.2.3 Outsourcing

For speed, simple cutting was outsourced to Aquajet. Ltd, a company capable of cutting metals of many thickness and geometries by water jet. This experienced professional helped mitigate project risks and reduced costs through their larger network of resources and lower overheads. Volume was added to the designs digitally, and this material would be precision finished away after water jet cutting was complete.

7.2.4 Manufacturing Techniques

After the team received the water jet parts, milling the edges and drilling the mounting holes were the next steps. A precision 3- axis milling machine was used on aluminium 60-82 T6 (10, 20 mm) and Stainless Steel to achieve the highest tolerance. Drilling techniques such as clamps, centre punching the holes, drill tool and chamfering the edges were consistent throughout the manufacturing process.

7.2.5 Manufacturing Challenges

The biggest strains on the project were integrating the numerous areas of concept design into one coherent mechatronic platform, and transforming conceptually-sound designs into a physically-feasible robot. This involved many seemingly-minor, yet crucial considerations such as bearings and thrust washers, drive connections and constraints to limit degrees of freedom. Other hindrances to progress were the large lead times for ordering of components, and lengthy admin processes which are highlighted in Table 16.

Table 16 – Lead times of key components

Crucial Items	Expected Date	Actual Delivery Date
Maxon Motors	13/12/2015	08/01/2015
MakerBeam® Components	26/01/2015	12/01/2015
Pico - ITX	13/02/2015	Still awaiting
Brushless Camera Gimbal	18/02/2015	18/03/2015

7.2.6 Manufacturing Summary

Following the completion of the manufacturing stage of the project, Orion was fully assembled and mechanically functional. See Figure 57 and Figure 58 for images of the assembled robot.

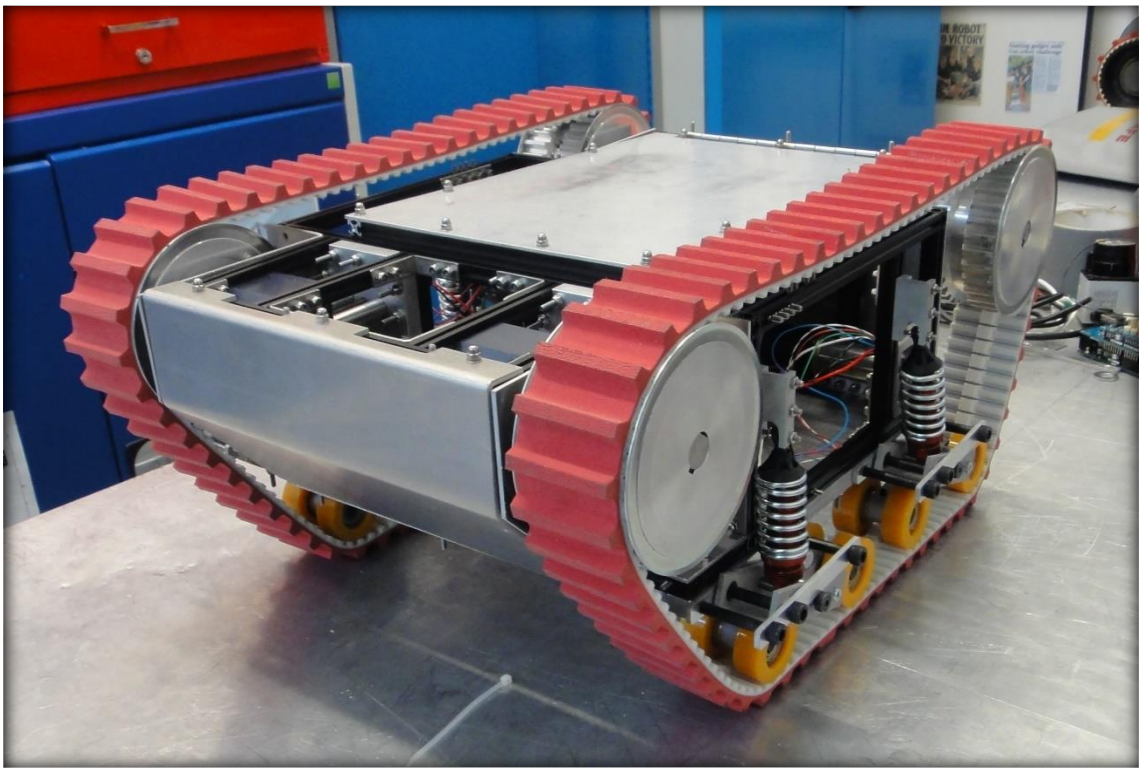

Figure 57 - Manufactured robot assembly isometric view

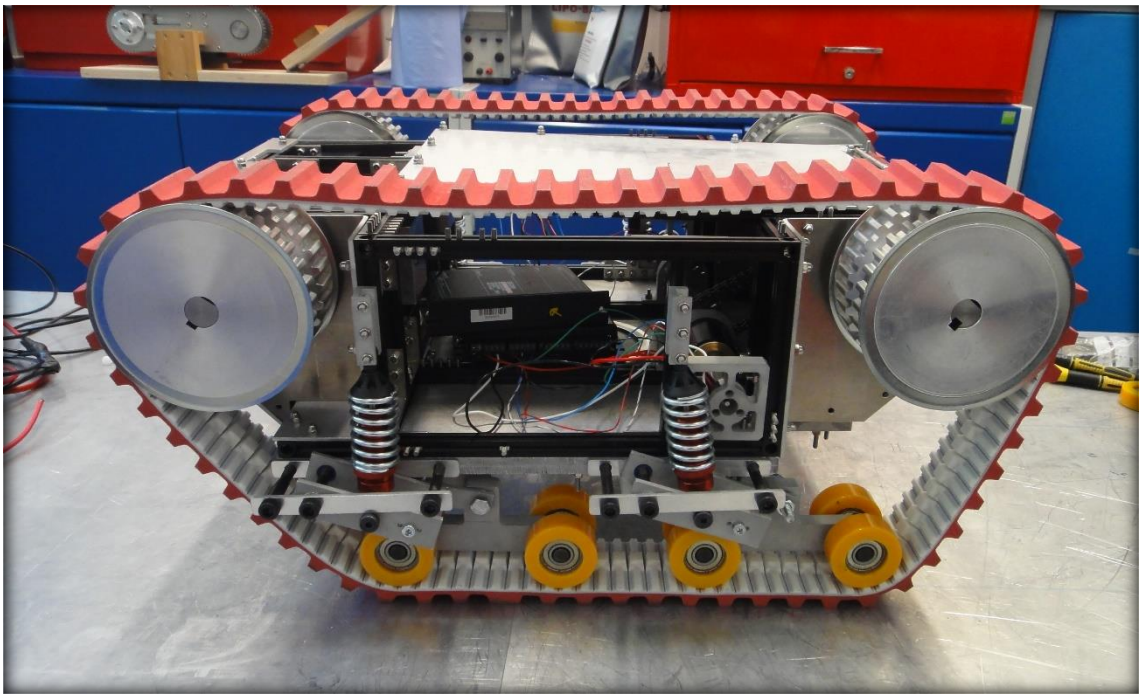

Figure 58 - Manufactured robot assembly side view

8 TESTING

8.1 Aims

Component and system testing were conducted over the duration of the project in order to ensure functional system operation, gauge the level of specification satisfaction and indicate levels of progress and achievement for WMR 2014/15.

8.2 Motor Testing

The new Maxon motors were tested against the Gimson Robotics GR02 motors used by the 2013/14 team. A seven-second pulse was sent to both motors to accelerate them to maximum rotational speed, which was held before decelerating back to zero. Graph 4 shows that the Maxon motors and the GR02 motors have a maximum no-load velocity of 20,000 rpm and 19400rpm respectively. The graph confirms that the implementation of the Maxon motors increases the acceleration (and deceleration) of the robot, increasing manoeuvrability when traversing dangerous terrain.

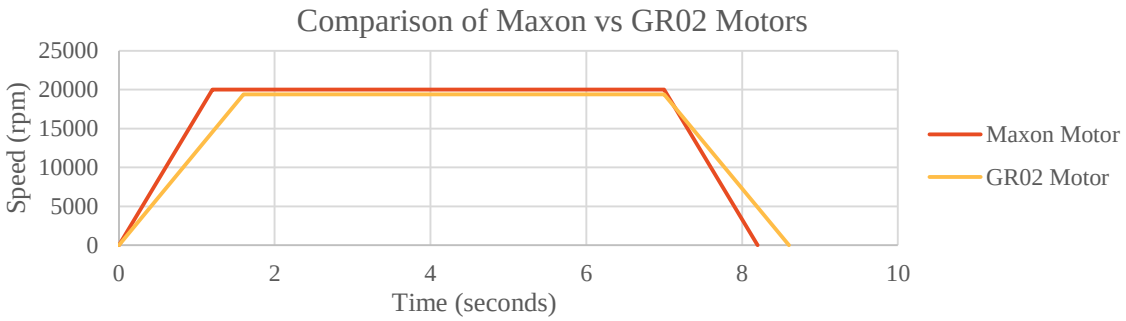

Graph 4 – Comparison of motors

8.3 Suspension Testing

Sophisticated calculations were conducted to estimate the stiffness of the springs required to adequately suspend the robot in Section 5.3.6.2. The calculations yielded the required spring rate to be approximately 15000N/m. In order to validate these calculations physical tests were conducted on a variety of springs. The chosen springs had to be capable of supporting a quarter of the total robot weight, which is approximately 6.25kg. For a suspension system it is recommended that the springs do not compress more than half of the total available spring travel, which was experimentally found to be 25mm. The maximum compression was therefore estimated to be 12mm.

Graph 5 shows the displacement experienced by three different springs under different loads. All three springs were found to displace a distance well under the maximum of 12mm. The

testing confirmed that the calculated spring rate would be sufficient to support the robot and hence the springs with a spring rate of 14350 N/m were chosen.

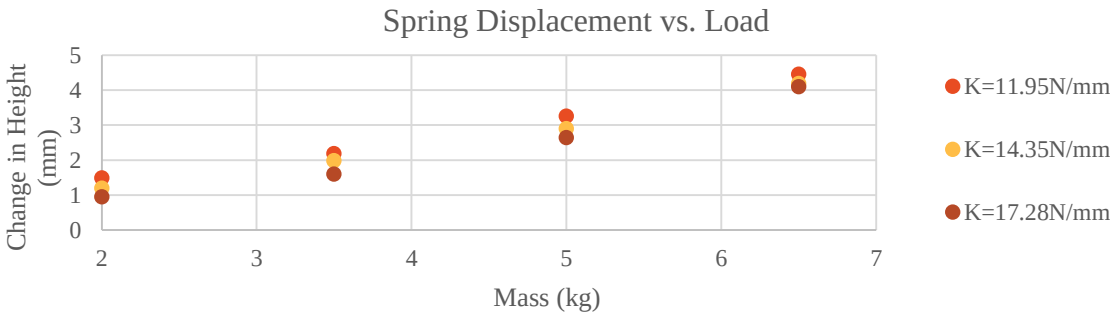

Graph 5 – Spring displacement test results

8.4 Weight and Mobility

Primary analysis confirmed that the robot was capable of mounting a 190mm step. These were purely mobility tests, without electronic components mounted or drive. Figure 59 shows Orion's suspension idlers adapting to the terrain for stability, and guard against toppling.

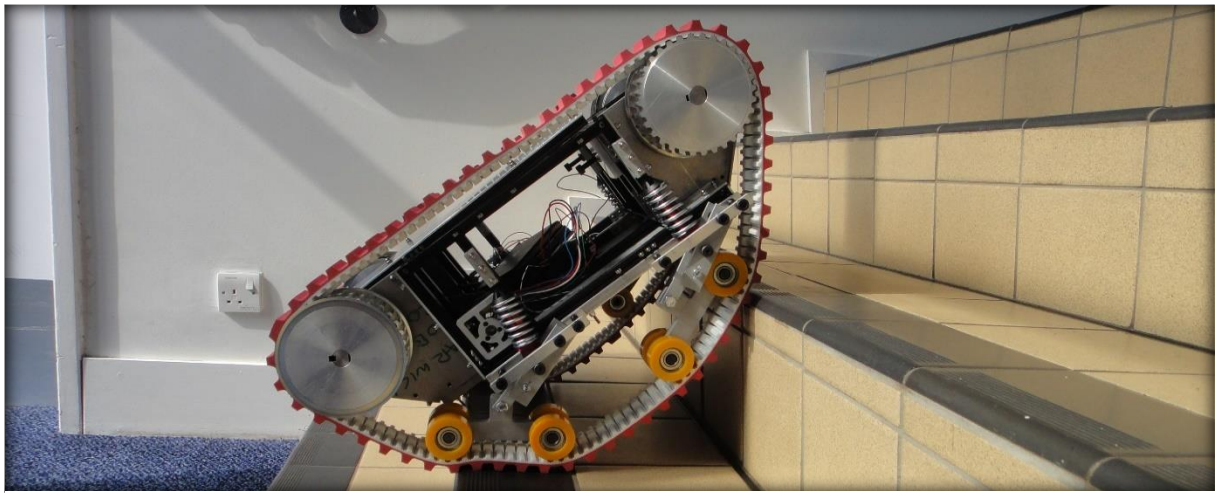

Figure 59 - Primary tests on Orion's mobility

8.5 Strengths & Weaknesses

The results from these tests and additional analysis conducted on Orion's design and manufactured components thus far yields the strengths and weaknesses in Table 17.

Table 17 - Strengths and weaknesses of Orion's design

Strengths	Weaknesses
+ Optimised drivetrain with tracks and suspension to enable multi-terrain travel	- Internal use of space could be more efficient
+ Strong & accessible chassis and shell	- Suspension is vulnerable to side impacts
+ Battery safety system through quick access and emergency stop	- Battery life shorter than anticipated
+ Modular and easily-adaptable mechanical and electrical systems	- Weight distribution

8.6 Degree of Specification Achievement

At the culmination of the project the level of achievement was obtained by analysing each aspect of the specification, as shown in Table 18.

Table 18 – Degree of specification achievement

ID	Parameter	Value / Description	Expected Achievement	Achieved
1	Accessibility			
1.1	Accessible Hatch Design	30 Seconds for a Battery Change	May 2015	✓
1.2	Deploy integrated USB access	Combine connections into a single USB port hub	May 2015	✓
2	Clearance			
2.1	High Track Radius	Climb stairs with a step height of 190mm at an angle of 38°	May 2015	✓
2.2	Low possibility of beaching	Minimum clearance of 100mm	May 2015	✓
3	Dimensions			
3.1	Capable of turning within a standard door width	Length < 460mm Width < 320mm Height < 242.5mm	May 2015	✓
3.2	Validate internal volume with calculations of cooling needs	Volume minimum of 3.9 x 10^{-3} m^3	May 2015	✓
3.3	Fan cool with ventilation	Minimum Flow rate of 0.31 Cmm	May 2015	✓
4	Weight			
4.1	Deployable by one person	Maximum weight of 25kg	May 2015	✓
4.2	Low lying centre of gravity	Centre of Gravity acts within the base on a 38° incline slope	May 2015	✓

5	Durability			
5.1	Vulnerable components inside chassis	Survive a 350mm drop impact	May 2016	✓
5.2	No cable connections through moving parts	Stationary, fixed internal connections	May 2015	✓
6	Drive			
6.1	Simple track design for high contact area and grip	Monolithic and rubber based tracks	May 2015	✓
6.2	Emphasis on controlled positioning	Accelerate at 0.3 m/s^2 Standard operation at 1m/s	May 2015	-
6.3	Return to base when upside down	Chassis within tracks	May 2015	-
6.4	Sufficient Torque to Climb Stairs	Minimum Torque of 20N/m	May 2015	✓
7	Electronics			
7.1	Provision for Development	Modular Architecture and additional ports	May 2015	✓
7.2	Capable of full tele-operated control when out of sight	Range of Speeds, standard operation at 1m/s	May 2015	✗
8	Sensory Array			
8.1	Sensory Array Design	Utilise LiDAR Technology	May 2016	✓

9 CRITICAL REVIEW

9.1 WMR Project

The WMR Team was assembled in October 2014 and by early April 2015 had constructed an innovative and versatile mechatronic platform for USAR development. The team had no prior robotics experience and this achievement is therefore a testament to the commitment of the WMR team. The group did well to re-evaluate early ambitions and aims in the project for more simplistic designs; six months is an intensely demanding time period to deliver a robot of any type, as the 2013/14 WMR team can testify to. Hence a three-year plan was deemed more realistic. A relatively simplistic design still proved to be a significant challenge, with external factors in ordering components dictating much of the progress. A clear strategy was in place from the project inception and was executed well. The team all logged a minimum of 330 hours of allocated project time in the pursuit of Orion, and the project easily came in under budget with a surplus of £1,156.82, or 15%. The team has also committed to documenting designs and programming in a dossier for next year's team, a luxury the 2014/15 team did not have, to ensure WMR 2015/16 hit the ground running and build on the progress achieved this year. A summary of key points and suggestions can be viewed in Section 10 Recommendations.

9.2 Design

Orion was intended to be particularly mobile with suspension to increase speed and ease of traversing obstacles. The robot return to base even when inverted with its innovative track layout, and all components are easily accessible through the shell hatches. Orion is small and lightweight and is capable of accessing confined spaces. There is provision for the addition of an arm and end-effector, and further functionality both mechanically and electronically as described in the three-year plan. The current specification adheres to RoboCup rules and Orion is a solid platform for development with the RoboCup as a long-term objective.

Industry expertise was incorporated through consultation with WMG technicians and component suppliers of including Transdev, and Maxon Motor. Conceptual designs were adapted several times to meet manufacturing requirements and to promote easy assembly, which was one of the most challenging aspects of the project. All these reasons indicate a successful and thorough design process. On evaluation of the final robot design, some points of improvement arose, which are on the following page.

- Centre of Gravity - the robot is designed with a narrow base in order to climb stairs and obstacles with an angled front. The addition of pulleys at the top corners of Orion result in an almost 'top heavy' robot, which reduces stability. This has been somewhat reduced by heavy components at the base of the chassis, including a 6kg 10mm aluminium base plate, which has proved to be effective.
- Internal Volume - though strict guidelines were put in place at the start of the project, increasing electronic requirements and additional components put pressure on available space inside the robot. Orientation of components also led to somewhat inefficient use of space.
- Suspension - highlighted as potentially vulnerable to side impacts. This could be rectified with a side guard.
- Battery Monitor Circuit – the robot in its initial stages of design used protoboard to design and build a battery monitor circuit. This is less space-efficient and less securely wired than a complete PCB.
- Battery Life – Due to chassis size constraints, only a single 6s 5Ah LiPo was used.

9.3 Manufacture

Manufacture was scheduled to begin in early 2015, with designs complete. This was the case, however the start of manufacture was delayed because of lengthy order processes and supplier lead times. Despite this, the team did well to take on responsibility of manufacture and training was sought for several applications, primarily drilling, and forward-thinking in design meant that the majority of custom components could be outsourced to water-jet cutting manufacturers. Assembly was achieved in a timely manner with input from the entire team.

9.4 Lessons Learnt

Valuable lessons taken from the project included the following:

- Consult expertise; as often as possible, both internally and externally
- Focus on simplicity; as is good engineering practice
- All issues stem from design; invest time and energy refining designs and benefit in manufacture
- Prepare for logistics; supplier lead times and lengthy processing dictated progress

10 RECOMMENDATIONS

In order to deliver a quality M-USAR that is fit for purpose in real world applications, it was recognised from the start of the project that further work would be continued through future seasons of the WMR project, in a three-year plan, see Figure 60. These developments were identified early on as requirements for competing at the RoboCup and arose through analysis of Orion's design. As a supplement for future teams to ensure progress, a detailed dossier of designs and programming has been compiled.

10.1 Further Work

- Review of internal arrangement to best utilise space and distribute heat.
- Sensory Array - all sensors have been designed, specified and provided for electronically and in the chassis design. They are also designed to be modular. Remaining tasks are implementation, and integrated design with an arm and end effector. There is ample USP provision on the Powerboard, so further sensory capability could be investigated. WMR owns several LiDAR sensors. An ideal design would include a spring loaded gimbal mount (to protect against damage in the event of being inverted) and a 360˚ camera would lend itself well to search and rescue.
- The battery monitor should hence be designed in the future using NI Ultiboard in the same manner the Powerboard was.
- Robot Arm and End Effector - several challenges at RoboCup, and in real world applications, require the use of a robotic arm to interact with targets. Orion has provision for this in its Powerboard design, and a large, supported upward facing area on top of the chassis is an ideal platform.
- The addition of an arm may destabilise Orion, and therefore an innovative solution could be sought to stabilise the robot while the arm is in operation.
- Future development should focus on the miniaturisation of sensor mountings. Consideration of a robotic Arm and head to relocate sensors would free internal chassis space to improve additional battery capacity.
- SoC (system-on-chip) ROS solutions are a relatively new technology and could be implemented in future iterations. This would aid miniaturisation, energy efficiency, and ease of code implementation. With a multitude of onboard connectivity options, the advantages of systems such as the CompuLab Utilite 2 should be considered (CompuLab, 2015).

- RoboCup rules state that bonus points are provided for 3D maps in addition to the compulsory 2D maps that must be submitted (Pellenz, 2014). Details of how to achieve this are included in the handover dossier.
- QR codes will be scattered across the RoboCup course and marks are awarded for correct identification of these codes. *Cob-Marker* is a ROS package that uses the camera to decipher the information in a QR code (Bohren, 2012).
- Implement the heartbeat generator mentioned in Section 5.4.5.6 to use as a diagnostics tool.
- Dynamic Tensioning - the tensioning system is well designed in that it can be both semi-static and dynamic. Currently a screw adjusts the position of the front axle and therefore degree of tension in the tracks. With the addition of specified springs this system can become dynamic.
- To increase performance in real-world applications, increasing the durability of Orion would be beneficial. This could be achieved by increasing its resistance to liquids; a welded, or composite shell would be an innovative development.

Following the hard work, forward-thinking and progress made by WMR 2014/15, the next chapter in the WMR three-year plan promises to be an exciting one for 2015/16 team, and the field of Urban Search and Rescue Robotics.

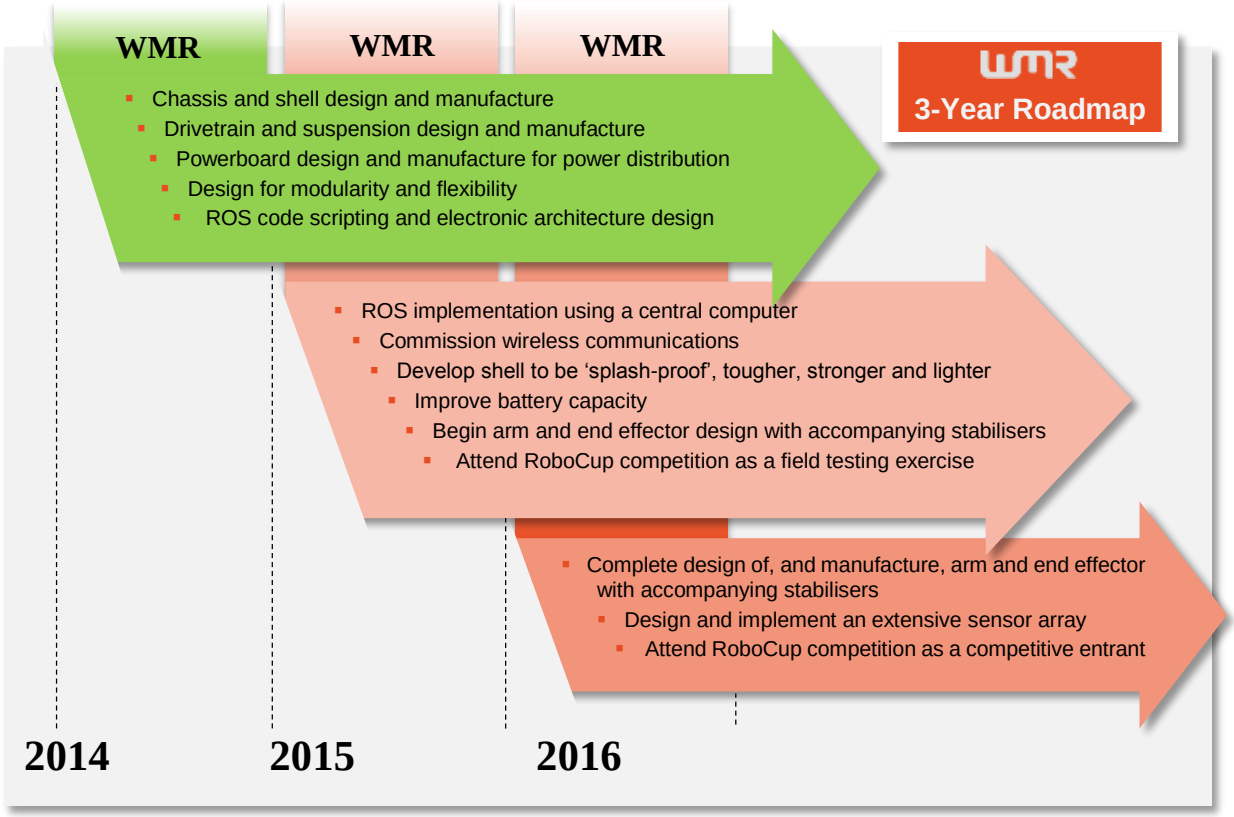

Figure 60 – WMR three year plan, first year achievement

11 CONCLUSIONS

"Success is the delivery of a product that meets expectation."

– James Leal, PID

The first year of the new WMR three-year plan having been completed, it is clear that extensive progress has been made in delivering a novel, exciting M-USAR robot. An innovative concept has been converted into a physical mechatronic platform with a good level of functionality, and provision made for further development both mechanically and electronically. In addition to this the WMR team have completed several Outreach programs, helping to inspire the next generation of engineers, details of which are outlined in the Cost Benefit Analysis. Through completing these tasks the WMR 2014/15 team have executed a strategy set out at the start of the 30 week project, and in doing so have achieved their aims and objectives.

The design of 'Orion' was built upon lessons learned from previous WMR projects and research into current competitors. Comprehensive background research and literature reviews were conducted before each aspect of design was undertaken, both mechanically and electronically. The WMR team, having had no previous robotics experience, undertook lengthy self-taught training to accomplish their considerable achievements. Integrating a full mechatronic design was the key challenge of the work, as well as tackling the significant obstacle of transforming a conceptually and theoretically sound design into good manufacturing practice, and a feasible assembly. All design decisions were justified with calculations, simulations and were made with the assistance of expertise from technicians and academics.

Orion has many competitive advantages and innovative features: it is lightweight and mobile, with high clearance, robust suspension, and easy access to its internal components via convenient access panels. A critical review from testing revealed the robot's vulnerabilities, which include its centre of gravity and stability. Scope for developments by future WMR teams has been included in the electronic architecture and a clear direction for such development has been outlined. Industry experts and suppliers were consulted throughout the design process: forging strong relationships for WMG and the University, whilst also gaining publicity for the WMR project.

Given the team's achievement of aims and objectives, delivery of the project 15% under budget, and the benefits to society offered including contributions to the important field of USAR robotics – it was felt that the 2014/15 WMR project should be considered a major success.


WMR
2014/15
Team

12 REFERENCES

4pcb, 2013. [Online]
Available at: http://www.4pcb.com/trace-width-calculator.html
[Accessed 29 January 2015].

Altium Ltd, 2004. [Online]
Available at:
http://www.altium.com/files/learningguides/ap0101%20polygon%20pours%20and%20copper%20regions.pdf
[Accessed 4 February 2015].

Anon., 2007. *VIA Motherboard Form Factor Comparison.* [Online]
Available at: http://www.flickr.com/photos/15932083@N05/2124071432/
[Accessed 01 03 2015].

Ashby, M. F., 2005. *Materials Selection in Mechanical Design.* 3rd ed. Amsterdam: Elsevier Butterworth- Heinemann.

ASUSTek Computer Inc, 2015. [Online]
Available at: http://www.asus.com/uk/Networking/RTAC66U/
[Accessed 20 January 2015].

Avago Technologies, 2013. *Avago HCPL-3120 Optocoupler.* [Online]
Available at: http://www.mouser.com/ds/2/38/AV02-0161EN_DS_HCPL-3120_2013-10-16-69256.pdf
[Accessed 1 February 2015].

Axiomtek, 2015. *PICO830.* [Online]
Available at:
http://axiomtek.com/Default.aspx?MenuId=Products&FunctionId=ProductView&ItemId=1036
[Accessed 22 2 2015].

BBC, 2014. *How robots are changing search and rescue.* [Online]
Available at: http://www.bbc.com/future/story/20140612-robots-to-the-rescue
[Accessed 10 April 2015].

Bohren, J., 2012. *cob_marker.* [Online]
Available at: http://wiki.ros.org/cob_marker

Buckstone, K. et al., 2013. *WMR ES410 Project Technical Report*, Coventry: University of Warwick.

Callister, W., 2007. *Materials Science and Engineering: an introduction.* 7th ed. New York: Wiley & Sons.

Carnegie Mellon University, 2015. *The DARPA Robotics Challenge.* [Online]
Available at: http://www.nrec.ri.cmu.edu/projects/tartanrescue/challenge/
[Accessed 10 April 2015].

Chavasse, C. et al., 2014. *Urban Search and Rescue Robotics: Technical Report*, Coventry: University of Warwick.

Chetwynd, D., 1992. *Foundations of Ultraprecision Mechanism Design*, Coventry: Gordon & Breach, Sciene Publishers.

CompuLab, 2015. [Online]
Available at: http://www.compulab.co.il/utilite-computer/web/utilite2-overview
[Accessed 2 April 2015].

DARPA, 2012. *No Bumps In The Road For DARPA's Robotic Suspension System.* [Online]
Available at: http://www.darpa.mil/NewsEvents/Releases/2012/03/22.aspx
[Accessed 17 March 2015].

Defense Update, 2009. *Weaponized RipSaw-MS2 UGV Evaluated for Convoy Security & Support.* [Online]
Available at: http://defense-update.com/products/r/ripsaw_ms2_141209.html
[Accessed 17 March 2015].

Engineering ToolBox, 2015. *Thermal Conductivity of Some Common Materials and Gases.* [Online]
Available at: http://www.engineeringtoolbox.com/thermal-conductivity-d_429.html
[Accessed 20 April 2015].

Fairhurst, G., 2008. *User Datagram Protocol.* [Online]
Available at: http://www.erg.abdn.ac.uk/users/gorry/course/inet-pages/udp.html
[Accessed 01 03 2015].

Farnell, 2015. [Online]
Available at: http://www.farnell.com/datasheets/1833179.pdf
[Accessed 29 January 2015].

Forum on Energy, 2013. *Rescue Robots: The Future of Nuclear Cleanup.* [Online]
Available at: http://forumonenergy.com/2013/12/30/rescue-robots-the-future-of-nuclear-cleanup/
[Accessed 10 April 2015].

fuRo, 2014. *fuRo.* [Online]
Available at: http://furo.org/en/works/quince.html

GE Industrial, 2015. [Online]
Available at: http://www.geindustrial.com/products/embedded-power/hammerhead
[Accessed 15 February 2015].

Gunderson, J. P., 2009. *Robots, Reasoning and Reification.* 1st ed. New York: Springer.

Harwin PLC, 2014. [Online]
Available at: http://www.harwin.com/products/M80-5000000M1-02-331-00-000/
[Accessed 30 November 2014].

Hudock, B. M., 2003. *Development of an urban search and rescue robot,* Annapolis, MD: US Naval Academy.

Hyperco, 2014. *Suspension Spring Rate and Wheel Rate Calculator.* [Online]
Available at: http://www.hypercoils.com/spring-calculator
[Accessed 20 April 2015].

Intersil Americas Inc., 2011. *Choosing and Using Bypass Capacitors.* [Online]
Available at: http://www.intersil.com/content/dam/Intersil/documents/an13/an1325.pdf
[Accessed 7 Feb 2015].

Kruijff, G.-J.et al., 2012. Recue Robots at earthquake-hit Mirandola, Italy: A field report. *2012 IEEE Internaional Symposium on Safety, Security and Rescue Robotics (SSRR),* Issue 5-8 Nov. 2012.

Lindell, D., 2014. *Crystallographic Effects in Corrosion of Austenitic Stainless Steels.* New York: Wiley & Sons.

LittelFuse Inc, 2014. [Online]
Available at:
http://www.littelfuse.com/~/media/electronics/datasheets/fuses/littelfuse_fuse_154_154t_154l_154tl_datasheet.pdf
[Accessed 30 November 2014].

Mascle, C., 2003. *Decision Support System in a Design for Assembly and Disassembly Methodology,* s.l.: IEEE International Symposium on Assembly and Task Planning.

Maxon, 2015. *Maxon EC 4-pole Brushless Motor.* [Online]
Available at:
http://www.maxonmotor.com/maxon/view/product/motor/ecmotor/ec4pole/323217

McGuigan, S. & Moss, P., 1998. A Review of Transmission Systems for Tracked Military Vehicles. *Journal of Battlefield Technology*, 1(3).

Milliken, W. F., 2002. *Chassis Design: principles and analysis.* 1st ed. Bury St Edmunds: Professional Engineering Publishing.

NHBC, 2014. Access to and use of buildings - dwellings. *Building Regulations Guidance Note.*

NHBC, 2014. *Building Regulations Guidance Note,* Milton Keynes: NHBC.

O'Kane, J. M., 2013. *A Gentle Introduction to ROS.* s.l.:s.n.

PEAK Electronics, 2012. [Online]
Available at: http://www.peak-electronics.de/dokumente/PEAK_Checkliste_Final_E,Nov12.pdf
[Accessed 7 February 2015].

Pellenz, J., 2014. *RoboCupRescue Robot League Rules for 2014.* [Online]
Available at: http://wiki.ssrrsummerschool.org/doku.php?id=rrl-rules-2014#changes

RCTanks, 2008. *Track Systems.* [Online]
Available at: http://www.rctankcombat.com/articles/track-systems/
[Accessed 18 March 2015].

Ringer, S. & Hono, K., 2000. *Materials Characterisation: Microstructural Evolution and Age Hardening in Aluminium Alloys.* Amsterdam: Elsevier.

RoboCup, 2013. *The robot that worked in Fukushima.* [Online]
Available at: http://www.robocup2013.org/the-robot-that-worked-in-fukushima/
[Accessed 10 April 2015].

Robocup, 2015. RoboCup Rescue. *RoboCup2015,* p. Accessed March 2015 at www.robocup2015.org/show/article/4.html.

ROS, 2011. *rosserial_arduino.* [Online]
Available at: http://wiki.ros.org/rosserial_arduino
[Accessed 28 2 2015].

ROS, 2013. *About ROS.* [Online]
Available at: http://www.ros.org/about-ros/.
[Accessed 12 02 2015].

ROS, 2014. *Technical Overview.* [Online]
Available at: http://wiki.ros.org/ROS/Technical%20Overview
[Accessed 01 03 2015].

Texas Instruments, 1995. *TI SN74ALS805B Hex 2-Input Nor Gate IC.* [Online]
Available at: http://www.farnell.com/datasheets/1850963.pdf
[Accessed 10 January 2015].

Tjinguytech, 2013. [Online]
Available at: http://www.tjinguytech.com/charging-how-tos/balance-connectors

TracoPower, 2015. *Traco Power TEN 40 DC-DC converters.* [Online]
Available at: http://www.tracopower.com/products/ten40.pdf
[Accessed 10 February 2015].

University of Bonn, 2015. *Autonomous Intelligent Systems: Nimbro Rescue.* [Online]
Available at: http://www.ais.uni-bonn.de/nimbro/Rescue/
[Accessed 10 April 2015].

Vishay Intertechnology Inc, 2014. [Online]
Available at: http://www.vishay.com/docs/93459/vs-fb190sa10.pdf
[Accessed 9 December 2014].

WMR, 2013. *WMR 2012-13 Technical Report.* [Online]
Available at:
http://www2.warwick.ac.uk/fac/sci/eng/meng/wmr/projects/rescue/reports/1112reports/wmr2012-tech_report.pdf
[Accessed 20 April 2015].

WMR, 2014. *Urban Search and Rescue Robotics*, Coventry: University of Warwick.

Wong, J., 1993. *Theory of Ground Vehicles.* 2nd ed. New York: J. Wiley.

Wurm, K. M. & Hornung, A., 2014. *An Efficient Probabilistic 3D Mapping Framework Based on Octrees.* [Online]
Available at: http://octomap.github.io/

Team Member: *Craig* **Sheet Last Updated:** *DATE*
Total Hours Worked: *355.5* **Av. Hours Per Week:** *12.2*

Date	No. of Hours	Activity Type	Activity Description
30 September 2014	1.0	Group Meeting	Induction meeting with Emma Rushforth
02 October 2014	1.0	Group Meeting	Initial project meeting to get to know each other and discuss preliminary project direction possibilities
07 October 2014	1.5	Non-Technical Role (eg. Finance, Sponsorship etc.)	Researching previous sources of sponsorship and editing Sponsorship Form from last year's team
08 October 2014	2.0	Technical Research	Researching materials and other robots to improve chassis
08 October 2014	0.5	Health and Safety	IMC Health and Safety briefing
08 October 2014	4.0	Non-Technical Role (eg. Finance, Sponsorship etc.)	Contacting Lisa Barwick regarding publicity and editing Sponsorship Form from last year's team
13 October 2014	0.5	Non-Technical Role (eg. Finance, Sponsorship etc.)	Writing generic sponsorship cover letter and sent sponsorship proposal to Makeblock
14 October 2014	1.0	Group Meeting	Weekly meeting with Emma Rushforth
14 October 2014	1.0	Non-Technical Role (eg. Finance, Sponsorship etc.)	Making Timesheet work correctly and sent sponsorship proposal to Makerbeam
15 October 2014	1.0	Design	Transferring Inventor files into SolidWorks
15 October 2014	2.5	Group Meeting	Defining basic to-do list, top level objectives, and robot area ownerships
15 October 2014	2.0	Report Writing/Formatting/Compilation etc.	Compiling to-do list for chassis
16 October 2014	2.0	Report Writing/Formatting/Compilation etc.	Compiling Gantt chart for chassis
17 October 2014	2.0	Non-Technical Role (eg. Finance, Sponsorship etc.)	Sponsorship form and website updating
20 October 2014	2.0	Report Writing/Formatting/Compilation etc.	Compiling Gantt chart for Milestone Report

APPENDICES

Appendix A: Project Documents

Appendix A1: Individual Timesheet

Appendix A2: Budget & Technology List

	Reference	Quantity	Supplier	Expected	Actual	Budget	Surplus	Ordered	Approval	Status of Order
Fan	http://uk.farnell.com/sunon/mb50100v2-0000-a99/fan-50x50x10mm-5vdc/	1	onecall	8.44	**£22.96**			yes	AP	Delivered
64 gb USB drive	http://www.memorybits.co.uk/product_info.php?products_id=27376	1		8.44	**£20.38**			yes	JS	
Brushless Gimbal	http://www.ebay.co.uk/itm/Gopro-Brushless-Camera-Gimbal-w-Motors-C	1	Ebay	8.44	**£33.20**			yes	JS	Ordered will be deliver
Soldering Tool and Braid			Vic					yes	JS	Delivered
LittelFuse 1A	http://uk.farnell.com/littelfuse/0464001-dr/fuse-fast-acting-smd-1a/dp/1817	10	Farnell	7.10	**£5.80**			yes	JS	Delivered
LittelFuse 3.5A	http://uk.farnell.com/littelfuse/015402-5dr/fuse-smd-omni-block-f-3-5a/dp	10	Farnell	8.80	**£7.20**			yes	JS	Delivered
LittelFuse 30A	http://uk.farnell.com/littelfuse/0456030-er/fuse-smd-30a-vi-fast-acting/dp	10	Farnell	15.60	**£12.80**			yes	JS	Delivered
10 PORT Powered USB	http://www.rapidonline.com/office-it/logilink-usb-2-0-hub-10-port-with-on-c	1	Rapid Online	20.92	**£20.92**			yes	JS	Processing, wk 22
Quad 2 input NOR (TI SN74HCT02N)	http://uk.farnell.com/texas-instruments/sn74hct02n/logic-quad-2-in-nor-g	5	Farnell	1.68	**£1.40**			yes	JS	Delivered
Hex 2 input NOR (TI SN74AS805BN)	http://uk.farnell.com/texas-instruments/sn74as805bn/logic-gate-nor-hex-	5	Farnell	9.70	**£7.95**			yes	JS	Delivered
Multicomp 20POS DIP socket	http://uk.farnell.com/multicomp/spol550l/dip-socket-20pos-through-hole	5	Farnell	0.66	**£0.55**			yes	JS	Delivered
optocoupler (AVAGO HCPL-3120-000E)	http://uk.farnell.com/avago-technologies/hcpl-3120-000e/optocoupler-2-5	3	Farnell	6.24	**£5.13**			yes	JS	Delivered
Battery Electronics					**£69.76**	£0.00				
Lipo Batteries					£69.76			yes	JS	Ordered, Finance has
Sensors				**£0.00**	**£73.74**	**£300.00**	£226.26			
CO2	http://www.dfrobot.com/index.php?route=product/product&product_id=10	1	dfrobot		£0.00			yes	JS	Delivered
IMU	https://www.xsens.com/wp-content/uploads/2013/11/mti-leaflet.pdf	1	xsens		£0.00			yes	JS	Delivered
LED	http://www.farnell.com/datasheets/1783696.pdf	2	CRE		£3.76			yes	JS	Delivered
Lidar	https://www.hokuyo-aut.jp/02sensor/07scanner/urg_04lx_ug01.html	1	hokuyo		£0.00			yes	JS	Delivered
camera	http://www.microsoft.com/hardware/en-gb/d/lifecam-hd-3000	1	microsoft		£49.99			yes	JS	Delivered
IR camera	http://www.flir.com/uploadedFiles/CVS_APAC/Cores_and_Components	1	flir		£0.00			yes	JS	Delivered
LCD	http://www.amazon.co.uk/SainSmart-Serial-Module-Display-Arduino/dp/E	1	SainSmart		£19.99			yes	JS	Delivered
Manufacturing					**£726.45**	**£500.00**	-£226.45			
Waterjet cutting	Cutting Edge Technology				**£300.00**			Yes	PM	Delivered
Spray/powder paint chassis					**£18.00**					
Engineering Stores Tab					**£408.45**					
Clothing				**£234.62**	**£234.62**	**£300.00**	£65.38			
Polo shirts (inc. 7 logos and personalised names)	Quote reference 50188	8	Acorn Printing	£234.62	£234.62			Yes	CF	Delivered
Total				**£1,603.91**	**£3,770.33**	**£4,800.00**	£1,549.43			

Appendix A3: Manufacturing Priority List

Table 19 – Testing Criteria

Appendix B: Testing Criteria

Testing Objective	Test	Desired Result
Volume and Cooling	Run motors on full load and record temperature distribution	Functional for a sustained period
Stair Climb	Drive up 5 Steps	Capability
Drop Impact	Drop from 350mm on hard floor	Minor/No Damage/Still functional
Durability - Multiple terrains	Drive over mud/ water/hard wood/sand	No Functional change
Traction	38’ ramp	Capability
Control - Return to base	Start robot upsides down	Capable movement
Control - variable speed	Test motors and drivetrain	3 speed modes
Sensory Array	Detection for sources of CO2, Heat etc	Sense signs of life

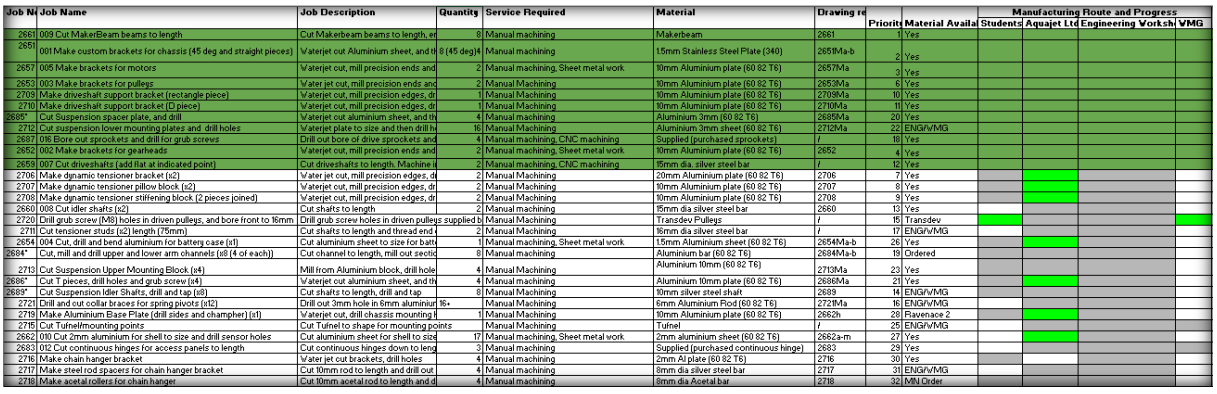

Job No	Job Name	Job Description	Quantity	Service Required	Material	Drawing re	Priority	Material Availa	Manufacturing Route and Progress			
									Students	Aquajet Ltd	Engineering Worksh	VMG
2661	009 Cut MakerBeam beams to length	Cut Makerbeam beams to length, er	8	Manual machining	Makerbeam	2661	1	Yes				
2651	001 Make custom brackets for chassis (45 deg and straight pieces)	Waterjet cut Aluminium sheet, and th	8 (45 deg)4	Manual machining	1.5mm Stainless Steel Plate (340)	2651Ma-b	2	Yes				
2657	005 Make brackets for motors	Waterjet cut, mill precision ends and	2	Manual machining, Sheet metal work	10mm Aluminium plate (60 82 T6)	2657Ma	3	Yes				
2653	003 Make brackets for pulleys	Water jet cut, mill precision ends and	2	Manual Machining	10mm Aluminium plate (60 82 T6)	2653Ma	6	Yes				
2709	Make driveshaft support bracket (rectangle piece)	Waterjet cut, mill precision edges, dr	1	Manual Machining	10mm Aluminium plate (60 82 T6)	2709Ma	10	Yes				
2710	Make driveshaft support bracket (D piece)	Waterjet cut, mill precision edges, dr	1	Manual Machining	10mm Aluminium plate (60 82 T6)	2710Ma	11	Yes				
2685*	Cut Suspension spacer plate, and drill	Waterjet cut aluminium sheet, and th	4	Manual machining	Aluminium 3mm (60 82 T6)	2685Ma	20	Yes				
2712	Cut suspension lower mounting plates and drill holes	Waterjet plate to size and then drill ho	16	Manual Machining	Aluminium 3mm sheet (60 82 T6)	2712Ma	22	ENGifVMG				
2687	016 Bore out sprockets and drill for grub screws	Drill out bore of drive sprockets and	4	Manual machining, CNC machining	Supplied (purchased sprockets)	/	18	Yes				
2652	002 Make brackets for gearheads	Waterjet cut, mill precision ends and	2	Manual machining, Sheet metal work	10mm Aluminium plate (60 82 T6)	2652	4	Yes				
2693	007 Cut driveshafts (add flat at indicated point)	Cut driveshafts to length, Machine a	2	Manual machining, CNC machining	15mm dia. silver steel bar	/	12	Yes				
2706	Make dynamic tensioner bracket (x2)	Water jet cut, mill precision edges, d	2	Manual Machining	20mm Aluminium plate (60 82 T6)	2706	7	Yes				
2707	Make dynamic tensioner pillow block (x2)	Waterjet cut, mill precision edges, dr	2	Manual Machining	10mm Aluminium plate (60 82 T6)	2707	8	Yes				
2708	Make dynamic tensioner stiffening block (2 pieces joined)	Waterjet cut, mill precision edges, dr	2	Manual Machining	10mm Aluminium plate (60 82 T6)	2708	9	Yes				
2660	008 Cut idler shafts (x2)	Cut shafts to length	2	Manual machining	15mm dia silver steel bar	2660	13	Yes				
2720	Drill grub screw (M8) holes in driven pulleys, and bore front to 16mm	Drill grub screw holes in driven pulleys supplied b		Manual Machining	Transdev Pulleys	/	15	Transdev				
2711	Cut tensioner studs (x2) length (75mm)	Cut shafts to length and thread end	2	Manual Machining	16mm dia silver steel bar	/	17	ENGifVMG				
2654	004 Cut, drill and bend aluminium for battery case (x1)	Cut aluminium sheet to size for batt	1	Manual machining, Sheet metal work	1.5mm Aluminium sheet (60 82 T6)	2654Ma-b	26	Yes				
2684*	Cut, mill and drill upper and lower arm channels (x8 (4 of each))	Cut channel to length, mill out sectio	8	Manual machining	Aluminium bar (60 82 T6)	2684Ma-b	19	Ordered				
2713	Cut Suspension Upper Mounting Block (x4)	Mill from Aluminium block, drill hole	4	Manual Machining	Aluminium 10mm (60 82 T6)	2713Ma	23	Yes				
2686*	Cut T pieces, drill holes and grub screw (x4)	Waterjet cut aluminium sheet, and th	4	Manual machining	Aluminium 10mm plate (60 82 T6)	2686Ma	21	Yes				
2689*	Cut Suspension Idler Shafts, drill and tap (x8)	Cut shafts to length, drill and tap	8	Manual Machining	10mm silver steel shaft	2689	14	ENGifVMG				
2721	Drill and cut collar braces for spring pivots (x12)	Drill out 3mm hole in 6mm aluminiur	16+	Manual Machining	6mm Aluminium Rod (60 82 T6)	2721Ma	16	ENGifVMG				
2719	Make Aluminium Base Plate (drill sides and champher) (x1)	Waterjet cut, drill chassis mounting h	1	Manual Machining	10mm Aluminium plate (60 82 T6)	2682h	28	Pavenace 2				
2715	Cut Tufnel/mounting points	Cut Tufnel to shape for mounting points		Manual Machining	Tufnel	/	25	ENGifVMG				
2682	010 Cut 2mm aluminium for shell to size and drill sensor holes	Cut aluminium sheet for shell to size	17	Manual machining, Sheet metal work	2mm aluminium sheet (60 82 T6)	2682a-m	27	Yes				
2683	012 Cut continuous hinges for access panels to length	Cut continuous hinges down to leng	3	Manual machining	Supplied (purchased continuous hinge)	2683	29	Yes				
2716	Make chain hanger bracket	Water jet cut brackets, drill holes	4	Manual machining	2mm Al plate (60 82 T6)	2716	30	Yes				
2717	Make steel rod spacers for chain hanger bracket	Cut 10mm rod to length and drill out	4	Manual machining	8mm dia silver steel bar	2717	31	ENGifVMG				
2718	Make acetal rollers for chain hanger	Cut 10mm acetal rod to length and d	4	Manual machining	8mm dia Acetal bar	2718	32	MN Order				

Appendix C: Specification Justification

Appendix C1: Robot Dimensions

The maximum external dimensions are limited by a 750mm wide doorway and 750mm wide hallway, based on NHBC building regulations. The robot needs to be able to pass through the doorway and fully rotate in the hallway as detailed in (NHBC, 2014).

For a known limited doorway and hallway width (a_1) and a chosen robot width (L_2), the maximum turning radius (r) can be calculated using Equation C1 and is dependent on the desired wall clearance (a_2). The maximum robot length (L_1) can be calculated using Equation C2.

$$r = \frac{a_1}{2} - a_2 \qquad (C1)$$

$$L_1 = \sqrt{(2r)^2 - L_2^2} \qquad (C2)$$

Table 20 – Robot external dimension parameters

Parameter	Notation	Dimension (mm)
Doorway / Hallway Width	a_1	750.0
Wall Clearance	a_2	20.0
Maximum Robot Length	L_1	580.0
Robot Width	L_2	410.0
Maximum Turning Radius	r	355.0

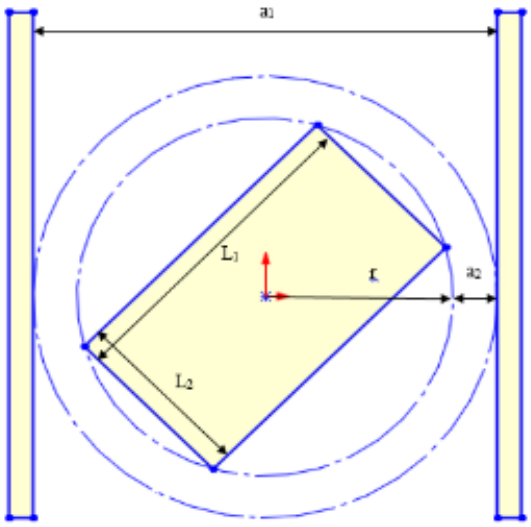

Figure 61 – Robot external dimension restrictions

Appendix C2: CoG Calculations

As depicted in Figure 62, the CoG needs to be in front of the rear pivot point of the robot on a slope of 38°. This angle is based on building regulations regarding staircases for a semi-public application. The resultant of the positive (clockwise) moments generated about the CoG and the negative (anti-clockwise) moments generated about the CoG must be positive to ensure the robot doesn't overturn on a staircase; $M_{pos} > M_{neg}$. These moments consider the acceleration of the robot, weight distribution and weight components at the CoG which are labelled on Figure 63.

Both figures take the form of a bicycle model, whereby the left and right tracks are lumped into one entity to simplify calculations. The model assumes the mass of the robot and the acceleration on the robot acts from the centre of gravity (CoG). The weight distribution is assumed to act at two points on the robot; one at the front and one at the rear. The incline is assumed to be of a constant gradient. The robot is assumed to have constant traction and not slip during acceleration. This model also negates any effects of air resistance, lift and rolling resistance.

Equations C3 to C8 describe how to solve the model.

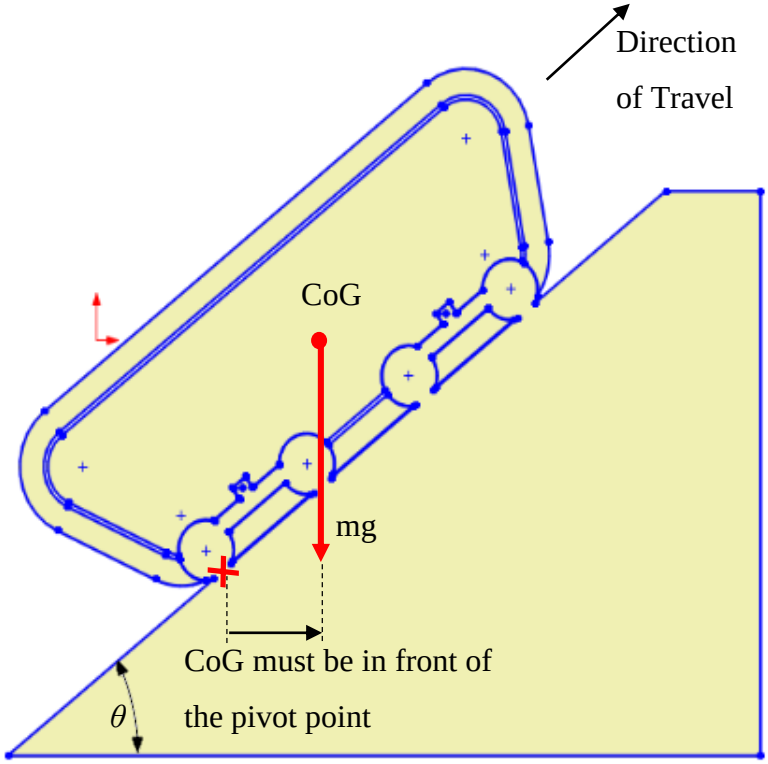

Figure 62 – Centre of gravity location relative to pivot

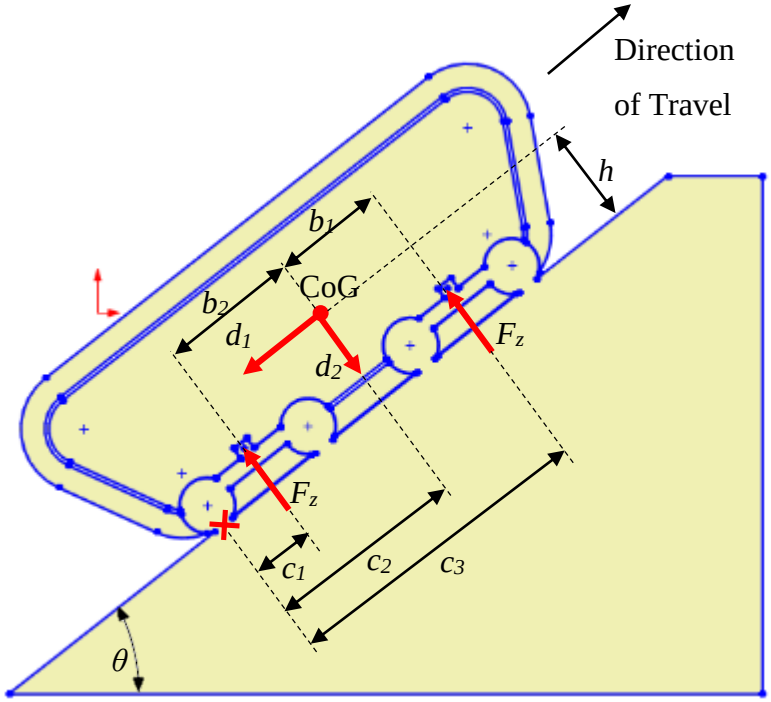

Figure 63 – Positive and negative moments about pivot point

$$F_{zF} = mg\left(\frac{b_2}{b_1 + b_2}\cos\theta - \frac{h}{b_1 + b_2}\sin\theta\right) - \frac{h\,m\,a}{b_1 + b_2} \quad (C3)$$

$$F_{zR} = mg\left(\frac{b_1}{b_1 + b_2}\cos\theta + \frac{h}{b_1 + b_2}\sin\theta\right) + \frac{h\,m\,a}{b_1 + b_2} \quad (C4)$$

$$d_1 = ma + mg\sin\theta \quad (C5)$$

$$d_2 = mg\cos\theta \quad (C6)$$

$$M_{pos} = c_2\,d_2 \quad (C7)$$

$$M_{neg} = c_1 F_{zR} + c_3 F_{zF} + h d_1 \quad (C8)$$

Table 21 – Parameters for robot centre of gravity and moments about pivot point

Parameter	Notation	Value
Gravity	g	9.81 ms^{-2}
Robot Acceleration	a	0.3 ms^{-2}
Angle of Incline	θ	38°
Front Normal Reaction Force	F_{zF}	To be designed
Rear Normal Reaction Force	F_{zR}	To be designed
Robot Mass	m	To be designed
CoG to Front Span	b_1	To be designed
CoG to Rear Span	b_2	To be designed
CoG Height	h	To be designed
Pivot Point to Rear Span	c_1	To be designed
Pivot Point to CoG Span	c_2	To be designed
Pivot Point to Front Span	c_3	To be designed
Mass and Acceleration Component (Horizontal)	d_1	To be designed
Mass Component (Vertical)	d_2	To be designed
Positive Moments About Pivot Point (Clockwise)	M_{pos}	$> M_{neg}$
Negative Moments About Pivot Point (Anti-Clockwise)	M_{neg}	$< M_{pos}$

Appendix D: Chassis

Appendix D1: Chassis Full Specification

Table 22 – Full Chassis Specification

ID	Parameter	Value / Description
1	Dimensions and Shape	
1.1	Chassis length	Maximum chassis length of 522.0 mm
1.2	Chassis width	Maximum chassis width of 369.0 mm
1.3	Chassis height	Maximum chassis height of 315.0 mm
1.4	Internal chassis volume	Minimum internal chassis volume of 3.9×10^{-3} m^3 to house all electronics and hardware
1.5	Clearance over obstacles	Front and rear of chassis underside must be chamfered or curved and underside of robot should be as high as practically possible above the ground
2	Mass	
2.1	CoG location	CoG must lie in front of the pivot point and be equally spread front to back along the chassis
2.2	Chassis weight	Maximum chassis and shell mass should be less than 5kg (20% of overall robot mass)
3	Load Resistance	
3.1	Fall resistance	Fall from 350 mm (vertical impact force of 655 N) must not affect operability
3.2	Crash resistance	Crash into an immovable object at 1.0 ms^{-1} (crash force of 250 N) must not affect operability
4	Accessibility	
4.1	Quick battery access	Use access panels to allow maximum battery change time of 30 seconds
4.2	Easy access to internal components	Use access panels to provide easy access to key internal components within the chassis
5	Manufacturability	
5.1	Chassis assembly	Chassis should be easy to assemble and fix in the case that some parts get damaged
5.2	Chassis design flexibility	Chassis design should be modular, allowing more components to be easily added to the frame as required

Appendix D2: Chassis Internal Volume

Table 23 – Chassis internal volume requirements

Component	Quantity	Estimated Volume (mm^3)
Electric Motor	2	37,000
Gearbox	2	70,000
Motor Controller	2	420,000
Power Board	1	576,000
Pico ITX	1	646,000
Arduino Mega 2560	1	240,000
Wireless Router	1	811,000
Li-Ion Battery Pack	1	533,000
Cooling Fan	1	12,000
Wiring Looms	N/A	70,000
Drivetrain System (drive shafts, sprockets, etc.)	N/A	150,000
Dynamic Track Tensioning System	2	294,000
Total Estimated Volume		**3,859,000 (3.9×10^{-3} m^3)**

Table 24 – Chassis design summary

Chassis Version	Length (mm)	Width (mm)	Height (mm)	Internal Volume (m^3)	Ratio of Internal Volume to LWH
V1	440	320	160	7.76×10^{-3}	0.34 (34%)
V2	440	223	160	6.69×10^{-3}	0.43 (43%)
V3	440	326	177	7.30×10^{-3}	0.29 (29%)
V4	440	323	120	13.61×10^{-3}	0.80 (80%)

Appendix D3: Fall Resistance - Equations of Motion

Equations D1 to D3 were used in calculating the fall impact and crash impact forces for simulations on the robot chassis.

$$v = \sqrt{2\,g\,s} \qquad (D1)$$

$$a = -{}^{v}/_{t} \qquad (D2)$$

$$F = ma \qquad (D3)$$

Appendix D4: Materials Comparative Study

Appendix D41 Aluminium

The microstructure and chemical composition of 2000 and 6000 series aluminium alloys are displayed in Table 25. As shown in the table, 2024T3 has a greater copper weight percentage than 6082T6. One can deduce that the former has been subjected to greater age- hardening. More specifically, (Ringer & Hono, 2000) outlined the saturated copper atoms form GP zones. The difference in these zones strain the lattice thus ongoing coherency and strain stress. These GP zones are, subsequently, replaced with a theta'' precipitation which are not fully coherent within the matrix. Furthermore, (Ringer & Hono, 2000) emphasised further growth leads to the metastable theta' phase which is isomorphous within the aforesaid lattice. Thus, these have a lower interfacial energy than equilibrium phases of a similar crystal structure. As the nature of the precipitation process has been identified, one can examine and identify how this is relevant to 2000 and 6000 aluminium alloys. Principally, a 2000 system is normally alloyed with copper, possesses high strength but lacks durability. In a 6000 series aluminium alloy system, GP zones (now magnesium and silicon atoms) are replaced with beta'' precipitation as opposed to theta. This stage is followed by beta' phase and then progressively to the equilibrium beta phase. The 6082T6 alloy is more formable and possesses medium strength compared to its 2000 counterpart applications. The use of 6082T is therefore favoured.

Table 25 - Chemical Composition (% weight) of the Alloys

	Cu	Mg	Mn	Fe	Si	Zn	Cr	Ti	Al
6082T6	0.08	0.78	0.48	0.39	0.95	0.04	0.03	0.05	97.2
2024T3	4.67	1.34	0.63	0.25	0.15	0.02	0.01	0.06	92.87

Appendix D42 Steel

Austenitic stainless steel has good microstructure stability and excellent resistance to corrosion (Lindell, 2014). These steels' microstructure are equiaxed austenite. This material stays in its face- centred cubic (fcc) lattice structure over the entire temperature range. Contrarily, ferritic steels transform drastically from a body-centred cubic lattice (bcc) to a face- centred cubic lattice of austenite. The chemical compositions within these 300 series alloys are depicted in Table 26.

Table 26 - Chemical Composition (% weight) of Chromium and Nickel in Stainless Steel

	304	321	347
Chromium	18-20	17-20	17-20
Nickel	8-11	9-13	0.63

In a forming context, 321 and 341 are preferred over the 304 as it is harder. Type 321 has better resistance to oxidation and corrosion compared to 304 and is a good choice in elevated conditions. Type 304 is more aesthetically pleasing than 321 and 341. All these steels possess superb welding qualities and toughness.

Table 27 – Sample Properties

Material Sample	Mass of Sample (kg)	Flexural Strength (MPa)	Specific Flexural Strength (MPa/kg)
Mild Stainless Steel	0.120	158	1316
6082-T6 Aluminium	0.041	95	2317
Makerbeam®	0.020	21	1050

Appendix E: Drivetrain

Appendix E1: Tracks Study

Continuous tracks are a type of vehicle propulsion systems used on military, construction and agricultural vehicles. Military vehicles tend to have tracks made from modular steel plates and lighter vehicles such as agricultural or construction vehicles tend to have tracks made from reinforced rubber. The main advantages for using tracks are added traction, low ground pressure and durability. Tracks distribute weight better than tyres/wheels due to the larger surface area and therefore prevent sinking into soft ground.

Appendix E10 Materials

Tracks are usually made out of the following materials:

- Metal - usually military vehicle tracks
- Plastic – usually robot tracks
- Rubber – usually agricultural or construction vehicles

Appendix E11 Size

Tracks come in lots of different sizes. Some companies give you the option to specify all dimensions but the majority just allow you to specify the overall length. This means that specific tracks with the desired width must be chosen. The track width on the new robot is currently 30mm and the old robot has a combination of 70mm tracks at the base and 50mm tracks on the flippers.

Appendix E12 Treads

Assuming rubber tracks are decided upon, there are few options in terms of tread. Options currently include:

- Horizontal treads (similar to old robot)
- V-shaped treads

There are many ways to design and make tracks. The following list describes how to make different types of tracks using everyday materials.

Appendix E13 Bicycle chain track

- Constructed using bicycle chain, rubber friction drive wheel and strips of plywood
- Tractions provided is very good because the rivets used to attach the treads to the chain dig into the ground
- Friction drive wheels allow the use of the full width treads on the tracks and therefore prevent debris getting lodged between the treads

Appendix E14 Treadmill track

- Require treadmill and wood
- Tracks must be properly tensioned and the friction surface must be kept clean
- Can easily travel on a variety of surfaces
- Edges of the tread provide excellent traction

Appendix E15 Roller chain track

- Use a single chain that goes down the middle of the track, a drive sprocket and an idler sprocket
- Limited flexibility of the track
- Durable but the heaviest form of track system

Appendix E16 Plastic conveyer track

- Strong, lightweight alternative to roller chain solutions
- No construction necessary
- Possible to buy the belt links and sprockets together
- Only need to adjust the length of the track
- There is no real way to modify the tracks
- Strong, lightweight and durable
- Good on hard, smooth surfaces
- Open spaces within track make traveling over soft surfaces difficult – it just sinks

Appendix E17 Moulded tracks

- Time consuming – requires making hundreds of little components
- Behave similarly to solid track system
- Unreliable – increases chance of breakage due to the quantity of small components

Appendix E18 Hinge track

- Based on standard door hinges
- All-steel and inexpensive
- Easy to build
- Has completely closed, steel pads; this prevents debris sticking between the pads
- Steel pads do not wear out on hard terrains
- Hinge pivots dig into the ground
- Works best with a rear drive wheel
- Track can be loose and sagging

Appendix E19 Chain and bolt track

- Made from simple, easily obtainable components
- Potential problems with tensioning
- Little side to side deflection of the track and that is why there are no guide teeth

Due to cost and complexity the form of transport was limited to tracks or wheels. Table 28 compares tracks and wheels in order to asses which are more suitable for use in a USAR robot.

Table 28 – Track and Wheel Comparison

ID	Constraint	Tracks	Wheels	Scale	Reason for choice
1	Cost	0	1	5	Wheels are more common and involve fewer parts leading to being cheaper
2	Mass	0	1	5	Tracks have more components than wheels, leading to a greater mass
3	Modular	1	0	5	Tracks can have parts mounted inside them, leading to the possibility of a self-contained unit
4	Size	1	0	4	Tracks are more flexible in shape/size of design
5	Adaptability	1	0	4	Tracks only need the tread to be changed for different levels of grip or clearance. Wheels need to be completely replaced to change these aspects
6	Repair/ Maintenance	1	0	3	If the tread breaks, the whole wheel needs replacing but the track just needs one tread element replacing
7	Complexity	0	1	3	Wheels have less components so are less complex
8	Durability	0	1	2	Generally made from thick rubber, so more durable then lots of little treads
9	Reliability	0	1	3	Tracks have more components so more can break than in a wheel
10	Torque	1	0	3	Although both have the same torque tracks can apply it more effectively
11	Traction	1	0	3	Wheels only contact the ground in a small area whereas tracks are much larger attaining better traction
12	Gap/ Obstacle crossing	1	0	5	Tracks length allows them to traverse gaps and obstacles which wheels would otherwise get stuck in/on
13	Clearance	0	1	3	Without special consideration, tracks give less clearance than wheels
14	Mobility	1	0	3	Greater gap and obstacle crossing capabilities give tracks better mobility
15	Power Source	-	-	-	As the power source will be the same for both, this will not be compared
16	Control	-	-	-	Control methods will be the same for
17	Wiring	-	-	-	Wiring to motors will not depend on wheels/tracks
18	Environment	1	0	3	Tracks have lower ground pressure and can therefore handle a wider range of environments e.g. sand/gravel
	Total	**33**	**21**		

The comparison determined that tracks were the most suitable form of motion for the new USAR robot.

Appendix E2: Clutch and Double Differential

Clutch Brake

In this design a single motor powers a driveshaft, which is connected to each track via a clutch as shown in Figure 64 , and when the clutches are engaged power is transmitted equally to both tracks. If (for example) a left turn is required then the left-hand clutch is disengaged, allowing the left-hand track to slow, and causing the vehicle to "free turn"*. If a sharper turn were required then the left-hand track would braked to further slow it – thus decreasing the turn radius.

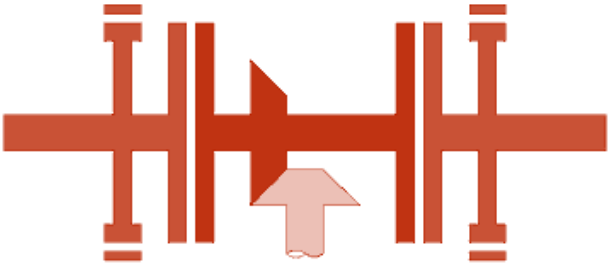

Figure 64 – Clutch-Brake Mechanism

Table 29 – Clutch-Brake: Advantages & Disadvantages

Advantages	Disadvantages
+ Relatively simple design	- Inefficient: braked turn slows the vehicle and causes significant frictional losses
+ Relatively easy to steer. (However see disadvantages for caveat)	- Steering can still be unpredictable as the braking force vs yaw curve is effectively flat – meaning that a small change in braking force can lead to a large change in turn radius
	- Unable to perform neutral turn

A derivative of the clutch-brake system is the 'braked differential' – which simplifies the clutch-brake design further by driving the two tracks through a differential, hence eliminating the need for clutches as shown in Figure 65 This design does, however, still carry the same shortcomings as the clutch-brake in terms of inefficiency, unpredictable steering and lack of neutral turn capabilities.

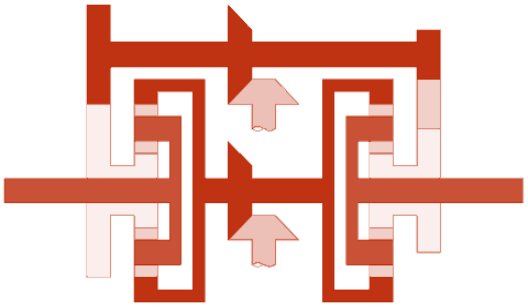

Figure 65 – Double Differential

Celtrac 'Controlled Differential', Double Differentials etc.

For this mechanism a specially-designed differential is made, through application of a brake, to rotate at specific rate, proportional to the speed of the vehicle - this allows for efficient turning at one fixed radius. Greater turn radii may be achieved by 'slipping' the brake, however this negates the efficiency advantage afforded by the fixed turning circle.

A refinement of the controlled differential is the "Maybach" double differential mechanism, wherein the differential gears, rather than precessing about a fixed gear, instead precess about a gear driven at a speed directly proportional to that of the motor. This provides a separate turn radius for each forward gear, as well as allowing neutral turns if the main gearbox is placed in neutral and the differential gears are rotated.

A further refinement of this concept is the "Wilson" double differential, whereby a second transmission between the motor and the initial transmission steering input is added. As a result the differential gears may be run at various rates proportional to motor speed – hence providing a number of turn radii, each in proportion to the forward gear chosen. This transmission is also not subtractive, unlike the Maybach design, meaning that when one track is slowed the other accelerates. This design is considered the father of all current-day, fast-track-laying steering systems. Introducing a third differential effectively gives a double-differential transmission combined with a braked differential for steering – this is used by practically all today's fast, tracked vehicles.

Table 30 – Double & Controlled Differential Advantages

Advantages	Disadvantages
+ Very efficient	- High complexity
+ Steers well	- Unnecessary at small scale
+ Allows multiple turn radii including neutral turn	

Appendix E3: Kinetic Friction Coefficient

The coefficient of friction was determined by placing a sample of AbbrX 55 material on a piece of the desired material, then adjusting the slope of the material until the sample slipped and descended the slope at a constant velocity. By simple force balancing the coefficient of friction was given by Equation E1. Results from this method are summarised in Table 31.

$$\mu = \tan\theta \qquad (E1)$$

Table 31 – Friction Coefficients

Material	Kinetic Friction Coefficient
Smooth Wood	0.61
Rough Wood	0.87
Brick	0.84
Concrete	0.97

Appendix E4: Drivetrain Calculations

In Figure 66 a wheel of mass, m, and radius, r, is being driven up an incline of angle, θ, at a steady velocity, u, by a torque, τ. There is a frictional force, f, acting up the slope.

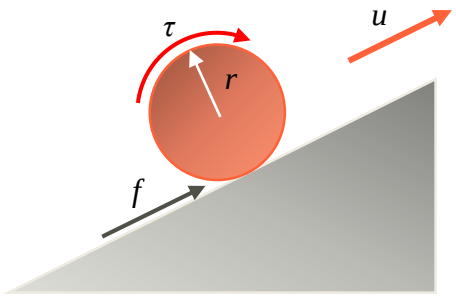

Figure 66 – Steady Torque Derivation

Then a simple moment balance gives,

$$\sum M = \tau - fr = 0$$

$$\tau = fr \qquad (E2)$$

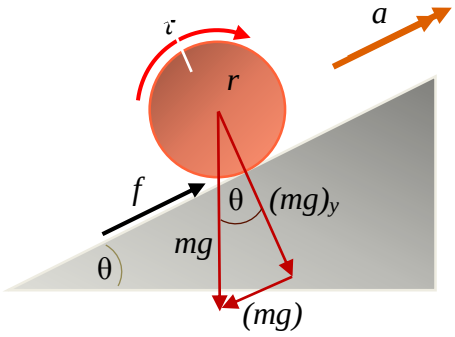

Figure 67 – Acceleration Torque Derivation

If, however, the wheel is accelerating up the slope then the situation is slightly more complex:

Summing forces in the x-direction, gives,

$$\sum F_x = f - (mg)_x = ma$$

$$ma + mg\sin\theta = f \qquad (E3)$$

Then substituting for f from Equation 8.1,

$$ma + mg\sin\theta = \frac{\tau}{r} \qquad (E4)$$

The required torque from the motor is then given by,

$$\tau = mr(a + g\sin\theta) \qquad (E5)$$

In the case of multiple motors the required torque will simply be divided by the number of motors multiplied by their efficiency:

$$\tau = \frac{mr(a + g\sin\theta)}{\varepsilon n} \qquad (E6)$$

Appendix E5: Suspension Calculations

Once the concept had been devised, theoretical modelling was required to determine various parameters including the required spring stiffness and the yield strength of the individual components. From the suspension model already shown in section 5.3.6.:

Summing moments about point A, gives

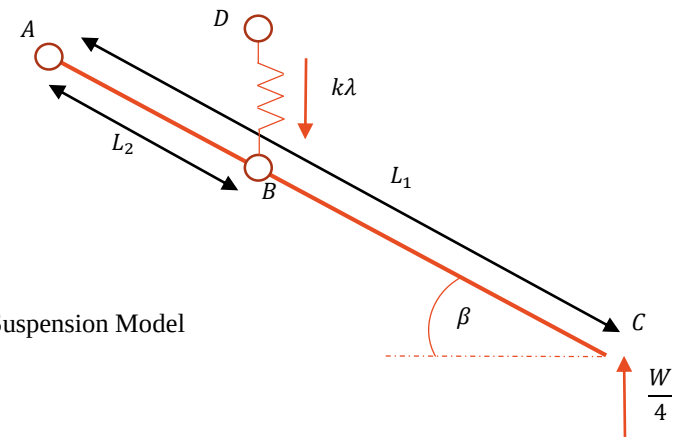

Figure 68 – Suspension Model

$$\sum M = (k\delta \cdot L_2\cos\beta) - [(W/4)\cdot L_1\cos\beta] \qquad (E7)$$

At equilibrium moments sum to zero, i.e.

$$(k\delta \cdot L_2\cos\beta) = [(W/4)\cdot L_1\cos\beta]$$

i.e.

$$k\delta L_2 = (W/4)\cdot L_1$$

$$k = \frac{L_1}{L_2}\frac{W}{4\delta} \qquad (E8)$$

Appendix F: Electronics

Appendix F0: Glossary

Powerboard – manages the power distribution from the battery to the various components.

DC-DC Voltage Converters – an electronic circuit which converts a source of direct current (DC) from one voltage level to another. It is a class of power converter.

VPN - a virtual private network (VPN) extends a private network across a public network, such as the Internet. It enables a computer or network-enabled device to send and receive data across shared or public networks as if it were directly connected to the private network, while benefiting from the functionality, security and management policies of the public network.

MCU - a microcontroller unit is a small computer on a single integrated circuit containing a processor core, memory, and programmable input/output peripherals.

PROTO PIC- a modified MCU

PWM - a technique used to encode a message into a pulsing signal.

PID - calculates an error value as the difference between a measured process variable and a desired setpoint. The controller attempts to minimize the error by adjusting the process through use of a manipulated variable.

Nyquist - the lower bound for the sample rate for alias-free signal sampling

Geotiff - is a public domain metadata standard which allows georeferencing information to be embedded within a TIFF file.

MOSFET - a type of transistor used for amplifying or switching electronic signals.

CMOS - a technology for constructing integrated circuits.

SR Latch - a circuit that has two stable states and can be used to store state information.

Appendix F1: Lithium Batteries

LiPo batteries are a relatively volatile charge storage medium, however they benefit from having extremely high charge density. LiPo batteries can overcharge, over-discharge, over-temperature, short circuit, crush and nail penetration may all result in a catastrophic failure, including the pouch rupturing, the electrolyte leaking, and possible combusting during a volatile reaction with air.

All Li-ion cells expand at high levels of State of Charge (SOC) or over-charge, due to slight vaporisation of the electrolyte. This may result in delamination and thus bad contact of the internal layers of the cell, which in turn brings diminished reliability and overall cycle life of the cell. This is very noticeable for LiPos, which can visibly inflate due to lack of a hard case to contain their expansion.

Lithium Polymer (LiPo) Batteries - Compatibility and Battery Life Considerations

Drawing inspiration from previous WMR robots 6s (6 cell) LiPo Batteries were used. LiPo batteries supply high stability DC voltage and each cell can be charged to 4.2V (25.2V total) and discharged to 3V (18V total). LiPo batteries must be monitored so as to prevent dangerous deep discharge, whereby the cell voltage goes far below the safe limit, which by general consensus is approximately 3.7V and below 3V. Deep discharge or overcharge is extremely dangerous due to the highly reactive electrolyte material. Battery mounting systems have been designed to allow rapid battery removal should failure occur, and the battery master switching circuit allows one to set a user defined threshold voltage at which point the preventative switching circuitry would disconnect the system with the power supply. This prevents damage to the rest of the electronic systems. Cells are oriented in parallel to increase the current capacity and the batteries have an allowable discharge rate of 45C continuous and 90C in short bursts of approximately 15 seconds.

Continuous Discharge current

Q=CV = Ixt (charge = current x time)

Battery Spec: 6S LiPo 5000mAh with 45C discharge rate

45C discharge rate x 5Ah

This equates to 225A of continuous discharge capability, a more than adequate current for the rest of the system calculated as below:

	Max Current Draw (A)	Current Draw inc. 35% Safety margin (A)
GE EHHD024A0A41	24	32.4
TRACO TEL 30 2412	2.5	3.375
Maxon ESCON 50/5	2 x 15 = 30	40.5
Total	56.5	76.275

Battery life considerations

Using 76.275A as the total current draw is unrealistic, since this load is unlikely to ever be drawn from the batteries. The present robot hardware configuration uses 5V components drawing a maximum total current of 9.585A (approximately 13A with 35% safety margin) from the GE EHHD024A0A41 converter and uses only a single 12V device, being the router drawing a maximum of 2A (2.7A with safety margin) using the Traco Tel 30 2412.

Additionally the motor controllers are configured to source a maximum of 15A, however these motors are expected to operate nearer their nominal current far lower than 15A, so each motor controller is arbitrarily expected to draw an average of 7A (9.45A with 35% safety margin).

Recalculating the average total current draw with these expected values:

$13+2.7 + (2 \times 9.45) = 34.6 \approx 35A$

Comparing this expected 35A total current draw of Orion to the 63.75A of the motors alone at max efficiency from 2013/14 m-USAR, it is clear to see that the new system is a great deal better. If considering the additional 15.7A of peripherals as an estimate based upon this year's peripherals, this value rises to approximately 80A

This equates to a theoretical 230% improvement in battery life between the Orion 2014/15 robot and the m-USAR of 2013/14.

Appendix F2: Arm Schematic Design

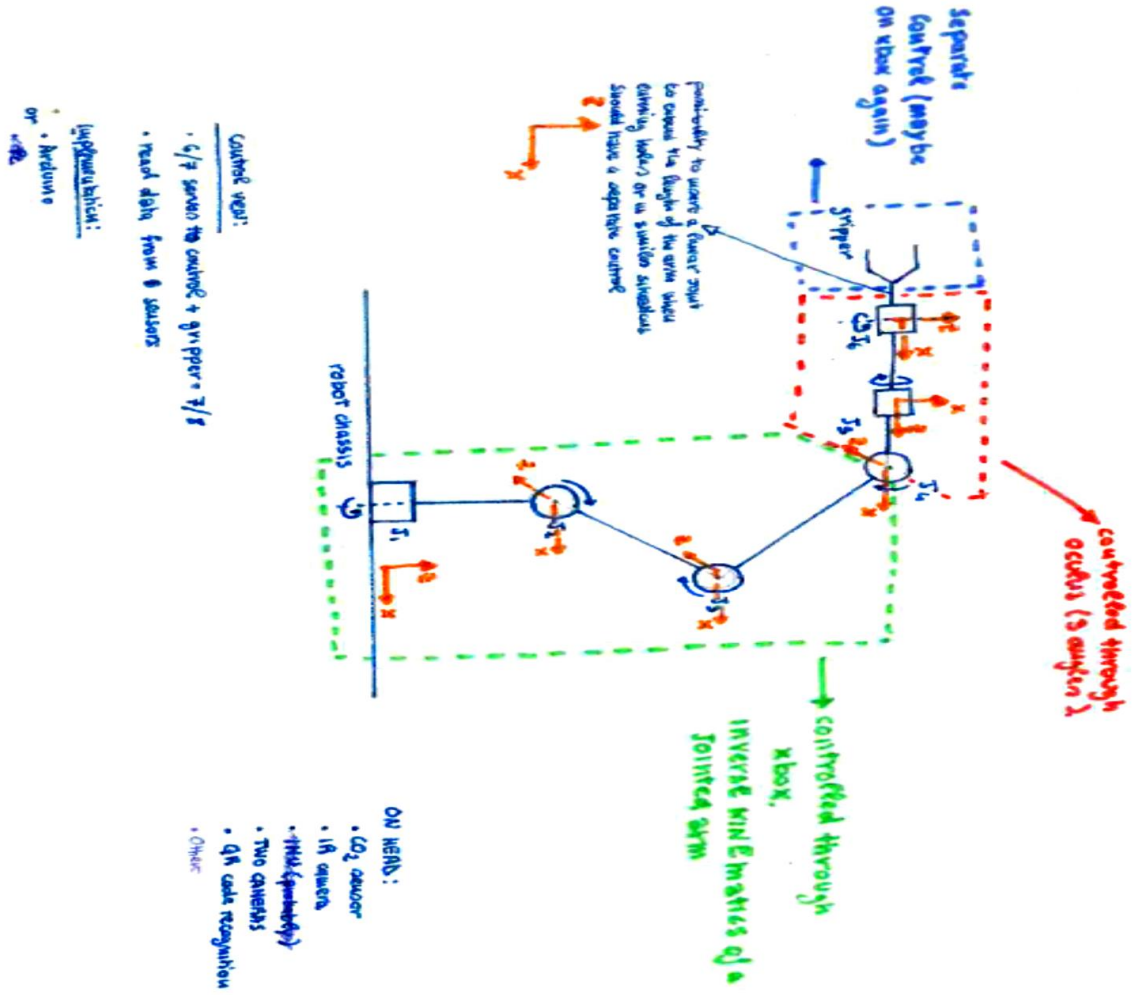

Figure 69 – Arm schematic

Appendix F3: Arduino

The Mega 2560 has 54 digital I/O pins, 16 analogue inputs, 4 UARTs (hardware serial ports), a 16 MHz crystal oscillator, a USB connection, a power jack, an ICSP header, and a reset button. It can be charged either through the USB connection, the dc supply or a battery. The addition of a USB shield is needed to provide the interface with a USB diagnostic and, eventually with a remote control. While the addition is simple in the design, the use of the serial communication reduces the voltage output of the pins to roughly 1V. This constituted a criticality in the interface with the motor controller and dictated the choice of PWM as the preferred control mode, since the control was based on the duty cycle and frequency of the control signal, rather than on its voltage level. Finally, Arduino allows to tailor the frequency output of its pins and this is a crucial characteristic in the adaptability of the controller to different sensors and motor controllers, each with its own frequency.

Appendix F4: Wireless Router

Initially the Ubiquiti HP Wireless Router was ordered because of its specifications. It is a powerful router using 802.11 b/g/n network protocols with an uninterrupted range of 200m whilst only using a 5V 2A supply, and so was an ideal choice. However, when the router arrived it was found that the router actually required a 24V supply (the router's motherboard had step down transformers inside to step down the voltage to 5 alongside many other voltages), which was more than the battery could provide stably. As opposed to WMR 2013/14, who supplied an undervoltage to their ASUS AC1750 Gigabit Router, it was deemed unacceptable to use such a high voltage router. As mentioned within the main body of the report supplying a voltage at under the required value will cause certain or sporadic 'failure-like' behaviour, or at best a markedly sub-optimal performance Therefore the less powerful Buffalo WZR2-G300N router used in the M-USAR was used in the robot as it only requires a 12V supply.

Appendix F5: PlayStation Controller

The controller has been programmed such that the left analogue stick is repeatedly sending a two dimensional input to the client ranging from 0 to 255. These numbers represent the stick's position on the x and y axis relative to the centre position. For example, if the control stick is held completely to the right, the controller will send a value of 255 for the x-axis to the client via bluetooth. The client will then relay this message using ROS via the VPN to ROS on the Pico-ITX. This message will then be interpreted by ROS to mean that it should send an output high Pin 2 on the Arduino (connected to the left motor) and an output low to Pin 11 (connected to the right motor). This will in effect cause Orion to turn right until a different value is sent by the Bluetooth controller.

Appendix F6: TurtleSim

One of the most useful packages in ROS is the TurtleSim package. It is used in many tutorials is ROS to explain various concepts. It is relevant to this project as it can be used as a diagnostic tool for the connection between the Sony PlayStation controller and ROS.

TurtleSim is effectively a program with a small turtle which can be controlled by the user in various ways. One of the functions of the program is the ability to move the turtle around the screen with the controller. Therefore TurtleSim can be used to check if ROS is reading the right values from the controller i.e. does the turtle's movement correspond with the movement of the analogue stick on the controller.

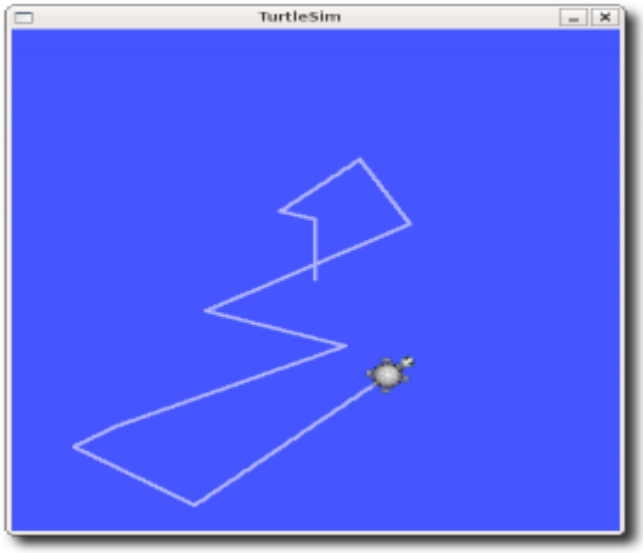

Figure 70 – ROS TurtleSim being used to test the controller

Appendix F7: Further Explanation of Battery Monitor SR - Latch

An innovative new system was designed to repurpose the GARTT voltage monitor/buzzer with some additional latching circuitry, to provide a signal to a power MOSFET to switch off the power to the Orion M-USAR.

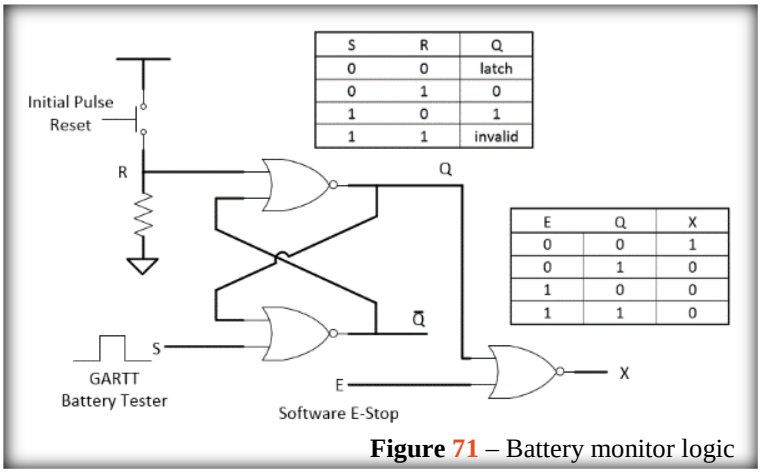

Figure 71 – Battery monitor logic

The buzzer, which originally 'flashed' on an off during the alarm, was used as the 'SET' input to an NOR SR latching circuit. This meant that upon 'flashing' the output remained at a constant latched logical 'High' level.

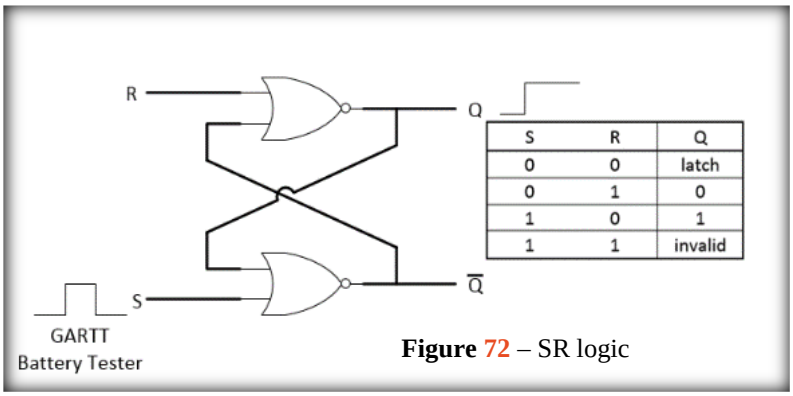

Figure 72 – SR logic

The operation of the GARTT buzzer did however 'flash' once upon plug in, which would force the output of the SR latch into a latched state. To remedy this, the 'RESET' input of the SR latch was designed to connect to a momentary pull up switch, which acts to reset the output into the 'low' state until the battery monitor once again flashes (this time, as a result of low cell voltage).

As an improvement to this initial design a Software Emergency-stop signal was incorporated into the monitor circuit. This is an innovative safety feature which makes use of the software heartbeat previously mentioned. Software 'bugs' or endless loops in are recognised by the Arduino which then sets an output high, preventing uncontrollable and potentially dangerous robot behaviour. If either the E-stop signal from the Arduino is 'set' high or the output from the battery monitoring SR latch is set 'high', the output 'X' would switch 'low'. By using this new configuration, the output would become active high, only switching low upon a failure in cell voltage or in software. This allows the circuit to be more easily used with drive circuitry to switch off the main Power MOSFET.

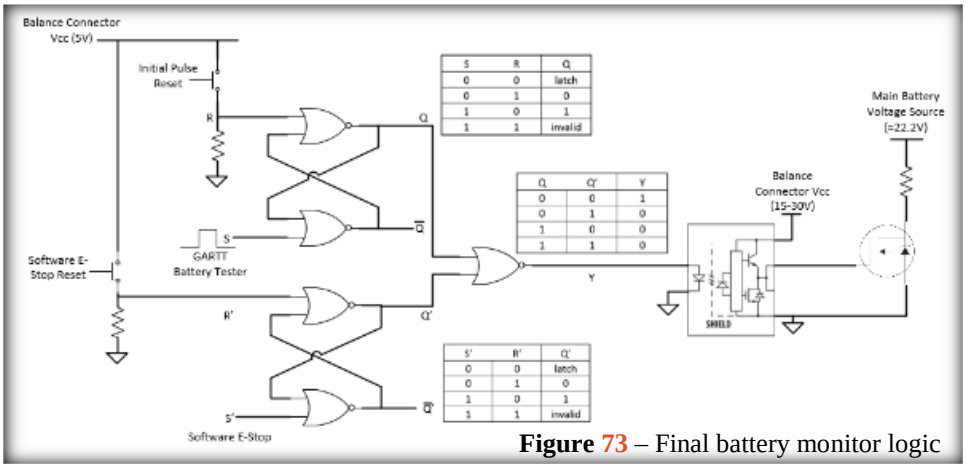

Figure 73 – Final battery monitor logic

The Software E-Stop was further improved by incorporating its own SR latching circuit. This meant that the 'high' output from the microcontroller upon an E-stop would cause an output that latched 'low' even after the power was cut. Since the robot modularity and code application allows a more simple Bluetooth control upon plugging a Bluetooth module into the robot, a momentary Reset switch was incorporated into the E-stop SR latch, meaning that if there is a bug during out-field operation, the Bluetooth module can be plugged in, and the reset switch can be pressed to restart power to the system (provided sufficient cell voltages). Since the Microcontroller code was written to detect the presence of a bluetooth dongle, upon restart the code executes a switch statement whereby it reverts to control over Bluetooth and ignores ROS commands and the output that was for the heartbeat is now held 'low' for operation. This different control medium allows retrieval of the robot at the worst-case software scenario, adding a vital safety feature to an already important heartbeat system.

A TI SN74AS805BN Hex 2-input NOR gate was used to prototype the NOR gate circuit. A Vishay FB180SA10P Power MOSFET, which is rated to 180A was chosen as the main power switch. This can easily handle any transient load on the battery, calculated at approximately 76A. A gate driver must be used as an intermediate stage between the logic and the MOSFET since the NOR gate output can only source a continuous 15mA at 2V when in logical 'high'. This is insufficient for the Vishay MOSFET as it requires a V_{GS} of at least 5V and ideally 15V to conduct sufficient current irrespective of the threshold voltage. An Avago HCPL-3120-300E was used, which when supplied with a voltage V_{CC} of above 13.5V sets the output to equal the supplied voltage upon an input current of above 7mA. This allows the NOR logic to force the gate driver to output sufficient voltage for the Power MOSFET to conduct and hence function correctly. Care was taken to ensure that the Vishay MOSFET was routed far from the Opto-coupler Gate Driver to prevent undesirable tuning and coupling.

Appendix F8: Overheating Modelling

For designing and combining power electronic systems in a chassis, it is imperative to understand rudimentary thermal issues such as the heat emanating from motors and heat dissipation in integrated circuits. Due to this, there needs to be productive thermal management of electronic components to prevent draining the battery, premature failure, overexerting these devices and improve power availability. In simple terms, these electronic components require cooling. Such techniques for heat dissipation include heat sinks and fan(s) for air cooling.

In this study, the total power dissipated from the electronic components totalled to 88 W. Refer to Table 32. To compensate, an aluminium 6082t6 shell was used to act as a heat sink. Heat

transfer by conduction can be used to model heat loss through this shell's wall. For a barrier of constant 2 mm thickness, the rate of heat loss is:

$$\frac{Q}{t} = \frac{kA(T_h - T_c)}{d} \qquad (F1)$$

Where Q is heat conduction, k is thermal conductivity, d is the thickness of aluminium shell, A is the area of the shell's wall.

By computation, the area of the shell is 396968.2 mm^2; the thermal conductivity of the 6082t6 alloy is 180W/mk; ambient temperature is 25 degrees and temperature inside the shell is assumed to be 40 degrees. Thus the heat loss rate is 535.9 KW.

However, heat sinks alone are insufficient and multiple literature have deemed factors such as air velocity, material and surface treatments substantially affecting power systems' performance. Due to this, cooling needs to occur to circulate air to move heat from the hot components to a cool area in the chassis. As shown in Table 32, the total power dissipated from the electronic components equated to 88 W.

Table 32 – Heat Power Loss of Each Component

Part	Heat Power Loss (W)
Motors x 2	45
Pico-ITX	1
Motor Controllers	22
Arduino	1
PMB	20 (approximation)
Battery	30

By calculation and considering the temperature of the components; heat transfer between the components; its environment; optimum airflow for cooling; the number of fans and the placement, majority of the heat dissipation would be derived from the motors and motor controllers. For sufficient cooling, a fan(s) would need to be placed at x, y, z end of the chassis to ensure an even temperature distribution throughout the chassis. Furthermore, one would opt for one fan parallel to the motor controllers and motors to pass air through the components. This would increase the flow throughout the entire robot chassis. Using this configuration, vents are not needed for this cooling system. Ideally, one recommends an additional smaller fan facing x, y, z to aid with cooling. However, due to space limitations, this was not possible.

Criteria for Fan

As the number and placement of the fan is known, it is necessary to choose the right fan configuration. This criteria is based on the thermal dissipation (CFM) factor, the supply voltage, the size and the geometry of the fan. Using the equation:

$$Heat\ Power = 0.316 \times CFM \times \Delta T$$

Where CFM is the cubic feet per minute i.e air flow measurement, ΔT is the difference between the intake air and exhaust air.

Taking Heat Power as 535.9 KW and ΔT as the maximum intake air and exhaust air of the hottest component- motor, the CFM is 11.03. Furthermore, it is important to have a supply voltage similar to the surrounding components to ease design constraints on the power board. Therefore, the average voltage of the components is 5V so the optimal fan's voltage would be 5V. For this application, a fan of low pressure, low system resistance and high flow rate is needed. A high flow rate is needed as one fan is being used.

Additionally, it is important to note that the main aim of this fan is to move air from a large space to another area. For this reason, an axial geometry is preferred over radial fans. Axial fans tend to rotate about their axis and move a column of air parallel to that axis. These blades are known to achieve a high efficiency factor. Radial fans induce airflow by the centrifugal force generated in a column of air that rotates. In particular, airfoil axial impellers provide uniform, high volume airflow with low power consumption for optimum efficiency.

The best possible fan within these aforesaid constraints is the SUNON MB50100V2-0000-A99 Fan, supplied by Farnell. This fan's dimensions are 50 x 50 x 10 mm, 5 VDC, 26 dBA in noise, 4 curves and CFM equals to 11.0.

Appendix F9: Methodology of a Topic Connection

The protocol for two nodes to start exchanging messages is as follows (ROS, 2014):

1. The subscriber reads the arguments from the command line to decide the topic name to use
2. The publisher similarly reads the command line remapping arguments to choose a topic name
3. The subscriber registers with the master via a XML remote procedure call (XML-RPC) protocol
4. The publisher also registers with the master via the same protocol
5. Once the publisher has been registered, the master notifies the subscriber of the new publisher via XML-RPC

6. The subscriber will then request to connect to the publisher to subscribe for a particular topic and the transport protocol will be negotiated (UDP in Orion's case)
7. The Publisher sends the subscriber the settings, who in turn establishes the connection with the publisher through the designated transport protocol

Appendix F10: Fuse Considerations

Fuses are required as a protection mechanism for the output peripherals, some of which are very expensive and are likely to break under subjection to high current spikes. The DC/DC converters of the Powerboard themselves are also not safe to use without external fuses:

"This power module is not internally fused. An input line fuse must always be used" - GE Critical Power EHHD024A0A4

It would be desirable to use fuses not susceptible to quickblow, whereby if connectors are removed or connected without the rest of the system being off, fuses will break. Quickblow fuses are vulnerable to hot plugging and hence slow blow fuses would be more appropriate if it is desirable to plug peripherals in when the system is powered. The LittelFuse Slo-Blo® design series has enhanced inrush withstanding characteristics over the NANO2 Fast-Acting Fuse. The unique time delay feature of this fuse design helps solve the problem of nuisance "opening" by accommodating inrush currents that normally cause a fast-acting fuse to open. For parts such as motors, slow blow fuses would be recommended, however do not provide sensitive protection for some more delicate peripherals such as the FLIR IR camera. For the particular use in protecting semiconductor devices, fast-acting fuses should be used. LittelFuse 476 series fast acting fuses were chosen to fulfill Powerboard requirements. This does however mean no connections can be made upon power on in the current configuration.

This issue is remedied somewhat by the the use of a powered USB hub, which provides double protection between the battery and the peripherals, allowing the USB powered devices to be plugged in during power on.

A minimum fuse value of 135% larger than the load current was chosen as recommended in the Optifuse fuse selection guide (OptiFuse, 2010).

LittelFuse Nano fuses provide an ideal product type, due to their miniaturized surface mount capability, but also provide a wide range of fuse ratings at a standard size, which can be placed

within an Omniblok fuse holder rather than having to solder each fuse direct to printed circuit boards. This is shown in the image below.

Figure 74 – LittleFuse Nano fuses in Omniblock holders

Appendix F11: Heartbeat Generator

Currently, the Arduino is programmed as such, that if it does not receive the heartbeat signal, it can send an output high; which will be used as one of the inputs of the SR latch configuration driving the Battery MOSFET master switching control; which in turn will shut down all the power to the robot. However, this simple but elegant program can be reprogrammed in different ways by future students working on Orion. A good setup would be to have different heartbeat signals for the core topics, such as the Motor and the LiDAR topics, with each heartbeat signal having different consequences based on the importance of the function. For example, if the heartbeat signal for the motors is not received, then the Arduino can be programmed to automatically send a disable signal to the motors. Similarly, if the LiDAR topic has stopped running, the LiDAR heartbeat signal will not be received by the Arduino, which in turn will turn on an LED, indicating to the users that the LiDAR has turned off. Therefore the heartbeat generator is a great way to know that the robot is fully functional and can prevent mishaps from software and hardware glitches.

Appendix F12: Powerboard Final Design

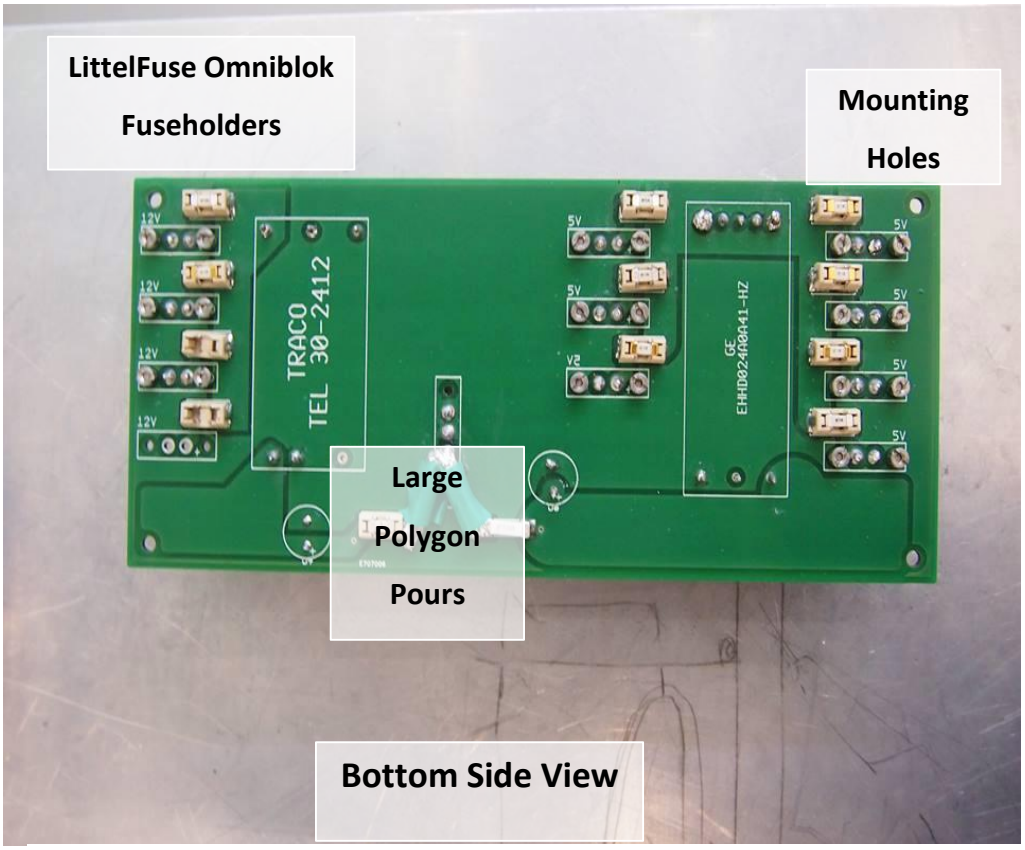

Figure 75 - Final Power Board Design (Bottom)

Appendix G: Manufacturing

Appendix G1: Health and Safety

As well as implementing safety mechanisms within the robot design, it was important that the students work in the safest manner possible. Therefore all students attended a safety workshop conducted by Paul Johnson, a member of the IMC workshop team, at the beginning of the academic year. This session informed the students on general safety within the laboratory including wearing steel-capped shoes at all the times and not eating/drinking in the lab.

Lithium-ion batteries were used to power the robot; which are vulnerable to overcharge, over-discharge, over-temperature, short circuit, crush and nail penetration which can all result in a catastrophic failure, including the pouch rupturing, the electrolyte leaking, and even a fire. Therefore all students who would be handling the batteries undertook a battery safety session at the Energy Innovation Centre during the first term. In addition, several other safety sessions were undertaken during the year by individual students utilising the hazardous tools in the lab such as the drill.

The team ensured safety was given paramount importance throughout the year and recommends that future students on the project follow suit.

Appendix H: System Testing

The following tests have been generated to verify the requirements stated in the specification.

- Requirements "Met" if fully verified through testing, observations or analysis,
- Requirements are "Partially Met" if some aspects of the requirement can be verified
- Requirements are "Not Met" if they cannot be verified.

Requirement to be tested	Observation/ Analysis/ Test	Method	Results	Requirement Met/Partially Met/Not met
The length of the robot will be no larger than 460mm.	Test	Measure length of the robot.	Is the length of the robot less than or equal to 460mm?	Met
The width of the robot will be no larger than 320mm.	Test	Measure the width of the robot	Is the width of the robot less than or equal to 320mm?	Met
The height of the robot will be no larger than 242.5mm.	Test	Measure the height of the robot.	Is the height of the robot less than or equal to 242.5mm?	Met
The volume of the robot must be equal to or larger than $0.013m^3$.	Test	Using the measurements of the length, width and height of the robot, calculate the internal volume of the robot.	Is the internal volume of the robot equal to or greater than $0.013m^3$?	Met
The weight of the robot must not exceed 25kg	Test	1. Place robot on weighing scales 2. Read off value of weight	Weight = Can a single person deploy the robot?	Met
It will be possible to change over a battery within 30 seconds	Test	1. Open side hatch on robot 2. Remove current battery 3. Insert new battery 4. Secure hatch for continued use	Battery changeover time = 30s	Met

The robot must be able to climb stairs with a step height of 190mm at an angle of 38°	Test	1. Place the robot at the bottom of a set of stairs with the required step height and angle 2. Initiate movement 3. Navigate the robot up the staircase	Does the robot slip down? Does the robot make it to the top of the staircase?	Partially Met
Test on kerb	Test			Met
The robot will survive a 350mm drop	Test	1. Suspend the robot 350mm above the ground 2. Release the robot 3. Confirm that the robot is undamaged and continues to function	Does the robot survive a 350mm drop?	Partially Met
There will be no cable connections through moving part	Observation		Are there any cable connections through moving parts?	Met
The robot will perform adequately over thin surface water	Test	1. Place robot on the ground near to a puddle 2. Initiate movement 3. Drive robot through puddle 4. Confirm robot successfully drives through puddle, is undamaged and continues to function	Can the robot successfully operate when driving through thin surface water?	Not Met
The robot will successfully	Test	1. Place robot near to muddy area.	Can the robot successfully	Not Met

traverse through mud		2. Initiate movement. 3. Drive robot through mud. 3. Confirm that the robot is undamaged and continues to function	travel through mud?	
The robot will successfully travel on hard floor	Test	1. Place robot on hard floor. 2. Initiate movement. 3. Drive robot through mud. 3. Confirm that the robot is undamaged and continues to function	Can the robot successfully travel on hard floor?	Partially Met
The robot will successfully traverse through sand	Test	1. Place robot near to a sandy area. 2. Initiate movement. 3. Drive robot through mud. 3. Confirm that the robot is undamaged and continues to function	Can the robot successfully travel through sand?	Not Met
The robot will successfully travel on wooden floor	Test	1. Place robot on wooden floor. 2. Initiate movement. 3. Drive robot through mud. 3. Confirm that the robot is undamaged and continues to function	Can the robot successfully travel on wooden floor?	Partially Met

It will be possible to vary the speed of the robot	Observation		Is it possible to vary the speed?	Met
The robot will be able to accelerate up to 0.3 m/s²	Test	1. Initiate movement. 2.	Can the robot accelerate up to 0.3 m/s²?	Partially Met
The robot will move comfortably at 1m/s	Test	1. Initiate movement. 2. Increase the velocity to 1m/s. 3. Confirm that the robot moves comfortably at this velocity.	Can the robot operate comfortably at 1m/s?	Partially Met
The robot will be able to return to base when it is flipped upside-down	Test	1. Turn the robot upside-down 2. Navigate the robot back to base whilst upside-down	Can the robot return to base whilst it's upside-down?	Partially Met
The robot will be capable of mapping out a room	Observation		Can the robot accurately map out a room using the LiDAR?	Met
The robot will be able to detect different levels of CO_2	Observation		Can the robot detect CO_2?	Partially Met
The robot will be able to replay an IR image of its surroundings to the user	Observation		Can the robot produce an IR image of its surroundings?	Partially Met
The robot will be capable of full tele-operated control when out of sight	Observation		Is the robot capable of full tele-operation when out of sight?	Not Met